

UNIVERSITY OF NAPLES FEDERICO II

School of Polytechnic and Basic Sciences



Department of Chemical, Materials and Industrial Production Engineering

*XXXI PhD Programme in
Industrial Products and Processes Engineering*

Smart Sensor Monitoring in Machining of Difficult-to-Cut Materials

PhD COURSE COORDINATOR

Ch.mo Prof. Ing. Giuseppe Mensitieri

PhD CANDIDATE

Ing. Francesco Napolitano

PhD SUPERVISOR

Ch.mo Prof. Ing. Roberto Teti

PhD CO-SUPERVISOR

Dr. Ing. Alessandra Caggiano



FRAUNHOFER JOINT LABORATORY OF EXCELLENCE ON ADVANCED PRODUCTION TECHNOLOGY

(FH-J_LEAPT UNINAPLES)

Index

LIST OF FIGURES.....	III
LIST OF TABLES.....	VI
1. INTRODUCTION	1
2. SENSOR MONITORING OF MACHINING PROCESSES.....	3
2.1 SENSOR MONITORING APPLICATIONS.....	3
2.1.1 <i>Tool conditions</i>	3
2.1.2 <i>Surface integrity</i>	4
2.1.3 <i>Process conditions</i>	4
2.1.4 <i>Chip form</i>	5
2.1.5 <i>Machine tool state</i>	5
2.1.6 <i>Other applications</i>	6
2.2 SENSORS FOR MACHINING PROCESS MONITORING	6
2.2.1 <i>Motor Power and Current</i>	6
2.2.2 <i>Force and torque</i>	7
2.2.3 <i>Acoustic emission</i>	8
2.2.4 <i>Vibration</i>	8
2.2.5 <i>Other sensors</i>	9
2.3 ADVANCED SENSOR SIGNAL PROCESSING METHODS	9
2.3.1 <i>Signal conditioning and pre-processing</i>	10
2.3.2 <i>Signal feature extraction</i>	11
2.3.2.1 <i>Time domain</i>	11
2.3.2.2 <i>Frequency domain</i>	11
2.3.3 <i>Signal feature selection</i>	12
2.4 DECISION MAKING SYSTEMS	13
2.4.1 <i>Neural networks</i>	15
2.4.2 <i>Fuzzy logic</i>	16
2.4.3 <i>Other decision making systems</i>	17
2.5 SENSOR FUSION TECHNOLOGY	18
2.6 CLOUD MANUFACTURING FOR MACHINING PROCESS MONITORING	19
2.7 RESEARCH GAP	20
2.7.1 <i>Gap identification</i>	20
2.7.2 <i>Objectives</i>	21
3. SMART SENSOR MONITORING OF TITANIUM ALLOY DRY TURNING	
.....	22
3.1 THE FRAMEWORK.....	22
3.1.1 <i>CAPRI project on “Landing Gear with Intelligent Actuation”</i>	23
3.2 EXPERIMENTAL TESTING CAMPAIGN	23
3.2.1 <i>Multiple sensor system setup</i>	24
3.2.2 <i>Workpiece material</i>	32

3.2.3 <i>Cutting tool specifications and process parameters</i>	33
3.3 TOOL WEAR MEASUREMENT AND WEAR CURVE CONSTRUCTION	34
3.4 SIGNAL PROCESSING AND FEATURE EXTRACTION	37
3.4.1 <i>Signal segmentation and resampling</i>	39
3.4.2 <i>Signal feature extraction</i>	41
3.4.3 <i>Signal feature selection</i>	42
3.5 TOOL WEAR CURVE RECONSTRUCTION AND GENERATION THROUGH INTELLIGENT METHODS	43
3.5.1 <i>Tool wear curve reconstruction</i>	43
3.5.2 <i>Tool wear curve generation</i>	44
3.6 RESULTS AND DISCUSSION	46
4. SMART SENSOR MONITORING OF CFRP/CFRP AND AL/CFRP STACK DRILLING	48
4.1 THE FRAMEWORK	48
4.1.1 <i>Applications</i>	50
4.2 EXPERIMENTAL TESTING CAMPAIGN	51
4.2.1 <i>Multiple sensor system setup</i>	51
4.2.2 <i>Workpiece material</i>	54
4.2.3 <i>Cutting tool specifications and process parameters</i>	57
4.3 TOOL WEAR MEASUREMENT AND WEAR CURVE CONSTRUCTION	58
4.4 SIGNAL PROCESSING AND FEATURE EXTRACTION	64
4.4.1 <i>Signal segmentation</i>	65
4.4.2 <i>Signal features extraction</i>	68
4.4.2.1 <i>Time domain features</i>	69
4.4.2.2 <i>Frequency domain features</i>	71
4.4.3 <i>Signal features selection</i>	76
4.4.3.1 <i>Feature dimensionality reduction</i>	77
4.5 TOOL WEAR CURVE RECONSTRUCTION THROUGH INTELLIGENT METHODS	79
4.6 RESULTS AND DISCUSSION	81
4.6.1 <i>Tool wear forecast in drilling</i>	81
4.6.2 <i>Feature dimensionality reduction</i>	84
5. SUMMARY AND FUTURE DEVELOPMENTS	86
5.1 CLOUD MANUFACTURING APPROACH	87
BIBLIOGRAPHY	88

List of Figures

Figure 1. Spindle motor with integrated sensor ring (G. Byrne and O' Donnell 2007).....	7
Figure 2. Advanced signal processing procedure (Teti et al. 2010).....	10
Figure 3. Frequency of usage of AI approaches in intelligent machining systems according to the references found in the research platform ISI-Web of knowledge from 2002 to 2007 (Abellan-Nebot and Romero Subirón 2010)......	14
Figure 4. Fuzzy inference system implementation steps (Teti et al. 2010).....	17
Figure 5. Doosan PUMA400LM CNC lathe.	24
Figure 6. Multiple sensor system mounted on the tool holder (Alessandra Caggiano, Napolitano, and Teti 2017).....	25
Figure 7. 3D Force sensor Montronix FS13-CXK-R-ICA.	25
Figure 8. Set-up of the Montronix TSFA3-ICA 3D force sensor amplifier.	26
Figure 9. Acoustic emission sensor Montronix BV-100.	27
Figure 10. Acoustic Emission sensor amplifier Montronix TSVA2-DGM-BV.	28
Figure 11. Vibration sensor Montronix Spectra TM Pulse.	29
Figure 12. National Instrument NI USB-6361 digitizing board.....	31
Figure 13. Cutting insert CNMG120404-MS MT9015.	33
Figure 14. Wear zone of the cutting edge(ISO 3685:1993).	34
Figure 15. Tool wear measurement on the acquired image.....	35
Figure 16. Dino Lite Microscope.	35
Figure 17. Dino Lite Microscope mounted on its magnetic support.....	36
Figure 18. Measured tool flank wear values vs machining time for $v_1 = 60$ m/min, $v_2 = 70$ m/min, $v_3 = 80$ m/min ($f = 0.2$ mm/rev, $d = 0.5$ mm).....	36
Figure 19. Measured tool flank wear values vs machining time for $d_1 = 0.5$ mm, $d_2 = 1$ mm, $d_3 = 1.5$ mm ($v = 60$ m/min, $f = 0.2$ mm/rev).....	37
Figure 20. Measured tool flank wear values vs machining time for $f_1 = 0.2$ mm/rev, $f_2 = 0.25$ mm/rev, $f_3 = 0.3$ mm/rev ($v = 60$ m/min, $d = 0.5$ mm).....	37
Figure 21. Acquired Force signals.....	38
Figure 22. Acquired Acoustic Emission RMS and Vibration Acceleration signals.	38
Figure 23. Acquired Acceleration signals.....	39
Figure 24. Moving average of F_x cutting force component signal and set threshold (red line).	39
Figure 25. Segmented F_x , F_y , F_z cutting force components signals.....	40
Figure 26. Segmented acoustic emission RMS and vibration acceleration RMS signals.	40
Figure 27. Segmented A_x , A_y and A_z vibration acceleration signals.....	41
Figure 28. Extracted statistical sensor signal features in time domain.	42
Figure 29. Average of F_z cutting force component signal, $F_{z_{av}}$, vs machining time for $f_1 = 0.2$ mm/rev, $f_2 = 0.25$ mm/rev, $f_3 = 0.3$ mm/rev ($v = 60$ m/min, $d = 0.5$ mm).....	43
Figure 30. Artificial Neural Network architecture.....	43
Figure 31. ANN output vs measured VB_{max} for turning test at $v = 60$ m/min, $f = 0.25$ mm/rev, $d = 0.5$ mm. ANN configuration: 9-18-1. MSE = 0.000639.....	46

Figure 32. ANN entire tool wear curve generation. The tool wear curve for $v_1 = 60$ m/min, $f_1 = 0.25$ mm/rev, $d_1 = 1.5$ mm is obtained using a training set comprising sensor signal features and corresponding tool wear values for $v_2 = 60$ m/min, $f_2 = 0.20$ mm/rev, $d_2 = 1.5$ mm and $v_3 = 60$ m/min, $f_3 = 0.30$ mm/rev, $d_3 = 1.5$ mm. ANN configuration: 12-24-1. MSE = 0.01373.	47
Figure 33. Drilling basic motions.	49
Figure 34. Multiple sensors system for drilling process monitoring setup.	52
Figure 35. (a) Kistler 9257 piezoelectric dynamometer; (b) Kistler 9277A25 piezoelectric dynamometer.	53
Figure 36. Kistler 5007 amplifiers.	53
Figure 37. Acoustic Emission and Vibration Acceleration amplifier settings.	54
Figure 38. (a) Vacuum bag moulding; (b) Autoclave.	55
Figure 39. Laminates profiles and their surface textures.	56
Figure 40. Standard geometry of a twist drill (Mikell P. Groover 2014).	57
Figure 41. (a) Innovative step drill bit. (b) Traditional twist drill bit.	58
Figure 42. Schematic representation of twist drill (Stephenson and Agapiou 2006).	59
Figure 43. Tool wear as a function of cutting time (Marinov 2004).	60
Figure 44. Effect of cutting speed on tool wear and tool life for three cutting speeds.	60
Figure 45. (a) Tesa Visio V-200 optical microscope, (b) clamping system.	61
Figure 46. VB max and VB tool wear measurement on innovative drill bit.	61
Figure 47. VB max and VB tool wear measurement on traditional drill bit.	62
Figure 48. Tool wear measurement scheme for drill bits (Dolinšek, Šuštaršič, and Kopač 2001).	62
Figure 49. Tool wear values and interpolated curves. Traditional drill bits.	63
Figure 50. Tool wear values and interpolated curves. Innovative drill bits.	63
Figure 51. Acquired Thrust Force signal.	64
Figure 52. Acquired Torque signal.	64
Figure 53. Acquired Acoustic emission RMS signal.	65
Figure 54. Acquired Vibration Acceleration signal.	65
Figure 55. Filtered Thrust Force signal.	66
Figure 56. Start point and end point on the acquired Thrust Force signal.	66
Figure 57. Segmented Thrust Force signal.	67
Figure 58. Segmented Torque signal.	67
Figure 59. Segmented Acoustic Emission RMS signal.	68
Figure 60. Segmented Vibration Acceleration RMS signal.	68
Figure 61. Sensor signal extracted features in the case study A.	69
Figure 62. Sensor signal extracted features in the case study C.	69
Figure 63. Thrust Force Average for traditional twist drill bit $d = 4.85$ mm.	70
Figure 64. Thrust Force Variance for traditional twist drill bit $d = 4.85$ mm.	70
Figure 65. Thrust Force Skewness for traditional twist drill bit $d = 4.85$ mm.	71
Figure 66. Thrust Force Kurtosis for traditional twist drill bit $d = 4.85$ mm.	71
Figure 67. Fibre cutting angle variations during CFRP drilling.	72
Figure 68. Diverse fiber orientations simultaneously along the cutting edge.	72

<i>Figure 69. Single-Sided Amplitude Spectrum of the Thrust Force signals acquired in drilling tests at 3000 rpm, 0.15 mm/rev.</i>	<i>73</i>
<i>Figure 70. Evolution of peaks detected in frequency domain using discrete Fourier Transform</i>	<i>73</i>
<i>Figure 71. Segmented and filtered thrust force signal with separation line for Aluminium drilling portion and CFRP drilling portion.....</i>	<i>74</i>
<i>Figure 72. Sensor signal extracted features in the case study B.....</i>	<i>75</i>
<i>Figure 73. Scree plot reporting the variance explained as a function of the principal components for all the drilling tests.</i>	<i>78</i>
<i>Figure 74. Scores of the first principal component, PC1, and measured tool wear values, VB, vs hole no. for test T3 ($v = 6000$ rpm, $f = 0.15$ mm/rev).</i>	<i>79</i>
<i>Figure 75. ANN architecture proposed in the case study A.</i>	<i>80</i>
<i>Figure 76. ANN architecture proposed in the case study C.....</i>	<i>81</i>
<i>Figure 77. RMSE prediction performance of the ANN trained with diverse numbers, m, of SFPVs for the tests with traditional drill bits.....</i>	<i>81</i>
<i>Figure 78. RMSE prediction performance of the ANN trained with diverse numbers, m, of SFPVs for the tests with innovative drill bits.</i>	<i>82</i>
<i>Figure 79. Worst case ANN forecast: experimental tests at 2700 rpm – 0.11 mm/rev with innovative drill bit.</i>	<i>83</i>
<i>Figure 80. Best case ANN forecast: experimental tests at 6000 rpm – 0.20 mm/rev with innovative drill bit.</i>	<i>83</i>
<i>Figure 81. Regression plot between ANN predicted and measured VB for test $v = 6000$ rpm, $f = 0.15$ mm/rev. ANN configuration: 3-3-1. RMSE = 4.09E-04.</i>	<i>85</i>

List of Tables

<i>Table 1. Comparison between main properties of Ti6Al4V and steel (Donachie 1983).....</i>	<i>22</i>
<i>Table 2. Characteristics of the force sensor (Teti et al. 2006).....</i>	<i>26</i>
<i>Table 3. Technical characteristic of 3D force sensor amplifier.....</i>	<i>27</i>
<i>Table 4. Technical specifications of Acoustic Emission sensor Montronix BV-100.</i>	<i>28</i>
<i>Table 5. Technical specifications of AE amplifier Montronix TSVA2-DGM-BV.....</i>	<i>29</i>
<i>Table 6. Technical specifications of transmission unit.</i>	<i>30</i>
<i>Table 7. Technical specifications of Spectra Pulse Vibration Sensor.....</i>	<i>31</i>
<i>Table 8. Technical characteristic of digitizing board NI USB-6361.....</i>	<i>32</i>
<i>Table 9. Cutting conditions employed in the experimental campaign.</i>	<i>33</i>
<i>Table 10. Verification of correlations based on Pearson correlation coefficient.</i>	<i>45</i>
<i>Table 11. Overall Mean Square Error (MSE) obtained by ANN tool wear reconstruction for all the turning tests carried out at $v = 60$ m/min.....</i>	<i>46</i>
<i>Table 12. Summary of the experimental setup for drilling case studies.....</i>	<i>51</i>
<i>Table 13. Chemical composition of the Aluminium 2024 alloy.....</i>	<i>56</i>
<i>Table 14. Physical, mechanical and thermal properties of the Aluminium 2024 alloy.</i>	<i>57</i>
<i>Table 15. Experimental testing conditions for case studies A and C.</i>	<i>58</i>
<i>Table 16. Experimental testing conditions for case study B.</i>	<i>58</i>
<i>Table 17. List of most correlated features (case study B).</i>	<i>77</i>
<i>Table 18. Overall Root Mean Square Error (RMSE) obtained by ANN tool wear estimation for all the drilling tests.</i>	<i>84</i>

1. Introduction

The research activities presented in this thesis are focused on the development of smart sensor monitoring procedures applied to diverse machining processes with particular reference to the machining of difficult-to-cut materials. This work will describe the whole smart sensor monitoring procedure starting from the configuration of the multiple sensor monitoring system for each specific application and proceeding with the methodologies for sensor signal detection and analysis aimed at the extraction of signal features to feed to intelligent decision-making systems based on artificial neural networks. The final aim is to perform tool condition monitoring in advanced machining processes in terms of tool wear diagnosis and forecast, in the perspective of zero defect manufacturing and green technologies.

The work has been addressed within the framework of the national MIUR PON research project CAPRI, acronym for “Carrello per atterraggio con attuazione intelligente” (Landing Gear with Intelligent Actuation), and the research project STEP FAR, acronym for “Sviluppo di materiali e Tecnologie Ecocompatibili, di Processi di Foratura, taglio e di Assemblaggio Robotizzato” (Development of eco-compatible materials and technologies for robotised drilling and assembly processes). Both projects are sponsored by DAC, the Campania Technological Aerospace District, and involve two aerospace industries, Magnaghi Aeronautica S.p.A. and Leonardo S.p.A., respectively. Due to the industrial framework in which the projects were developed and taking advantage of the support from the industrial partners, the project activities have been carried out with the aim to contribute to the scientific research in the field of machining process monitoring as well as to promote the industrial applicability of the results.

The thesis was structured in order to illustrate all the methodologies, the experimental tests and the results obtained from the research activities. It begins with an introduction to “Sensor monitoring of machining processes” (Chapter 2) with particular attention to the main sensor monitoring applications and the types of sensors which are employed in machining. The key methods for advanced sensor signal processing, including the implementation of sensor fusion technology, are discussed in details as they represent the basic input for cognitive decision-making systems construction. The chapter finally presents a brief discussion on cloud-based manufacturing which will represent one of the future developments of this research work.

Chapters 3 and 4 illustrate the case studies of machining process sensor monitoring investigated in the research work. Within the CAPRI project, the feasibility of the dry turning process of Ti6Al4V alloy (Chapter 3) was studied with particular attention to the optimization of the machining parameters avoiding the use of coolant fluids. Since very rapid tool wear is experienced during dry machining of Titanium alloys, the multiple sensor monitoring system was used in order to develop a methodology based on a smart system for on line tool wear detection in terms of maximum flank wear land. Within the STEP FAR project, the drilling process of carbon fibre reinforced (CFRP) composite materials was studied using diverse experimental set-ups. Regarding the tools, three different types of drill bit were employed, including traditional as well as innovative geometry ones. Concerning the investigated materials, two different types of stack configurations were employed, namely CFRP/CFRP stacks and hybrid Al/CFRP stacks. Consequently, the machining parameters for each experimental campaign were varied, and also the methods for signal analysis were changed to verify the performance of the different methodologies. Finally, for each case different neural network configurations were investigated for cognitive-based decision making. First of all, the applicability of the system was tested in order to perform tool wear diagnosis and forecast. Then, the discussion proceeds with a further aim of the research work, which is the reduction of the number of selected sensor signal features, in order to improve the performance of the cognitive decision-making system, simplify modelling and facilitate the implementation of these methodologies in a cloud manufacturing approach to tool condition monitoring.

Sensor fusion methodologies were applied to the extracted and selected sensor signal features in the perspective of feature reduction with the purpose to implement these procedures for big data analytics within the Industry 4.0 framework. In conclusion, the positive impact of the proposed tool

condition monitoring methodologies based on multiple sensor signal acquisition and processing is illustrated, with particular reference to the reliable assessment of tool state in order to avoid too early or too late cutting tool substitution that negatively affect machining time and cost.

2. Sensor monitoring of machining processes

In the last years many studies showed that the availability of real-time data regarding the process operating conditions is the base of the success of modern flexible manufacturing systems. Due to the difficulties to find reliable models of production systems performance prediction it is necessary to assemble improved multiple sensors systems and to develop more sophisticated techniques for processing the sensor data output, in order to increase the efficiency of the actual monitoring systems employed for process monitoring and control of production.

Several authors of recent research studies have shown the effectiveness of sensor monitoring techniques based on the signal analysis (Teti et al. 2010). The aim of sensor monitoring is to increase the machining information reliability in order to make proper diagnosis about the status of the process through the selection of the appropriate features.

2.1 Sensor Monitoring Applications

Advanced monitoring of machining operations may have several objectives such as tool condition monitoring (TCM), surface integrity, process conditions monitoring, chip form classification and monitoring of the machine tool state (Teti et al. 2010).

2.1.1 Tool conditions

The following list summarizes some of the most important and notable applications in tool condition monitoring:

- Analysis of acoustic emission (AE) using the wavelet packet decomposition method (WPD) for automatic classification of tool wear in milling (S. Wu et al. 2014).
- Development of correlations in broaching between tool conditions and output signals of multiple sensors, i.e. AE, vibration, cutting force, hydraulic pressure and spindle power of the broaching machine, mounted on the machine tool (Dragos A Axinte and Gindy 2003). The spindle power signal was used for tool condition monitoring in milling, drilling and turning, it turned out to be successful in continuous turning and drilling but not efficient in discontinuous milling.
- Application to identify real-time tool breakage in milling operations based on the analysis of indirect measurements of cutting force through feed drive AC motor current (JM Lee et al. 1995).
- Development of a laser displacement meter for online tool geometry (Ryabov, Mori, and Kasashima 1996).
- Development of an online tool condition monitoring system based on vibrations and cutting forces monitoring (D. Dimla and Lister 2000).
- Online estimation of drill wear during drilling operations based on spindle motor power signal (H. Y. Kim et al. 2002).
- Use of micro-scale thermal imaging to identify effects of steel machinability on cutting zone temperature and related tool wear mechanisms (Arrazola et al. 2008).
- Analysis and comparison of cost effective methods for tool breakage detection by performing trials on ultra-precision micro-milling machine (Gandarias et al. 2006).

2.1.2 Surface integrity

Concerning monitoring and control of surface integrity in manufacturing processes, a number of applications and studies have been developed. The most remarkable are illustrated below:

- Online estimation of surface roughness (Ra) and dimensional deviation (DD) in turning using neural network. Cutting feed, depth of cut and two components of the cutting force (the feed and radial force components) appears to be the most significant features to be monitored (Azouzi and Guillot 1997).
- Correlation of surface and cutting force in end milling processes based on a statistical approach (Huang and Chen 2003).
- Prediction of surface roughness in turning based on cutting vibration parameters and FFT analysis (Abouelatta and Mád1 2001).
- Decomposition of the vibration signals for in-process prediction of surface roughness in turning based on singular spectrum analysis (Salgado et al. 2009).
- Real-time surface roughness prediction and machining trouble during cutting operation through time series analysis of vibration acceleration signals measured (Song et al. 2005).
- Assessment of machined surface quality after broaching, in terms of geometrical accuracy, burr formation, chatter marks and surface anomalies, based on the monitoring of multiple sensors signals, i.e. acoustic emission, vibration and cutting force. Cutting force in broaching proved to be efficient in detecting of small surface anomalies (Dragos Axinte et al. 2004).
- Development of a real-time monitoring system in hard machining to correlate AE parameters and white layer, surface finish and tool wear. The results showed that AERMS, frequency and count rate seems to be correlated with white layer formation and therefore suitable to monitor surface integrity factors (Guo and Ammula 2005).
- Recognition of grinding burns in cylindrical plunge grinding processes through AE signal analysis (Kwak and Song 2001).
- Real-time surface roughness prediction method based on a simple linear regression model using the displacement signal of spindle motion (Chang et al. 2007).
- Process monitoring in abusive broaching and milling of difficult-to-machine aerospace materials for surface anomalies detection based on AE signals and cutting force data (D Axinte et al. 2005; Marinescu and Axinte 2009).
- Analysis of the dynamics of broaching of complex part features. Inclined chatter surface marks, because of cutting edges specific geometry were linked through force and acceleration signal analysis revealed (D A Axinte 2007).
- Detection of workpiece surface discontinuities during multiple cutting edge machining through an array of three AE sensors (A. Axinte, Natarajan, and Gindy 2005; Marinescu and Axinte 2008).
- Determination of the cutting speed and feed rate effect on the quality of drilled holes in carbon fibre composites through cutting forces and temperature analysis (Rawat and Attia 2009).

2.1.3 Process conditions

The monitoring of process conditions represents another relevant aspect concerning the machining process analysis. Below are reported important applications and developments:

- Classification of drilling operations in normal and abnormal, e.g. tool breakage or missing tool, based on spindle power signals (Brophy, Kelly, and Byrne 2002).
- Fault detection method in tapping under different fault conditions based on torque and radial force (Mezentsev et al. 2002).

- Development of an online machining monitoring system for machining operations of aero engine materials experimentally validated on PXI and LabVIEW platforms (Shy, Axinte, and Gindy 2007).
- Development of a process monitoring system in Al alloy milling based on sound energy sensors, frequency analysis and cognitive processing of audible sound signal features to identify variable process conditions (Rubio and Teti 2009).
- Implementation of a generalised internet-based process monitoring facility for process optimisation and simulation forming a Remote Machine Monitoring System (RMMS) (Chen et al. 2002).
- Development of an online polishing expert system based on AE signals integrated with a multiple sensor system which can detect in real time polishing status and subsequently adjust the polishing parameters initially set (Ahn et al. 2001).
- Assessment of cutting variables, such as shear angle, chip thickness, tool vibration amplitude, strain, strain rate, and chip type in orthogonal turning tests using high speed photography combined with laser printed square grid (Pujana, Arrazola, and Villar 2008).
- Development of an innovative non-stationary process condition monitoring method based on time-frequency distribution analysis and a singular value decomposition approach (Gu, Ni, and Yuan 2002).

2.1.4 Chip form

As regards the applications developed for chip conditions, the following papers illustrates effective applications:

- Filtered AE spectrum employ components for chip form classification (Govekar, Gradisek, and Grabec 2000).
- Monitoring method based on neural network and spindle motor power to detect the state of chip disposal in drilling (H. Y. Kim et al. 2002).
- Chip form recognition based on wavelet packet transform (WPT) and spectral estimation of cutting force signals (Teti et al. 2006).
- Chip form characterization (chip entanglements, chip size, and chip shape) under different dry cutting conditions using geometric transformations of the control variables (Venuvinod and Djordjevich 1996).
- Development and testing of a system for the automatic chip breaking detection using frequency analysis of cutting forces (Andreasen and De Chiffre 1998).

2.1.5 Machine tool state

Finally, as far as machine tool state monitoring, the main applications studied and developed are the followings:

- Detection and comparison between characteristic parameters of signals available in controlled drives (position, speed and motor current) and the current ones (Verl et al. 2009).
- Design and implementation of an integrated intelligent monitoring system, with modular and reconfigurable structure. This system monitors a total of 72 diagnostic features (power, vibration, temperature and pressure of the drives and spindles) (Zhou et al. 2000).
- Condition monitoring technique based on vibration, acoustic emission, Shock Pulse Method (SPM) and surface roughness for fault detection of critical subsystems identified by a failure frequency analysis (Saravanan, Yadava, and Rao 2006).

2.1.6 Other applications

The sensor monitoring could be also used for other objectives. One of these further applications is the monitoring of energy consumption, especially in the green technology perspective several models were developed in order to evaluate the energy efficiency through the monitoring of energy consumption with the aim to avoid excessive waste of energy resources (Herrmann and Thiede 2009; Hu et al. 2012; Diaz et al. 2009; Vijayaraghavan and Dornfeld 2010).

Another application of the sensor monitoring systems concerns the machine maintenance. One study is focused on the implementation of monitoring system in order to perform a proactive maintenance instead of the traditional reactive sensor-based maintenance (Jay Lee 1995). Moreover, a review of methods and systems for diagnostic and prognostic of mechanical systems through condition-based maintenance paradigm allows to compare the different models, algorithms and technologies for data processing and maintenance decision-making (Jardine, Lin, and Banjevic 2006).

2.2 Sensors for machining process monitoring

The optimization of the machining process performance is the purpose of the application of sensors in machining processes to continuously monitor the manufacturing operations. This monitoring is done through diverse measuring techniques that can be distinguished as direct and indirect approaches.

Referring the techniques to the measurement of the actual quantity of a given variable, e.g. tool wear, is has the direct techniques. Other examples of direct measurement techniques applicable to monitoring of machining processes are the use of cameras for visual inspection, radioactive isotopes, laser beams, and electrical resistance. These type of technique may be limited by the access problems during machining, illumination and the use of cutting fluid so they remain confined only to laboratory environments. However, the direct measurement techniques are highly accurate and for this reason are extensively employed in research laboratories to monitor fundamental measurable variables during the machining processes.

Concerning the indirect measurement techniques, the actual quantity of a measured variable is correlated to an auxiliary quantity through an existing correlation. For this reason they are less accurate compared to direct method but give the advantage of being less complex to apply in the machining process and more appropriate to use in the industrial environments.

2.2.1 Motor Power and Current

Electric drives and spindles provide the mechanical force for material removal from the workpiece. The measurement of motor power or current or other motor related parameters can give some information about process and tool conditions. It is important that the embedded devices employed to monitor the motor related parameter do not influence negatively the machining process, it is possible to measure power through the drive control loop, particularly interesting in production environment (G. Byrne et al. 1995).

A cheap and economical monitoring solution in machining operations is retrofit power measurements. Nowadays the direct access to motor power and motor current signals using numerical controller is ensured by the most recent control systems (Oliveira et al. 2008). Recently there is the development of software integrated in the CNC control with the aim to improve the use of Human Machine Interface (HMI). The internal control signals and the additional sensors, now implemented in the machines, are based on the extension of Adaptive Control Optimise (ACO) and Adaptive Control Constraint (ACC) algorithms (Klocke, Wirtz, and Veselovac 2009). Power

measurement is already enabled in the drive controller and is adequate for use in the machining environments (G. Byrne et al. 1995). The power measurement technology leads to the application of another technique in order to demonstrate high quality signal information for process condition monitoring (Pritschow and Kramer 2005)

2.2.2 Force and torque

The mechanical machining processes require the application of mechanical forces in order to separate and remove the material from the raw workpiece. So the monitoring of cutting forces is essential for the process condition identification, cutting tool failure detection and workpiece quality assessment (G. I. Byrne, Dornfeld, and Denkena 2003). Similarly to the cutting force, also the measurement of the torsional applied load, measured by torque sensors, could be useful for the process characterization. Even though the measurement technology is the same, the application and the method of signal transmission of torque and force sensors are quite different. Force and torque sensors are generally used to measure the deformation of an elastic element and convert it into the applied force element or torsional load. The types of sensors employed for these acquisitions can be divided into two basic groups: piezoelectric and strain based sensors.

For direct force measurement, piezoelectric sensors should be mounted in line with the force path, multicomponent force transducers are employed where flexibility requirements exist such as experimental laboratory environments. Other types include rotating cutting force dynamometers that are able to acquire torque and the three components of the force. These devices have been used in monitoring of high speed milling where the speed is up to 20,000 rpm. Nowadays the integration of force and torque sensors in the CNC structure is increasing especially in drilling (G. Byrne and O' Donnell 2007) and milling (Qiao and Zhu 2012) machine tools. Figure 1 shows an integrated force sensor ring in the motor spindle, for the integration is required the isolation of the process phenomena from spindle and machine dynamics (Jun et al. 2002; Korkut 2003).

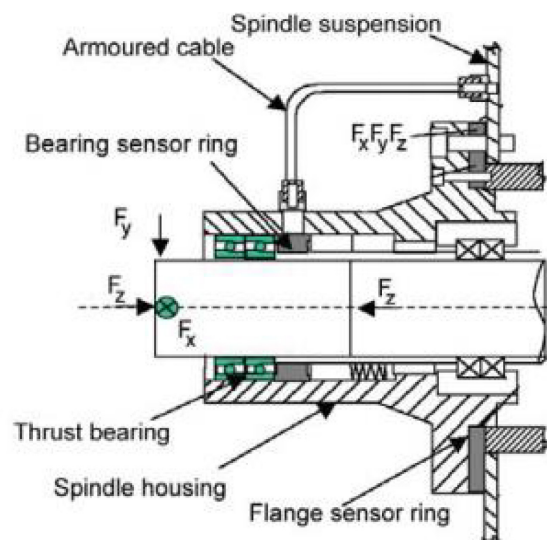


Figure 1. Spindle motor with integrated sensor ring (G. Byrne and O' Donnell 2007)

The strain gauges are considered stable and offer reasonably high frequency response, they are force sensors which deform when a force is applied. An application for the acquisition of static and dynamic forces is developed by combining strain gauges and piezoelectric sensor into a single instrument (J. Kim and Kim 1997). Another application provides the detection and measurement of the three cutting components of the force during milling, this is ensured by the development of a

strain based force sensor (Korkut 2003). Also on the development of a strain based sensor is based another application in which this sensor is placed between the cutting tool and the tool holder for conventional milling monitoring (Smith, Smith, and Tlustý 1998).

2.2.3 Acoustic emission

The acoustic emission (AE) is also measured and acquired during the machining processes, in order to do this measurement the piezoelectric sensor is one of the most adequate technology (Rogers 1979). Wide bandwidth is required in order to detect a big part of the phenomena in machining (100 to 900 kHz), it could be also used as root mean square (RMS) signal in order to reduce the dimension of the data to manage (X. Li 2002).

The principles to detect and monitor AE signals are based on capacitance or piezoelectric. In the first case the capacitance in the sensor changes as the distance between two parallel plate changes. This technique is considered highly accurate especially for the calibration of other AE sensors but these sensors are highly sensitive and are highly affected by position and mounting so they are inadequate in monitoring machining processes where the operating environment is harsh (Hundt et al. 1994). In the second case the piezoelectric thin film sensor is placed between the cutting insert and the tool holder, this makes the sensor more sensitive to changes due to the fact that is very closely located to the cutting process and it is also characterized by a very large frequency bandwidth.

The use of fibre optics allows to develop alternative and innovative approach (Carolan et al. 1997a, 1997b), the main advantage of this method is constituted by the fact that is a no contact method and it allows the transmission of the signal between the source and the sensor, this technology has other several strengths such as flat frequency, absolute calibration and the broader bandwidth compared to the other conventional methods. However the piezoelectric thin film sensor and fibre optics based AE sensor types have been extensively employed in laboratory environments but not yet in industrial contexts.

Regarding the AE signals, they are characterized by high frequency and low amplitude and this makes these signals suitable for transmission through a coupling fluid. As a matter of fact if the sensor is placed on the coolant supply nozzle, the coolant represents the transmission mechanism (Inasaki 1998). This application is also used with a nonintrusive coupling fluid to link the AE sensor to the spindle drive shaft (Hutton and Hu 1999; X. Li, Dong, and Yuan 1999). The method of coupling fluid is suitable in milling, drilling and other machining processes with rotating cutting tools.

It reports slip rings, inductive coupling and radio frequency transmission between the other available techniques for signal transmission and coupling between the AE sensor and the AE signal processor (Karpuschewski, Wehmeier, and Inasaki 2000; Inasaki 1998). Another research study proposed that the AE signal should be continuously reflected by the inner surfaces of the structure where the AE sensor is mounted (Krzysztof Jemielniak 2001).

2.2.4 Vibration

In the wide variety of devices to detect vibrations, the piezoelectric transduction is the most commonly employed in the machining operations. The vibrations generated during metal cutting can be considered dependent or independent from the cutting process. For example the vibration generated by other machines or by machine components are considered independent from the machining process. Instead the interrupted cutting can be considered as vibrations derived from metal cutting. As mentioned before the conditions of the cutting tool determine the aspect of the signals acquired so they have a significant impact also on the vibrations produced; chatter, which

is defined as self-excited vibration, is one of the common known types of vibration in machining, it is very destructive and negatively affects surface finish and tool life.

2.2.5 Other sensors

Beyond the most employed sensors in the machining process monitoring there are several other types which have been studied and used by the researchers in the same field of applications:

- micro sensors for temperature measurements in the cutting tool insert (Biermann et al. 2013; Yang et al. 2014).
- Other devices for temperature monitoring and measurement (Davies et al. 2007)
- Vision systems for tool condition monitoring based on temperature measurement (Kurada and Bradley 1997; Pittalà and Monno 2011)
- Lasers for cutting edge profile measuring of cutting tool in milling (Ryabov, Mori, and Kasashima 1996).
- Strain and temperature sensors (Shinno and Hashizume 1997).
- Sound and image analysis (Mannan, Kassim, and Jing 2000).
- Ultrasound techniques (Abu-zahra and Yu 2000).
- Laser light with reflected light intensity measurement (Wong et al. 1997).
- Bifurcated optic fibre with reflected light intensity measurement (Choudhury, Jain, and Rama Rao 1999).

2.3 Advanced sensor signal processing methods

The sensor signals properly acquired can be used to extract a proper number of sensor signal features (SFs) which are indicative of the machining process state. The features extracted can be correlated to the monitoring output, e.g. tool wear and process conditions (D. S. Dimla 2000; Sick 2002; X. Li 2002).

In Figure 2 is illustrated the sequence of the actions which can be done in order to apply the advanced signal processing methodology. In the first stage there are the signal pre-processing operations (filtering, amplification, A/D conversion, and segmentation), if it is necessary in this stage the signal transformation into frequency or time-frequency domain happens (Fourier Transform, wavelet transform, etc.). In the next stage the features are extracted and in the last stage the features selection takes place because there are many diverse descriptors from different sensor signals so it is important to identify the most relevant for process description. Finally they will be integrated into the tool or process condition diagnosis system.

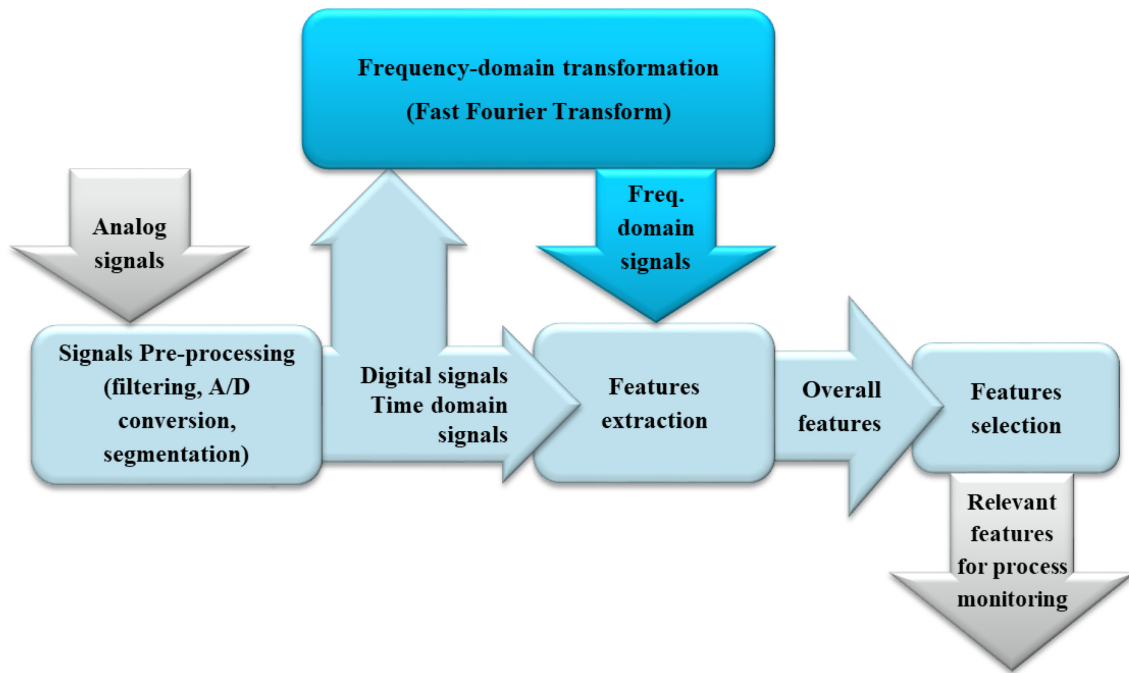


Figure 2. Advanced signal processing procedure (Teti et al. 2010)

2.3.1 Signal conditioning and pre-processing

Analogue signals require pre-processing operations in order to be converted into digital signals. The conditioning procedure is applied at each sensor (e.g. charge amplifier, piezotron coupler, etc.).

The piezoelectric AE sensor, the dynamometers and the accelerometers which are located close to the cutting zone have high impedance and they should be connected to an amplifier. The buffer amplifier transforms the raw voltage signal derived from the sensor in a proportional voltage signal. The filtering is necessary in order to avoid high frequency noise on the analogue signal.

The proper sampling frequency of the raw AE signals could reach 1MHz, so high sampling frequency is required (>1 MS/s) or could be necessary to perform a Root Mean Square operation on the raw signal in order to acquire the AERMS signal which require cheaper devices.

All signals are amplified before the A/D conversion in order to achieve the best possible accuracy. Moreover with the aim to reduce the frequency bands that are not related to the analysed process, digital filtering could be necessary. The digital filters could be also interesting in order to extract some features, for example was proposed an application to investigate the signal features characterizing the tool wear in interrupted turning through the application of digital filters to divide cutting force signals into two frequency ranges (Scheffer and Heyns 2004). Another application using a low-pass filter of cutting force signals was proposed in order to detect the catastrophic tool failure in turning (Jemielniak & Szafarczyk, 1992). In several applications, a digital signal filtering is necessary to avoid signal oscillations and high frequency noise (Ghosh et al. 2007; X. Li, Ouyang, and Liang 2008).

The pre-processing methods comprehend also the segmentation which is the operation that allows to remove the transient portion of the signal in order to preserve only the steady portion in which the machining is in progress. This is the only part of the signal on which will be performed the feature extraction because the tool is removing the material from the workpiece and the signal reports important information on the tool and process conditions (Bhattacharyya, Sengupta, and Mukhopadhyay 2007; Marinescu and Axinte 2008).

2.3.2 Signal feature extraction

2.3.2.1 Time domain

In the time domain a certain number of SFs can be extracted that will be selected based on their ability to describe the signal and preserve the information related to the process and tool conditions.

The most common features extracted in the time domain are:

- arithmetic mean, average value, magnitude (Dong et al. 2006; Salgado and Alonso 2006; Sick 2002; Ghosh et al. 2007);
- effective value (root mean square) (Sick 2002; Ghosh et al. 2007);
- conventional statistical features:
 - ✓ variance (or standard deviation) (Scheffer and Heyns 2001; Guo and Ammala 2005; Dong et al. 2006; Ghosh et al. 2007);
 - ✓ skewness (Al-Habaibeh and Gindy 2000; Zhu, Wong, and Hong 2009; Dong et al. 2006; Salgado and Alonso 2006);
 - ✓ kurtosis (Binsaeid et al. 2009; Al-Habaibeh and Gindy 2000; Zhu, Wong, and Hong 2009);
 - ✓ signal power (Al-Habaibeh and Gindy 2000; Bhattacharyya, Sengupta, and Mukhopadhyay 2007; Binsaeid et al. 2009);
- peak-to-peak range, or peak-to-valley amplitude (Sick 2002; Scheffer and Heyns 2004; Al-Habaibeh and Gindy 2000; Ghosh et al. 2007);
- crest factor (Sun et al. 2004; Scheffer and Heyns 2001; Sick 2002; Dong et al. 2006);
- ratios of the signals, signal increments (René de Jesús et al. 2004; Sick 2002).

There are some signal features relevant only for vibration and acoustic emission signals:

- ring down count or pulse rate, i.e. the number of times the AErms signal exceeds the threshold level (Krzysztof Jemielniak 2000; Kwak and Song 2001; Sick 2002; Guo and Ammala 2005);
- pulse width, i.e. the percentage of time during which AErms remains above the threshold level (Krzysztof Jemielniak, Kwiatkowski, and Wrzosek 1998; Krzysztof Jemielniak 2000);
- burst rate, i.e. number of times AERMS signal exceeds pre-set thresholds per second (Krzysztof Jemielniak 2000; X. Li 2002; Binsaeid et al. 2009);
- burst width, i.e. percentage of time AERMS signal remains above each threshold (Krzysztof Jemielniak, Kwiatkowski, and Wrzosek 1998; Krzysztof Jemielniak 2000).

The reported features are very useful for the detection of the catastrophic tool failure (K Jemielniak 1998) and for the monitoring of the cutting tool flank wear (Kannatey-Asibu Jr and Dornfeld 1982).

2.3.2.2 Frequency domain

Usually the discrete Fast Fourier Transform method (FFT) is used to perform the signal features extraction in the frequency domain. This method needs the conversion of the signals from their original domain (time or samples domain) to the frequency domain and this is performed using the Discrete Fourier Transform (DFT). The main aim behind FFT is to give an inside view of the process. An example would be its use for tool wear influences (Prakash, Kanthababu, and Rajurkar 2015).

The signal features usually taken into consideration are:

- amplitude of dominant spectral peaks (Kwak and Song 2001; Sick 2002; Marinescu and Axinte 2008; Binsaeid et al. 2009);
- signal power in particular frequency ranges (Govekar, Gradisek, and Grabec 2000; Krzysztof Jemielniak 2000; Sick 2002; Sun et al. 2004; Binsaeid et al. 2009);
- energy in given frequency bands (Altintas and Park 2004; Scheffer and Heyns 2001; Marinescu and Axinte 2008);

- statistical characteristics of band power spectrum: mean frequency, variance, skewness, kurtosis (Binsaeid et al. 2009);
- frequency of the spectrum highest peak (Abouelatta and Mädl 2001; Sick 2002; Guo and Ammula 2005).

The FFT provides all the frequency components over the entire signal duration, but due to the dynamic rather than static behaviour of the signals this is not completely suitable. The Short Time Fourier Transform can be usefully adopted to make a time-frequency analysis and to analyse the frequency components in different time intervals using a sliding window. For this sample of data, spectral coefficients are calculated and the window is moved to a new position where the calculation procedure is repeated. This method allows to obtain information along different consecutive short time intervals and, consecutively, put them together. The Short Time Fourier Transform was applied in milling operations to acoustic emission signals to identify tool and workpiece failures (Marinescu and Axinte 2008, 2009).

Using the Short Time Fourier Transform is not possible to obtain high time and frequency resolution at the same time so with the aim to overcome the problem of the window width was introduced the wavelet transform (Mallat 1989; Daubechies 1990). According to the frequency values to be investigated, the authors use different windows, wide windows are used for low frequencies analysis while narrow windows are used for high frequencies.

Nowadays there are several cases in literature that report the use of wavelet transform for the machine condition monitoring (Liu, Li, and Shen 2014; Kungpeng, San, and Soon 2012), flank wear estimation (Kamarthi and Pittner 1997; Kamarthi, Kumara, and Cohen 2000), tool failure and breakage (Hong, Rahman, and Zhou 1996; Tarnng and Lee 1999; Kwak 2006) very often in combination with neural network (Tansel, Mekdeci, and McLaughlin 1995).

Through discrete wavelet transform (DWT), the original signal may be decomposed into scaling coefficients and wavelet coefficients representing the signal convolution and its impulse response to the filters applied.

The coefficients obtained using wavelet transform method are considered and treated as signals from which, it is possible to extract significant features:

- average (Y. Wu and Du 1996; Hong, Rahman, and Zhou 1996);
- crest factor (Y. Wu and Du 1996; Scheffer and Heyns 2001);
- kurtosis (Teti et al. 2006; Y. Wu and Du 1996; Scheffer and Heyns 2001);
- peak-to-peak and peak-to-valley values (Y. Wu and Du 1996; Teti et al. 2006);
- Root Mean Square (Teti et al. 2006);
- standard deviation and variance (Grzesik and Bernat 1998; Y. Wu and Du 1996; Teti et al. 2006).

2.3.3 Signal feature selection

As mentioned before not all the extracted SFs will be used to describe the process conditions but it is necessary to apply a proper selection methodology in order to obtain only the most relevant features. The number of the selected features should be appropriate in order to avoid possible disturbances caused by any single SF. Some decision making systems, such as neural networks, require large number of training samples when faced with a bigger number of features (Hong, Rahman, and Zhou 1996). If the system should work after the first training session, a large number of SF inputs might not be adequate due to the fact that the amount of training samples is not big enough (Krzysztof Jemielniak 2000). Therefore, the SFs selection procedure may be able to maintain the relevant system information by eliminating repeated or irrelevant SFs, the application

of this methodology in the industrial contexts leads to a minimum operator intervention, i.e. the selection of the relevant SFs should be automatic.

As concern tool wear condition monitoring, the Pearson correlation coefficient r and the Spearman correlation coefficient r_s have been used to find the features that can best identify the measured values (Quan, Zhou, and Luo 1998; Hauke and Kossowski 2011). The correlation coefficient (r) represents the correlation between a selected feature (x) and a tool wear value (y), where \bar{x} and \bar{y} represent the average values:

$$r^2 = \frac{(\sum_i (x_i - \bar{x})(y_i - \bar{y}))^2}{\sum_i (x_i - \bar{x})^2 \sum_i (y_i - \bar{y})^2}$$

The Spearman correlation coefficient is defined as the Pearson correlation coefficient between the ranked variables. For a sample of size n , the n raw scores X_i, Y_i are converted to ranks rgX_i, rgY_i and r_s is computed from:

$$r_s = \frac{cov(rgX, rgY)}{\sigma_{rgX} \sigma_{rgY}}$$

Where $cov(rgX, rgY)$ is the covariance of the rank variables and $\sigma_{rgX}, \sigma_{rgY}$ are the standard deviations of the rank variables.

The correlation coefficient represents the measure of the linear correlation between two variables and it ranges from -1 to +1. Usually, a lower value of r means that that SF is not correlated with the phenomenon, so the probability to select it is low (Scheffer and Heyns 2001, 2004). The tendency is to consider the absolute value of correlation coefficients > 0.7 as good correlated, the values greater than 0.3 and lower than 0.7 as moderate correlated and the values lower than 0.3 as weak correlated.

Automated feature selection methods have a major drawback. The selection of very similar SFs, which are dependent on each other, using these methods is one of the undesired characteristics so the sensor fusion through automated feature selection methods cannot be completed. In such cases, manual intervention of engineers and scientists would be required for feature selection instead of automated methods. Nevertheless the manual procedures or interventions are not appropriate in the industrial applications and they remain confined in the laboratory experimental environments. A method to remove the undesired additional SFs would be calculating the Root Mean Square Error (RMSE), set a threshold and then select the best SFs (Krzysztof Jemielniak and Bombinski 2006; K Jemielniak, Bombin, and Aristimuno 2008; K Jemielniak and Arrazola 2008). Any SFs having an RMSE higher than the set threshold was rejected. Following the most adequate signal features are selected and the ones correlated to them are rejected.

2.4 Decision making systems

The multiple sensor monitoring systems have to be paired with a cognitive decision making systems based on a proper cognitive computing method in order to constitute the complete system to be employed for modern manufacturing systems (Teti and Kumara 1997; Abellan-Nebot and Romero Subirón 2010; Teti et al. 2010). Several paradigms, schemes, and techniques have been developed during the last years with the aim construct decision making support systems based on sensor monitoring and signal features extraction and processing. These cognitive paradigms include, neural networks, fuzzy logic, hybrid systems and more others that can combine different capabilities.

Figure 3 shows the AI approaches applied in machining monitoring systems according to the references found in the research platform ISI-Web of knowledge from 2002 to 2007.

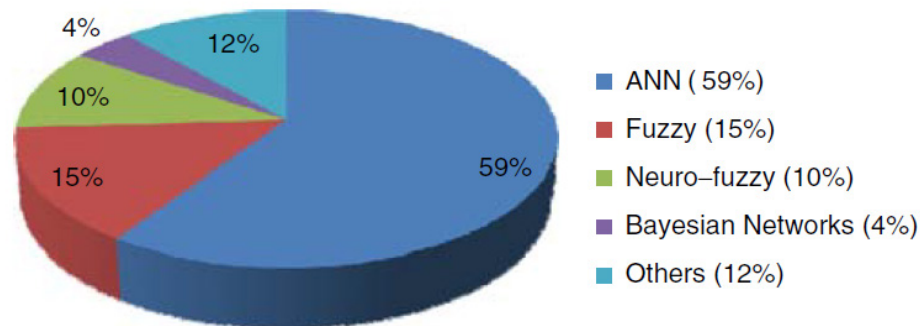


Figure 3. Frequency of usage of AI approaches in intelligent machining systems according to the references found in the research platform ISI-Web of knowledge from 2002 to 2007 (Abellan-Nebot and Romero Subirón 2010).

Machine learning methods can be classified in supervised learning and unsupervised learning methods. Every instance in any dataset used by machine learning algorithms is represented using the same set of features. If instances are given with known labels (the corresponding correct outputs) then the learning is called supervised, in contrast to unsupervised learning, where instances are unlabelled.

Supervised learning is where there are input variables (x) and an output variable (Y) and an algorithm is used to learn the mapping function from the input to the output: $Y = f(X)$.

The goal is to approximate the mapping function so well that, when there is new input data (x), the system can predict the output variable (Y) for that data.

It is called supervised learning because the process of an algorithm learning from the training dataset can be thought of as a teacher supervising the learning process. The correct answers are known, the algorithm iteratively makes predictions on the training data and is corrected by the teacher. Learning stops when the algorithm achieves an acceptable level of performance.

Supervised learning problems can be further grouped into regression and classification problems. A classification problem occurs when the output variable is a category, such as “red” or “blue” or “disease” and “no disease”; a regression problem occurs when the output variable is a real value, such as “dollars” or “weight”.

Some popular examples of supervised machine learning algorithms are:

- Linear regression for regression problems.
- Random forest for classification and regression problems.
- Support vector machines for classification problems.

Supervised learning is typically performed in the context of classification, when it wants to map input to output labels, or regression, when it wants to map input to a continuous output. In both regression and classification, the goal is to find specific relationships or structure in the input data that allow to effectively produce correct output data. Note that “correct” output is determined entirely from the training data, so while it doesn’t have a ground truth that our model will assume is true, it is not to say that data labels are always correct in real-world situations. Noisy, or incorrect, data labels will clearly reduce the effectiveness of the model.

Unsupervised learning is when the algorithm has only input data (X) and no corresponding output variables.

The goal of unsupervised learning is to model the underlying structure or distribution in the data in order to learn more about the data.

This is called unsupervised learning because unlike supervised learning above there are no correct answers and there is no teacher. Algorithms are left to their own devices to discover and present the interesting structure in the data.

The most common tasks within unsupervised learning are clustering, representation learning, and density estimation. In all of these cases, it aims at learning the inherent structure of the data without using explicitly-provided labels. Some common algorithms include k-means clustering, principal component analysis, and autoencoders. Since no labels are provided, there is no specific way to compare model performance in most unsupervised learning methods.

Two common use-cases for unsupervised learning are exploratory analysis and dimensionality reduction. Dimensionality reduction, which refers to the methods used to represent data using less columns or features, can be accomplished through unsupervised methods.

Unsupervised learning problems can be further grouped into clustering and association problems. A clustering problem occurs when it wants to discover the inherent groupings in the data, such as grouping customers by purchasing behaviour. An association rule learning problem occurs when it wants to discover rules that describe large portions of your data, such as people that buy X also tend to buy Y.

Some popular examples of unsupervised learning algorithms are:

- k-means for clustering problems.
- Apriori algorithm for association rule learning problems.

2.4.1 Neural networks

Within machine learning, artificial neural networks (ANNs) are a family of models based on the functioning of the central nervous system such as the brain. The developing and the adjusting of the connections between the neurons (or nodes), which operate in parallel is the base for the computation capability. Neural Network (NN) looks like a map in which input points are associated with their corresponding output points. This correlation between input and output nodes is based on given values, e.g. class membership.

NNs have several positive aspects and they can be summarized in the following list:

- the knowledge domain is based on known examples
- they are able to handle continuous and discrete data
- they have a good generalisation capability

The construction of the NN knowledge is made in the training phase. A typical NN training method is the supervised training, which consist in providing both input and the corresponding output patterns. The error between the output values predicted and the expected ones is used to adjust the weights of the links between the neurons of the network. Feeding the NN only with the input pattern vectors it obtains the unsupervised training, the NN learns and divides these input pattern vectors in groups depending on similarities between them.

There are several supervised learning paradigms. One of those is Backpropagation Neural Network (BPNN), it has been very popular for their performance and is based on the calculation of a loss function according to the descent gradient so it requires a pattern of output values. With the aim to obtain satisfactory results, random distortions to the weight system may be introduced in order to lead the NN performance function in local minima. Considering other supervised NN paradigms there are artificial cellular neural network (ACNN) (Daisuke and Tomoharu 2001), fuzzy logic neural network (FLNN) or neuro-fuzzy inference systems (NFS) which combines the benefits of

both paradigms (Halgamuge and Glesner 1994), probabilistic neural network (PNN) (Specht 1990), recurrent neural network (RNN) (Schmidhuber et al. 2007).

Contrary to supervised learning, in the unsupervised learning methods only inputs are fed to the NN. The NN tends to organise and sort the given data in such a way that the hidden processing nodes respond equally or similarly to closely related group of stimuli which represent distinct real concepts. Several unsupervised learning paradigms exist, between these, the self-organising map (SOM) NN is known for its high performance (Kohonen 1997, 1988). This paradigm uses the input data to create a 2D feature map, keeping the order of the data, if two or more of these input vectors are similar, they will be mapped to close processing elements in the 2D layer representing the features of the input data.

A probabilistic neural network was used for the detection and classification of tool malfunctions in broaching monitoring the cutting force acquired data (Dragos A Axinte 2006). The simulation of the roughing industrial broaching stage was performed using short broaching tools. These trials were carried out to produce square profile slots while detecting cutting force signals.

Simple NN architecture was repeatedly used in turning operation for tool wear evaluation (Bukkapatnam, Kumara, and Lakhtakia 2000; Bukkapatnam et al. 2002; Kamarthi, Kumara, and Cohen 2000). Another applications requires the use of two accelerometers and a monoaxial force sensor to develop an intelligent multi-sensor detection system for milling (Kuljanic, Totis, and Sortino 2009). A combined approach was employed for decision making using artificial cellular neural network for acceleration signals (Daisuke and Tomoharu 2001) and a fuzzy neural network for axial force signals. The NN gave good results for each sensor signal monitoring, the NN outputs were then combined in order to realise the concept of multi-sensor chatter detection. A decision making system was developed for milling process and is based on the spindle motor power monitoring and neural networks paradigm to evaluate the state of chip disposal (H. Kim and Ahn 2002). From the acquired data, selected features were extracted and combined into input vectors to be fed to a feed-forward back-propagation neural network system.

The operators of the machining processes are able to evaluate the process state and the presence of the machining problems thanks to their experience. Audible sound energy appears to be a good sensing technique that could adequately replace operator's experience based knowledge. The techniques based on the audible sound energy are not widely investigated in literature within the process condition monitoring of machining operations but one application was developed in milling analysing the sound energy deriving from band sawing of Al alloy and C steel with the aim to realize an automatic process monitoring system with cheap sensors (Rubio and Teti 2009). A NN approach was then realized and applied; it showed successful results to monitor tool conditions.

2.4.2 Fuzzy logic

Nowadays, fuzzy logic (FL) is used in two different contexts. In the first context, it used as an extension of the many-valued logic (or multi-valued logic), i.e. the infinite-valued logic, but most widely it is associated with the fuzzy set theory (Klir and Folger 1988). A fuzzy set is considered a set without clear boundary. They are an extension of the classical notion of set in which the membership of the elements in a set is assessed in binary terms (1 if the element belongs to the set, 0 otherwise). Instead, the fuzzy set theory introduces the concept of (membership function" as the gradual assessment of the membership of elements in a set. The shape of membership functions may be, most commonly, triangular or trapezoidal, and also rectangular, Gaussian, sigmoidal, etc. In the Figure 4 is illustrated the implementation, step by step, of the most common fuzzy inference system.



Figure 4. Fuzzy inference system implementation steps (Teti et al. 2010).

In order to monitor the cutting force components during turning process a decision making support system based on fuzzy logic was design and it has the objective to estimate the tool wear (Balazinski and Jemielniak 1998; Ren et al. 2015; Roy 2015). The three components the FDSS are: a knowledge base consisting of if-then rules, an inference engine and a user interface. The system consists of the linguistic term set, fuzzy rules and inference engine, and user interface. The decision support system described above allows to accurately assess the tool wear monitoring.

During the quasi orthogonal cutting of metal alloys were extracted features from acoustic emission signals and was performed a frequency analysis, the selected features have been used in a fuzzy logic system for tool wear and workpiece heat treatment monitoring (Teti 1995; Teti and Manzoni 1998). With a success rate higher than 75%, the system results adequate for monitoring scopes.

A fuzzy logic knowledge based system for tool wear monitoring using a genetic algorithm was developed (Achiche et al. 2002), then this system was compared to the classical tool wear estimation approaches (fuzzy logic and neural networks). Finally it can be said that the construction of a fuzzy logic knowledge base system requires appropriate skills and expertise, therefore FL systems are rather difficult and complicated to implement manually. The fuzzy logic knowledge based system may be built using a genetic algorithm to overcome this problem. Furthermore, the system complexity can be set according to the accuracy to be achieved.

2.4.3 Other decision making systems

Genetic algorithms (GA) were considered between the other methods for pattern recognition and decision making. It is a search heuristic inspired by biological phenomena and particularly useful to solve complex problems. To adopt this method, the first step is the development of the computer model able to represent the problem under investigation. Each element of the population was then convert in numerical representation and this is known as chromosome, a binary string. The population was ranked according to the fitness function. For the reproduction and the creation of the new population using genetic operators (e.g. crossover and mutation) the strings that perform the best solutions are selected. Thus, the evolution of the population was performed according to both exploration, i.e. explore the workspace solution, and exploitation, i.e. search in the best solution area already identified. These algorithms are considered to be simple in biology perspective, they are also considered sufficiently complex to catch the complexity of real world problems and provide good solutions.

Between the other decision making systems there are neuro-fuzzy systems and Bayesian networks. Adaptive neuro-fuzzy inference systems are applications where the aim is to add previous knowledge and also to extract hidden knowledge from experimental data in rule-form. In these systems the data set is composed of a medium number of samples and inverse problem has to be solved. Since neuro-fuzzy systems are a hybridisation of ANN and fuzzy systems, the recommended applications are similar to both ANN and fuzzy applications.

Adaptive neuro fuzzy inference system (ANFIS) to predict the effect of the machining variables on the surface finish of Alumic-79 was employed with effective results (Dweiri, Al-Jarrah, and Al-

Wedyan 2003). An adaptive-network based fuzzy inference system (ANFIS) was used to predict the workpiece surface roughness after the end milling process (Lo 2003).

Bayesian Networks are applications where the aim is to add previous knowledge and also to extract hidden knowledge from experimental data in the form of causal relationships and probabilities. These applications are suitable for modelling systems with highly stochastic behaviour and in which the prediction reported is given with an expected uncertainty level. When the experimental data set is composed of a large/very large number of samples depending on the variable discretisation ranges and the expected accuracy these systems are useful to be employed. BN is recommended in highly stochastic machining processes for cutting-tool diagnosis, prediction of part accuracy and the selection of cutting parameters in order to meet part specifications.

One work proposes a multi-sensor system for indirect monitoring of machining processes based on Bayesian Networks (BN) framework, in which classical modelling techniques are compared to BN models in order to show the important advantage and their ability to deal with the stochastic nature of the machining process (Nebot et al. 2007). Another author studied a process monitoring and diagnosis approach based on a Bayesian belief network for incorporating multiple process metrics from multiple sensor sources in sequential machining operations to identify the root cause of process variations and provide a probabilistic confidence level of the diagnosis (Dey and Stori 2005).

2.5 Sensor fusion technology

In monitoring of machining operations, the use of a single sensor and its signal features may not be sufficient to make a reliable diagnosis about the process status. Therefore, the methodology based on the fusion of signals coming from multiple different types of sensors was widely investigated in the literature. The aim of the sensor fusion paradigm is to extract a number of SFs related to the tool and/or process conditions (Segreto, Simeone, and Teti 2014; D. S. Dimla 2000; Sick 2002; X. Li 2002). The combined features allow to obtain more accurate, complete and robust information compared to that obtained using separate sources.

Also the industrial projects investigated the implementation of a multi-sensor fusion concept for process monitoring (Teti et al. 2008; Teti, Segreto, and Harzbecker 2008; Segreto and Teti 2008). Each machining process monitored requires specifically type of sensors, also work materials and monitoring scopes can determine changes in the sensors chosen. Summarizing the sensors employed in these applications include acoustic emission, audible sound, cutting force, motor current, optical and vibration sensors. The monitored machining process are: broaching, drilling, orthogonal cutting, milling, and turning. The materials tested are: composite materials, Ni alloys, Ni–Ti alloys, steels, and Ti alloys. The monitoring scopes investigated are: chip form, machinability, tool wear, process and work material conditions.

The features were extracted from both time and frequency domain and were used to construct a vector which contains the selected signal features belonging to different sensor sources this vector was named Sensor Fusion Pattern Vector (SFPV). The SFPVs represent the data input for pattern recognition paradigms (Duda and Hart 1973).

In reconfigurable multi-sensor monitoring systems, pattern recognition and decision making are provided by the decision making support systems described in the previous paragraph.

The methodology proposed was widely and successfully applied to the neural network approach, e.g. for the cutting of difficult-to-machine materials by monitoring both acceleration and cutting force signals (Nath, Rahman, and Andrew 2007).

The neural network training was realized using three different configurations of signal feature vectors:

- single sensor (single cutting force or acceleration component);
- integration of the three cutting force components or three acceleration components;
- sensor fusion pattern vectors combining cutting force and acceleration feature vectors;

The NN output was composed of coded values for process condition and machinability evaluation. The first configuration provided an accuracy range from 78% to 85%. Accuracy improved notably using the second configuration (92–97%). Finally, the sensor fusion concept implementation allows to obtain the highest accuracy values (99–100%).

Another example of fusion concept could be the combination of force sensor and vision system for online monitoring and detection of tool breakage and tool wear during milling (W. H. Wang et al. 2007). The tool wear estimation was performed taking the images of tool flank during the machining operations. Two features are extracted in-process from the cutting force and appropriately pre-processed. These two features closely indicate flank wear. After each cutting pass, the features extracted from the force sensor signals and the measured flank wear values were fed to a self-organizing map network for the online prediction of the flank wear. Moreover, the detection of tool breakage was performed using the time domain extracted features coming from the force sensor. The empirical findings highlight that this approach is adequate for tool condition monitoring in milling operations and regardless of cutting conditions.

2.6 Cloud manufacturing for machining process monitoring

Machining process monitoring applications in nowadays Industry 4.0 framework can benefit from the implementation of a cloud-based manufacturing process monitoring architecture for on-line smart diagnosis services. Such architecture allows to share process monitoring tasks between different resources, which can be geographically dislocated and managed by actors with different competences and functions. Distributed resources with enhanced computation and data storage capability allow to improve the efficiency of process condition diagnosis and enable more robust decision-making exploiting large information and knowledge sharing. Diagnosis on process conditions is offered as a cloud service, using an architecture where the computing resources in the cloud are connected to the physical manufacturing system realising a complex cyber-physical system using sensor and network communication. Based on sensorial data acquired at the factory level, smart on-line diagnosis on process status is carried out through knowledge-based algorithms and cognitive pattern recognition paradigms. On the basis of the cloud diagnosis, the local server activates the proper corrective action to be taken, such as process halting, parameters change, or tool replacement, sending the right command to the machine tool control (Alessandra Caggiano 2018).

The evolution of modern industrial systems for smart production in the perspective of Industry 4.0 leads to the development of multiple sensors systems integrated in internet communication systems (Cyber-Physical Systems) which can perform monitoring actions. The major contributions to this development coming from the increasing integration of information and communication technologies (ICTs) in the production environment, realising the so-called ‘Smart factories’ (Smit et al. 2016; László Monostori 2014; L. Monostori et al. 2016; L. Wang, Tornngren, and Onori 2015). The environment created by the cloud technologies contributes to the sharing of distributed manufacturing resources including knowledge, computing and software tools, as well as physical resources via the internet networking infrastructure (Zhang et al. 2012; Xu 2012; Tao et al. 2011; B. H. Li et al. 2010).

Cloud manufacturing may be defined as ‘an integrated CPS that can provide on-demand manufacturing services, digitally and physically, at the best utilisation of manufacturing resources’ (L. Wang, Tornngren, and Onori 2015). In this model software and computational resources are managed at the same time of physical resources such as manufacturing facilities and capabilities. This paradigm gives to the user ubiquitous access via cloud to CPPS, including smart machines and large amount of data provided by sensors or generated by intelligent computing, and it may significantly change the way to access and to provide manufacturing services (D. Wu et al. 2015). Diverse authors in the very recent literature have proposed innovative cloud manufacturing applications in order to tackle the main research gaps of the cloud manufacturing paradigm which can be summarized as follow:

- interfaces between cloud and production systems,
- real-time capability of production cloud,
- service-based provision of automation functionalities,
- cloud-based control platforms.

An approach to realise condition-based preventive maintenance of machine tools was developed using advanced monitoring techniques (Mourtzis, Vlachou, Milas, et al. 2016). Another approach for cloud-based adaptive process planning taking into account availability and capabilities of machine tools proposes to gather data from shop-floor machine tools using sensors and input from the operators and machine schedules in order to provide different information about process planning status using the information fusion technique (Mourtzis, Vlachou, Xanthopoulos, et al. 2016). Expanding the cloud computing paradigm to the field of computer-aided design and manufacturing was proposed the concept of Cloud-Based Design and Manufacturing (CBDM) which represents a service-oriented networked product development model (D. Wu et al. 2015). The predictive maintenance through the parallel implementation of machine learning algorithms on the cloud was proposed (D. Wu et al. 2016). Collecting data remotely and dynamically on the shop floor via sensors and data acquisition systems is possible to perform a prognosis of the machining condition to be used as the basis for preventive maintenance planning (Gao et al. 2015).

The machine condition monitoring is actually the main field of application for cloud manufacturing paradigm but there are a lot of other scopes which include monitoring of tool conditions, chip form, process parameters, surface integrity, chatter detection, etc. Cloud-enabled diagnosis in online TCM could constitutes a future development of this research work. It can provide several benefits compared to traditional TCM methodologies because data are remotely and dynamically gathered on the shop floor via sensors and data acquisition systems, already installed on the machines and which will illustrated in the other chapters, while data analysis can be performed in remote, where expert knowhow can be made available and shared in the cloud, realising the knowledge base referenced on-demand by users through the Internet (Alessandra Caggiano 2018).

2.7 Research gap

2.7.1 Gap identification

Nowadays, the importance of TCM is growing due to the increase in the development and employment of sensor monitoring systems as well as the development and integration of machine learning systems for online detection or estimation of tool condition status.

In the literature, a tool wear monitoring system based on ANN was developed with the aim to monitor turning of mild steel (Silva et al. 1998). Other authors used a MATLAB GUI to develop a tool wear detection system for turning of difficult-to-cut materials such as Inconel 718 based on the acquisition of force and vibration components (Mali, Telsang, and Gupta 2017). Acceleration and

vibration signals were analysed to perform an investigation which has the aim to establish the correlations between signal anomalies and chip formation, tool wear and surface roughness which are produced in turning of carbon steel (Bhuiyan, Choudhury, and Dahari 2014). A relevant topic is represented by online monitoring: different techniques for online tool wear detection were studied, one of them is based on optical sensor monitoring in order to feed an artificial neural network (Choudhury, Jain, and Rama Rao 1999), another research study has the aim to estimate tool wear through the employment of fuzzy neural network in turning of steel (Chungchoo and Saini 2002). As regards the online monitoring of dry turning, one study reports the methodology to perform tool wear prediction using adaptive neuro-fuzzy inference system (ANFIS) in dry turning of steel (Rizal et al. 2013).

Some authors discuss about sensor monitoring of drilling process for tool wear detection. Thrust force, torque, motor current signals and process parameters are used to feed artificial neural networks for tool wear evaluation in drilling of mild steel (Sanjay, Neema, and Chin 2005; Patra, Pal, and Bhattacharyya 2007) or copper (Lin and Ting 1996). Machine learning systems are usually employed for process parameters optimization: among the reported research works, one is focused on copper drilling (Kannan et al. 2014) while another one compares different machine learning algorithms with the aim to correlate the process parameters to the acquired sensor signals and surface roughness (Shunmugesh and Panneerselvam 2016) in drilling of CFRP. Features extracted from vibration signals using both time domain analysis and frequency domain analysis were used in order to perform tool wear detection with ANN in drilling of carbon steel (Abu-Mahfouz 2003). Moreover, different machine learning methods were proposed for tool wear prediction in cast iron drilling using thrust force torque and vibration signals (Panda, Chakraborty, and Pal 2008).

2.7.2 Objectives

The reported research works have highlighted the lack in scientific research of a procedure for signal analysis acquired during dry turning of Ti6Al4V, which is widely employed in the aerospace industry, and no methodology for online monitoring of tool wear status during this process is reported. This machining process could be potentially very dangerous due to the nature of the material which is classified as difficult-to-cut and also due to the nature of the machining process, because without lubricant the cutting conditions are more severe. The first objective of this research work is to fill this gap in the research studies, through the development of a proper procedure for tool wear detection through smart sensor signal analysis in dry turning of Ti6Al4V and then to propose the methodology for the implementation of an industrial cognitive system which is able to perform the online tool condition monitoring.

As regards drilling, the literature review highlights the absence of a consistent procedure for tool condition monitoring during drilling of CFRP/CFRP stacks or hybrid Al/CFRP stacks. The importance of tool wear monitoring during these drilling processes was considered crucial due to their large application in the aerospace industry as structural materials, so it is very important to have a strict control on the process behaviour which allows to have a strict control on the products. The second objective of this research work intends to fill this existing gap in the research and in the industrial practice. The development of sensor signal analysis procedures in drilling CFRP/CFRP stack or Al/CFRP stacks was carried out with the aim to build the cognitive systems for tool wear detection and estimation. The final aim, which is represented by the implementation of the cognitive systems in the industrial framework, leads to another development which is the improvement of sensor features selection through features dimensionality reduction in order to integrate these systems in the aerospace industry using the guidelines of Industry 4.0.

3. Smart sensor monitoring of Titanium alloy dry turning

3.1 The framework

In the last few years, manufacturing industries are facing new challenges related to sustainability of their operations, with particular reference to energy and resource efficiency improvement and environmental impact reduction (Duflou et al. 2012). These goals are particularly challenging when dealing with machining of difficult-to-machine materials such as titanium alloys, requiring extensive use of lubricant and coolant fluids which are undesirable in a green technology perspective.

Within the aerospace industry, Ti6Al4V is probably the most widespread titanium alloy, displaying very high tensile strength and toughness at high temperatures combined with low density. The mechanical and thermal properties of Ti6Al4V are reported in Table 1 (Donachie 1983). This alloy has the same tensile strength of steel being 45% lighter, a modulus of elasticity 50% lower than steel, and a very low thermal conductivity (down to 1/5 of steel). Moreover, an allotropic transformation occurs in the titanium structure at 882 °C (beta transus), with change from alpha titanium (EC structure) to the more deformable beta titanium (CCC structure) (Donachie 1988, 1983).

Properties	Ti6Al4V	Steel
Density (g/cm ³)	4.43	7.86
Melting point (°C)	1649	1454
Thermal conductivity (W/mK)	7.2	11.2-36.7
Elastic modulus (GPa)	114	210
Tensile strength, ultimate (MPa)	1000	827
Tensile strength, yield (MPa)	880	552

Table 1. Comparison between main properties of Ti6Al4V and steel (Donachie 1983).

Because of the material properties described above, two critical issues arising during turning of Ti6Al4V alloy cylindrical parts are represented by taper and excessive vibrations due to bar inflection and the very high temperatures in the workpiece and at the tool cutting edge (~ 1100°C) due to the material low thermal conductivity. These phenomena are intensified when turning under dry conditions, as the high temperatures in the cutting zone cause rapid tool wear and changes in the workpiece structure close to the cut zone (Ezugwu and Wang 1997; Ginting and Nouari 2009; Che-Haron and Jawaid 2005; Che-Haron 2001).

During titanium turning, the heat produced is absorbed by the cutting tool rather than by the workpiece due to the inherent material properties. This is often cause of premature tool failure although usually machining takes place at low rotational speeds.

Titanium is also highly flammable with related security risks, therefore tools should be able to work at high speeds, do not overheat, increase yield and complete the manufacturing without breaking.

With the aim to allow for dry turning of Ti6Al4V alloy, monitoring and on-line diagnosis of tool wear state during the process is required. To achieve this goal, a cognitive sensor monitoring procedure based on the acquisition and processing of cutting force, acoustic emission and vibration

signals during turning is implemented. The developed procedure based on sensor signal feature extraction, selection and cognitive pattern recognition via artificial neural networks allows for an accurate diagnosis on tool wear state (Teti 2015; Alessandra Caggiano et al. 2016; Segreto, Caggiano, and Teti 2015; Balsamo et al. 2016; Teti et al. 2010; Quan, Zhou, and Luo 1998). This diagnosis can be used for tool replacement strategies based on actual tool wear state instead of preventive strategies, allowing to fully exploit the entire tool life (Alessandra Caggiano, Segreto, and Teti 2016).

3.1.1 CAPRI project on “Landing Gear with Intelligent Actuation”

The CAPRI Project, acronym for “Carrello per atterraggio con attuazione intelligente” (Landing Gear with Intelligent Actuation), is a project promoted by the Campania Technological Aerospace District (DAC). The overall aim is to develop integrated solutions for an innovative landing system for civil aircrafts, destined primarily to the regional transport market. The goal is to reduce global development costs by reducing the number of fatigue tests, and operating costs by reducing scheduled maintenance tasks. Other objectives are:

- maximization of security;
- reduction of cost and weight of the landing gear system;
- increase of reliability and reduction of development and maintenance costs;
- promotion of the use of innovative materials and technologies;
- development and application of innovative technologies;
- implementation of low environmental impact technologies.

Within this wider project, the research activities developed in this thesis are focused on the low environmental impact machining of Ti6Al4V to be used as an innovative lightweight material for landing gear systems. In the green technologies perspective, which involves avoiding the use of the coolant fluids during the machining process, dry machining of this alloy is investigated. Due to the Ti alloy material properties, rapid wear of the cutting tool is expected: therefore, an intelligent multiple sensors monitoring system is required in order to monitor the tool conditions during the machining process. The study of the machining processes has the objective to develop and set-up processes characterized by greatly improved performance in terms of costs reduction, resources and materials optimization, environmental impact reduction. The optimization of materials and resources was achieved through the reduction of machining waste, due to errors during the product manufacturing process or through the full utilization of the cutting tools life adopting a condition based approach for tool replacement instead of a traditional time based approach.

The research program involves the participation of different partners including manufacturing industries and academic partners. One of the academic partners is the University of Naples Federico II, in particular the Fh-J_LEAPT UniNaples (Fraunhofer Joint Laboratory of Excellence on Advanced Production Technology) at DICMaPI (Department of Chemical, Materials and Industrial Production Engineering), which was particularly involved in the project activities on dry turning of Ti6Al4V with reference to the green technologies objective. The Magnaghi Aeronautica company assumed the role of coordinator thanks to its experience in aeronautic industry process, it defines the priority and innovative technologies, industrial implications, and project goals.

3.2 Experimental testing campaign

To investigate low environmental impact machining of Ti6Al4V to be used as an innovative lightweight material for landing gear systems, an experimental testing campaign of dry turning of Ti6Al4V bars was carried out.

The experimental testing campaign consists of turning tests under different cutting conditions. Each turning test involves consecutive cylindrical turning passes of 100 mm length on 60 mm diameter Ti6Al4V alloy bars up to complete tool wear. During each turning pass, the sensor signals were acquired using a multiple sensor system installed on the machine tool. In order to measure the tool wear after each pass, an image of the tool flank was taken using an electronic portable microscope.

3.2.1 Multiple sensor system setup

The CNC lathe Doosan PUMA400LM (Figure 5) is equipped with a multiple sensor system (Figure 6) including a Montronix FS13-CXK-R-ICA 3D force sensor, a Montronix BV100 acoustic emission sensor and a Montronix Spectra Pulse 3D vibration sensor. The first two sensors, providing analogue signals, are connected to a NI USB-6361 DAQ board for digitalization and acquisition on PC of the three cutting force components (F_x , F_y , F_z) and the Root Mean Square of acoustic emission (AERMS) signals. The 3D vibration sensor is a digital wireless sensor which acquires and sends to the PC the sensorial data corresponding to the three vibration acceleration components (A_x , A_y , A_z).

The DAQ board allows to set the signal sampling rate; following the Nyquist-Shannon sampling theorem, 10 kS/s was selected as a sufficient sampling rate to allow capturing all the original signal information. On the other hand, the digital vibration acceleration sensor directly carries out the signal sampling with a fixed rate of 3.24 kS/s.



Figure 5. Doosan PUMA400LM CNC lathe.

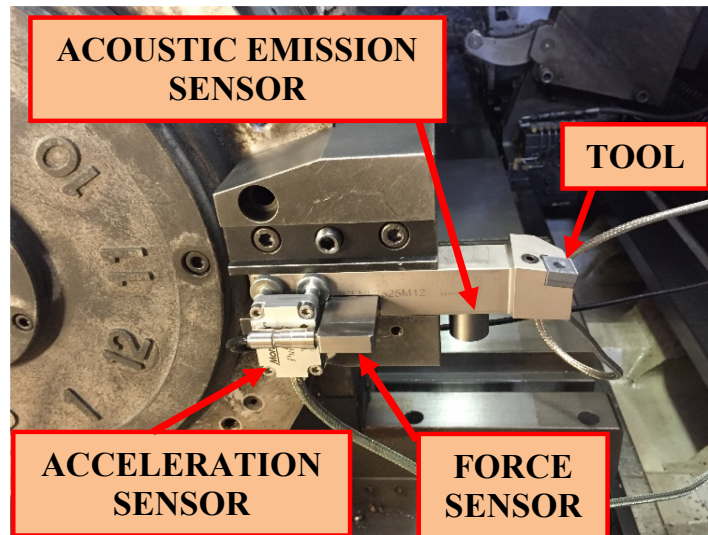


Figure 6. Multiple sensor system mounted on the tool holder (Alessandra Caggiano, Napolitano, and Teti 2017).

The Montronix FS13-CXK-R-ICA sensor is a piezoelectric force sensor with an integrated charge amplifier (ICA) for use in hard work conditions (Figure 7). It is able to make three dimensional cutting force measurements on the X, Y, Z axes. The integrated amplifier provides output signals with high sensitivity, low deviation and low impedance. Sensor monitoring of the cutting forces in turning was widely used by researchers because the forces are extremely sensitive to the process conditions. This category of sensors allows to identify strains and forces acting on the tool directly and with a good reliability. Moreover, they can be used to detect overloads or collisions, tool defects, tool breakage, and some applications tool splinter or tool wear.



Figure 7. 3D Force sensor Montronix FS13-CXK-R-ICA.

The Montronix FS13-CXK-R-ICA sensor is generally integrated in the machine tool and is used in lathe applications that require higher control performance that are not obtainable with a single-axis sensor. Table 2 shows the technical specifications of the force sensor.

The characteristics of this sensor make it ideal for a wide range of industrial monitoring applications:

- they are available either in an externally installed version or in a traditional version, designed to integrate the sensor inside the machine structure;
- improve reliability and simplify maintenance operations in industrial applications for process monitoring;
- provide a quick response time in detecting force variations due to tool breakage.

MONTRONIX FS13-CXK-R-ICA FORCE SENSOR TECHNICAL SPECIFICATIONS	
Sensitivity, 2 selectable field	Range I (low gain): Fx, Fy: 500 N/V, Fz: 1000 N/V Range II (high gain): Fx, Fy: 100 N/V, Fz: 200 N/V
Linearity	±1% FSO
Hysteresis	±1% FSO
Output Impedance	<100 W max
Output voltage	± 5 V
Power	± 15 VDC
Reset time	<1 ms
Noise Signal (<1 kHz)	<2 mVeff
Power consumption	ca. 11 mA
Overload capacity	from 6 to 25 kN preload
Dimensions	(L × W × H) 57 × 20 × 10 mm, cable excluded
Material	Stainless steel
Weight	Without cable ca. 30 g
Protection class	IP67
Temperature	working: from 0 to +60 °C depot: from -10 to +70 °C
Relative humidity	from 0 to 95% (condensation not allowed)
Cable	A 7 wires with internal shield, PUR sheath (polyurethane), length of ca. 5 m

Table 2. Characteristics of the force sensor (Teti et al. 2006).

In Figure 8, the Montronix TSFA3-ICA force sensor amplifier and its electronic set-up used during the experimental campaign is shown. It is a 3-channel force sensor amplifier used, in the experimental campaign, in combination with the Montronix FS13-CXK-R-ICA force sensor. Gain, filters, and effective values can be set individually for each channel, optimizing the amplifier adjustment for each new tool. Table 3 shows the technical characteristics of the force amplifier.

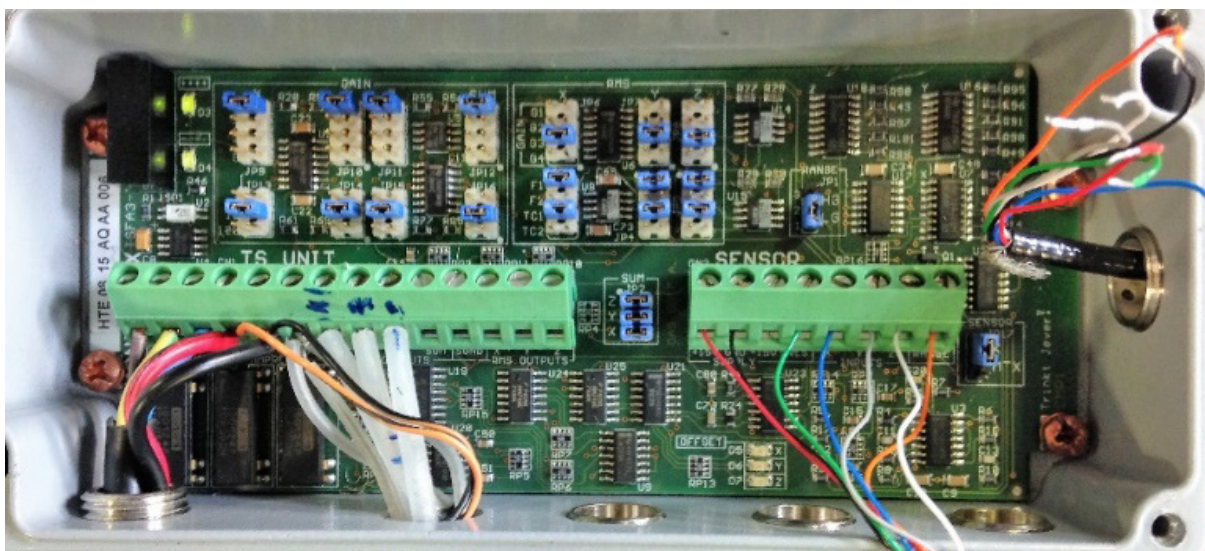


Figure 8. Set-up of the Montronix TSFA3-ICA 3D force sensor amplifier.

MONTRONIX TSFA3-ICA FORCE SENSOR AMPLIFIER TECHNICAL SPECIFICATIONS	
Amplification	1, 2, 4, 8, 10, 20, 40, 80, 100, 200, 400, 800
Gain error	±2%
Power supply voltage	±15 VDC
Power	+15 VDC @ 70mA, -15 VDC @ -20 mA
Temperature range	0° to 60° C
Connections	PG9 /specific sensor
Weight	700 g.
Input Signals	1, 2 o 3

Table 3. Technical characteristic of 3D force sensor amplifier.

Another element of the multiple sensor system used during the experimental campaign is the Montronix BV-100 acoustic emission and vibration sensor shown in Figure 9. The BV100 sensor is provided with two channels and it measures the mechanical vibration of the machine structure resulting from the cutting process (up to 10 kHz) to detect missing tools, broken tools, and severe process faults. It can also be used to monitor excessive vibration on bearings or spindles. This sensor also measures acoustic emission (AE) energy - the high frequency (50 kHz to 400 kHz) energy signals produced by the cutting process.



Figure 9. Acoustic emission sensor Montronix BV-100.

The acoustic emission sensor is characterized by (see also technical specifications in Table 4. Technical specifications of Acoustic Emission sensor Montronix BV-100. Table 4):

- an extremely wide frequency response for greater sensitivity in monitoring of tools with small and large diameters;
- easy installation: cable length of 5 m;
- compliance with IP67 and NEMA 6 standards, it is highly shielded against electromagnetic interference (EMI, Ce-EMV) and it is totally shield, internally and externally;
- the internal cladding in polyurethane protects cable against the damage of the coolant while the external plait in stainless steel protects it against hot chips and sharp edges.

MONTRONIX BV-100 ACOUSTIC EMISSION SENSOR TECHNICAL SPECIFICATIONS	
Frequency range	0.1 Hz -500 kHz
Output Impedance	< 100 Ω
Insulation resistance to mass	> 1 M Ω
Impact resistance, overload pulse (0.5 ms pulse)	7.000 g
Power	\pm 15 VDC
Power consumption	3-6 mA
Assembly	A screw M6 \times 1 \times 16
Dimensions	(L \times W \times H) 38 \times 20 \times 18 mm, without connecting cable
Material	Stainless steel
Weight	300 g
Protection class	IP67

Table 4. Technical specifications of Acoustic Emission sensor Montronix BV-100.

The acoustic emission sensor signal is amplified through a Montronix TSVA2-DGM-BV amplifier shown in the Figure 10 with its electronic set-up.

It is a two channels amplifier connected to the Montronix BV100 acoustic emission sensor (broadband sensor). Each amplifier channel has an analog output.

The amplifier has two channels:

- the yellow on the top (channel 1) is dedicated to the Vibration Acceleration signals amplification;
- the red on the bottom (channel 2) is dedicated to the AE signals amplification.

The gain set for the Vibration Acceleration signals is equal to 2 while the gain set for the AE signals is equal to 10 in order to properly visualize the signals without exceeding the maximum threshold of 10 V imposed by the data acquisition (DAQ) board. It is possible to set-up both the amplification and filtering values, and also the effective value for each channel.

Both the AE and Acceleration signals have been acquired as Root Mean Square (RMS) signals using a time constant equal to 0.12 ms. RMS is a technique used to rectify a raw signal and convert it to an amplitude envelope, which is easier to view. The rectification process converts all the numbers into positive values rather than positive and negative. Table 5 shows the technical characteristics of the acoustic emission amplifier.

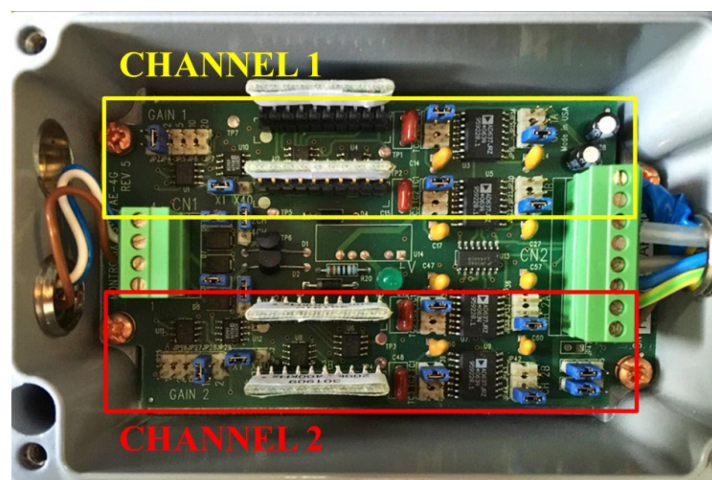


Figure 10. Acoustic Emission sensor amplifier Montronix TSVA2-DGM-BV.

MONTRONIX TSVA2-DGM-BV AE AMPLIFIER TECHNICAL SPECIFICATIONS	
Output signal	from 0 to 10 VDC
Gain error	±2%
Power supplied by the sensor	±15 VDC
Power	130 mA @ +15 V, -80 mA @ -15V
Current supplied by the sensor	4 mA DC
Assembly	2 screws M4
Weight	500 g.
Dimensions	(L × W × H) 176 × 83 × 35 mm
Material	Aluminium
Protection class	IP66
Temperature	Working: da 0 a 60 °C Depot: da -40 a 90 °C

Table 5. Technical specifications of AE amplifier Montronix TSVA2-DGM-BV.

The last component of the multiple sensor system is the Montronix Spectra TM Pulse Vibration sensor (Figure 11). It allows to measure the acceleration of the vibrations generated during machining along the axis X, Y, Z.

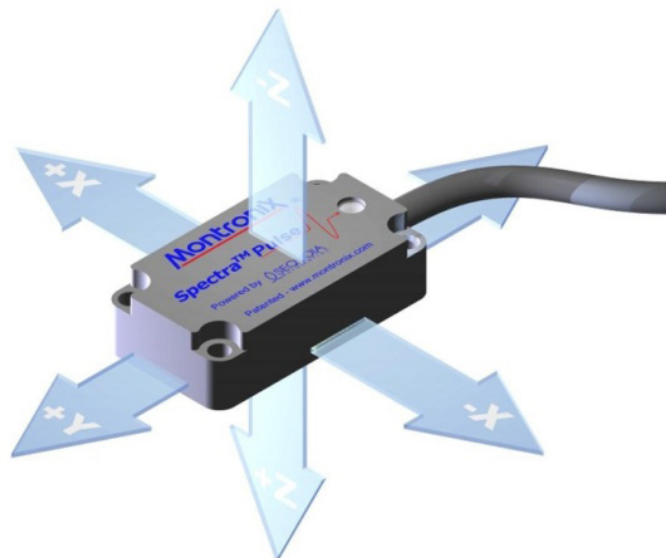


Figure 11. Vibration sensor Montronix Spectra TM Pulse.

The Spectra Pulse Vibration Sensor is a highly sophisticated sensor that uses new technologies, with advanced hardware and software developments, to permit an accurate and reliable monitoring system. The acquisition software is provided with the sensor, so the file acquisition and management are made using it. Furthermore, it is an intelligent sensor that performs digital analysis and communication.

The main characteristics of the vibration sensor are:

- integration of multiple functions in one device;
- small dimensions;
- configurable device;
- high performance;
- low energy consumption;
- easy installation.

This sensor can be used for a wide range of applications, including impact monitoring, vibration monitoring, analysis and detection of the inclination, centrifugal force measurement in all location. The general features are:

- linear DC bandwidth up to 2500 Hz;
- high linearity;
- low hysteresis;
- integrated temperature sensor.

Inputs/Outputs

- 3 digital outputs;
- 2 digital inputs (maximum voltage to apply: 24V);
- 1 RS232 (User Interface and Remote Configuration);
- 1 USB (User Interface and Remote Configuration);
- Power supply 20 ÷ 36 VDC, 200 mA;
- Cable: 2m.

In addition to the vibration sensor, which is a triaxial accelerometer, a long wire connects the sensor with the wireless transmitter which sends the acquired vibration signals directly to the computer. The Battery Net Box is equipped with a lithium-polymer battery that provides 6 hours of autonomy by the AC/DC Adapter. This sensor is different from the others because, being a gravity-based accelerometer, it allows a measurement not only in time domain but also in space domain. The Spectra Pulse Sensor and Transmitter Units are equipped with strong magnets for quick positioning and, thanks to Wireless technology, allow to operate safely without cable restrictions. The IP67 protection permits the acquisition of vibration signals, disequilibrium and the problems generated by mechanical parts movement even when working condition are with or without coolant. Offline analysis allows predictive maintenance planning and therefore can be used to replace the damaged/worn component with a condition based approach.

The following tables (Tables 6-7) show the technical characteristics of the wireless transmitter and the vibration sensor.

TRANSMISSION UNIT TECHNICAL SPECIFICATIONS	
Connections	Wireless LAN
Power	24V max.1A DC (10-30V)
Operative frequency	2,4 GHz
Operative area	300m (Air to Air)
Transmission power	100 mW
Bandwidth	1-54 MBit/s
Protection degree	IP54
Temperature range	0-50°C (working) 0-100°C (depot)
Humidity	0-100%
Battery	Lithium Polymer 3,6V 2,4Ah
Dimensions	(L × W × H) 130 × 85 × 51 mm

Table 6. Technical specifications of transmission unit.

SPECTRA PULSE VIBRATION SENSOR TECHNICAL SPECIFICATIONS	
Sensor	Triaxial accelerometer
Sensor type	MEMS Technology
Operation range	± 18 g
Bandwidth	DC 0 to 2500Hz
Shock breaking	1000g
Material	Aluminium
Weight	55 g
Protection degree	IP 67
Dimensions	(L × W × H) 55 × 30 × 15 mm
Certifications	CE

Table 7. Technical specifications of Spectra Pulse Vibration Sensor.

The monitoring system is also composed by a digitizing board that digitizes the analog signals originated from the sensors previously described and sends them to the PC using a USB cable. The 3D force sensor and the acoustic emission sensor are connected to this board. The digitizing board used in the experimental campaign is the National Instrument NI USB-6361 (Figure 12). It allows to choose different sampling rates (up to 2 MS/s), in the experimental campaign a 10 kS/s sampling rate was chosen.

The Nyquist-Shannon sampling theorem provides a recommendation for the nominal sampling interval required to avoid aliasing, i.e. the effect that causes different signals to become indistinguishable when sampled. The theorem states that the sampling frequency should be at least twice the highest frequency contained in the signal:

$$f_s \geq 2 * f_c$$

where:

f_s is the signal sampling frequency and f_c is the highest frequency observed in the signal.

The data acquisition software used is the NI SignalExpress 2015. It is possible, also, to use one of the board channels to acquire a 5 V signal, which will be used as a trigger to identify the beginning of the machining and consequently the start of the signal acquisition. The software allows to quickly acquire, analyse and visualize data using the software interface.



Figure 12. National Instrument NI USB-6361 digitizing board.

Table 8 shows the technical specifications of the digitizing board.

NATIONAL INSTRUMENT NI USB-6361 DIGITIZING BOARD	
Analog Inputs (AI)	16
Max AI Sampling Rate (1-Channel)	2MS/s
Max Total AI Throughput	2MS/s
Analog Outputs (AO)	2
Max AO Update Rate	2.86 MS/s
Digital I/O Lines	24
Max Digital I/O Rate	10 MHz
Triggering	Analog, Digital

Table 8. Technical characteristic of digitizing board NI USB-6361.

3.2.2 Workpiece material

Ti6Al4V is a titanium alloy, containing aluminium and vanadium, that owns excellent engineering properties in term of exceptional combination of resistance and toughness with high corrosion resistance. However, this titanium alloy is a very difficult to cut metal material, so that machining processes of this workmaterial can be very challenging and expensive.

This alloy has found great industrial development and its consumption is about 50% of total titanium production. The aerospace industry employs more than 80% of the production, the medical implants sector about 3%, while the rest is divided among the remaining industrial uses. This alloy is characterized by high versatility, as demonstrated by the various uses in very different fields, and can also be used at temperatures between 400 and 500 °C. Ti6Al4V assumes thermal and electrical insulating properties (in relative terms) thanks to a halved thermal conductivity and a thermal resistivity (which, as known, represents the inverse of electrical conductivity) more than three times the pure Titanium.

The main characteristics of that alloy are:

- low density and therefore remarkable lightness: its specific weight is about 4.5 kg/ dm³ and makes it particularly advantageous (with the same mechanical performance, a piece of titanium requires half of material in weight compared to steel);
- high melting point: it allows the use at particularly high temperatures;
- low value of Young's modulus: coupled with high strength resistance makes it a material that absorbs a lot of elastic energy (coupled with high flexibility);
- low thermal expansion: very close, and therefore compatible, to glass and ceramic;
- good heat transmission: low thermal conductivity of titanium may consider it inappropriate for heat exchange, however it has high corrosion resistance and it has high mechanical and structural characteristics that allow the use of this metal in manufacturing with very thin thicknesses, increasing considerably heat transfer;
- excellent corrosion resistance: this depends on the characteristic of titanium to coat spontaneously titanium with a passive dioxide film (just exposed to air, water or most oxidizing media) that has an exceptional corrosion resistance (even if damaged gets reformed instantly).

The previous characteristics results in other properties of material such as: erosion resistance and stress corrosion cracking or biocompatibility due to corrosion resistance in natural environments (the thin layer of titanium dioxide is one of the most inert substances existing and is unable to accommodate bacteria and microorganisms).

The most important mechanical characteristics are:

- good specific strength: given by the relationship between traction load and density. This characteristic between 200 and 500 °C is a key factor for aerospace applications;

- good resilience: low fragility resulting from the ability of the material to withstand impacts by absorbing the energy that develops in the impact;
- high traction yield stress: measures the stress corresponding to an elongation of 2% of a material sample and varies with the chemical composition.
- Compared to other materials such as Steel, Aluminium, Magnesium, Nickel, the Ti6Al4V has:
- low thermal conductivity; steels and magnesium have twice values and even those typical of aluminium are about 50% higher;
- the thermal expansion coefficient is just below value of pure metal and significantly lower than the other materials considered;
- excellent corrosion resistance;
- lower deformation value (on average 15 always in percentage terms), which remains higher than value of good reclaiming steels (7-10%).

3.2.3 Cutting tool specifications and process parameters

The cutting tool employed during the experimental turning tests is a Mitsubishi CNMG120404-MS MT9015 turning insert (Figure 13). It is an uncoated tungsten carbide tool, specific for titanium machining and suitable for medium material removal conditions, with ISO S15 carbide grade composition.



Figure 13. Cutting insert CNMG120404-MS MT9015.

Analysing the commercial name, some characteristics can be highlighted:

- C (geometry of the cutting insert): rhombic 80°
- N (cutting angle): 0°
- 04 (thickness of the cutting insert): 4.76 mm
- 04 (radius of the cutting edge): 0.4 mm
- MS: Shape of chip breaker

A full factorial experimental design was applied for the turning tests: three factors corresponding to the cutting parameters, i.e. cutting speed, v , feed rate, f , and depth of cut, d , were taken into consideration, and three different levels of each factor were tested according to the experimental plan in Table 9.

Parameter	Minimum	Intermediate	Maximum
Cutting speed (m/min)	60	70	80
Feed rate (mm/rev)	0.10	0.25	0.30
Depth of cut (mm)	0.5	1.0	1.5

Table 9. Cutting conditions employed in the experimental campaign.

The testing procedure was planned in accordance with the requirements indicated by the standard on tool-life testing with single-point turning tools (ISO 3685:1993).

3.3 Tool wear measurement and wear curve construction

The final aim of this work is to find correlations between the multiple sensor signals acquired during dry turning of Ti6Al4V and the tool wear conditions. Tool wear describes the gradual degradation of cutting tools due to machining operation. During the experimental campaign was studied tool wear development, taking into account the working process, the working material and the parameters used for each set of turning tests. Tool wear includes flank wear in which the erosion is relative to the portion of the tool in contact with the machined part, and crater wear in which the erosion is relative to the rake face that is in contact with chips.

In our campaign, flank wear was considered as the most significant wear relative to our aim of study. Flank wear was measured according to the prescriptions of current regulations about "Tool-life testing with single-point turning tools" ISO 3685: 1993 (E).

For tool wear measurements, the cutting edge is divided in four zones as showed in Figure 14:

- Zone C: is the curve part of the cutting edge.
- Zone B: is the right part of the cutting edge between zone C and zone A.
- Zone A: is the quarter part of the worn cutting edge.
- Zone N: extends beyond the contact zone between tool and workpiece for about 1 mm to 2 mm along the cutting edge.

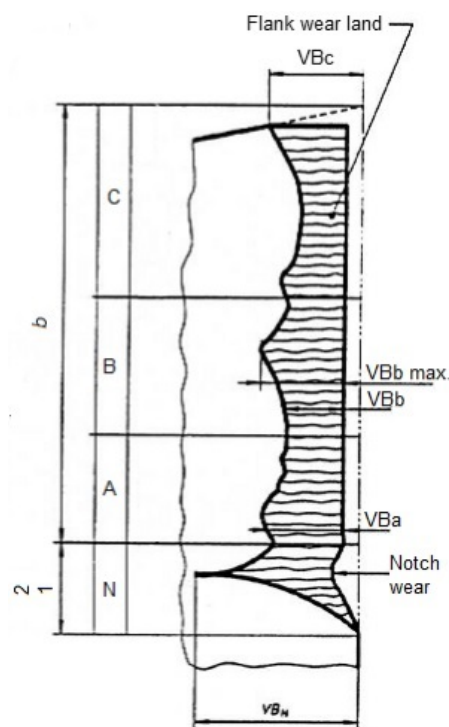


Figure 14. Wear zone of the cutting edge(ISO 3685:1993).

The flank wear is measured referring to the maximum value VB_{max} indicated graphically in the Figure 15. The criterion for the end of tool life was established by setting a 0.6 mm threshold for the highest acceptable VB_{max} value.

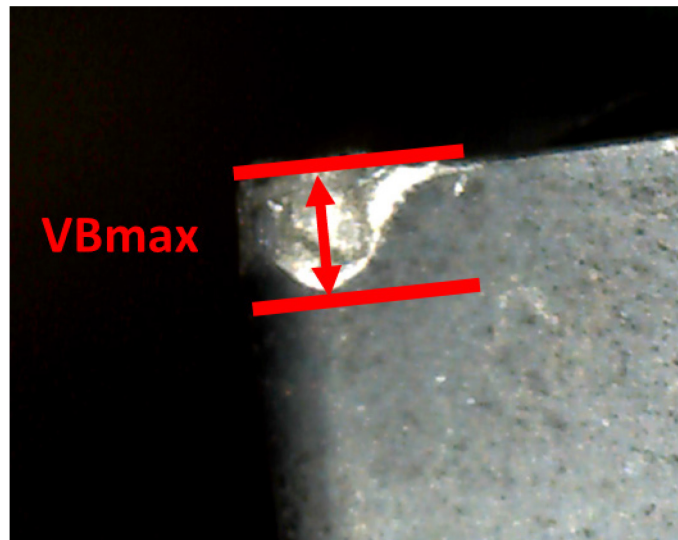


Figure 15. Tool wear measurement on the acquired image.



Figure 16. Dino Lite Microscope.

The procedure for VBmax calculation starts from images acquisitions at the end of each turning machining. The metrological instrument used to acquire images relative to the flank was the Dino Lite digital microscope shown in Figure 16.

The digital microscope has been coupled to the CNC lathe using a specifically created magnetic support, equipped with metal arms, in order to change the microscope positioning and so allow to photograph the cutting edge from different positions (Figure 17). Another advantage is the possibility to make photo and consequently to measure the tool wear without movement of the cutting edge from its position on tool at the end of each turning operation, accelerating considerably the time for measurement operations. The software used for image acquisitions is DinoCapture 2.0 and it is provided with the microscope.

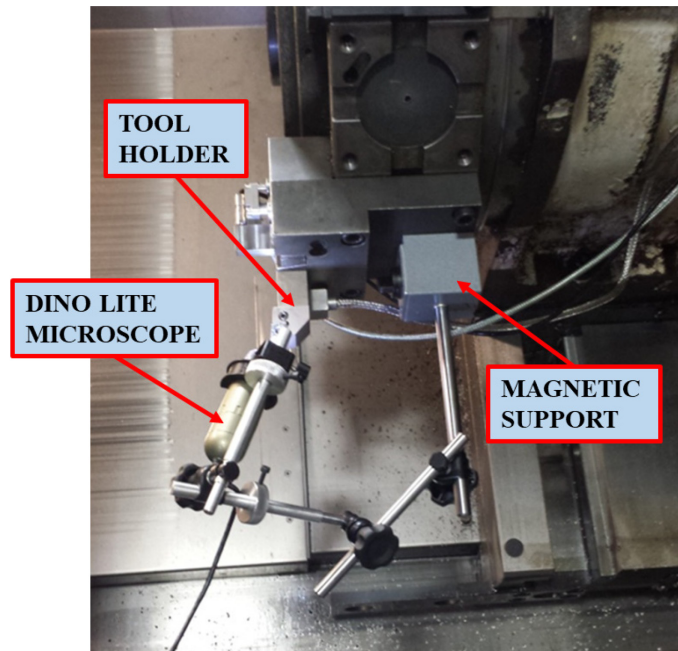


Figure 17. Dino Lite Microscope mounted on its magnetic support.

The tool wear curve reconstruction shows a good correspondence between these curves and the tool wear curves found in literature. The results on tool wear development confirm that cutting speeds 70 m/min and 80 m/min are too high for dry turning of Ti6Al4V. As a matter of fact, by increasing the cutting speed, a large increase in tool wear rate and a notable reduction of machining time and material removal carried out with a single tool are observed (Figure 18). As regards the differences between tool wear development at 60 m/min and 70 m/min, they are smaller at low feed rate and depth of cut, but significantly increase with growing feed rate and depth of cut.

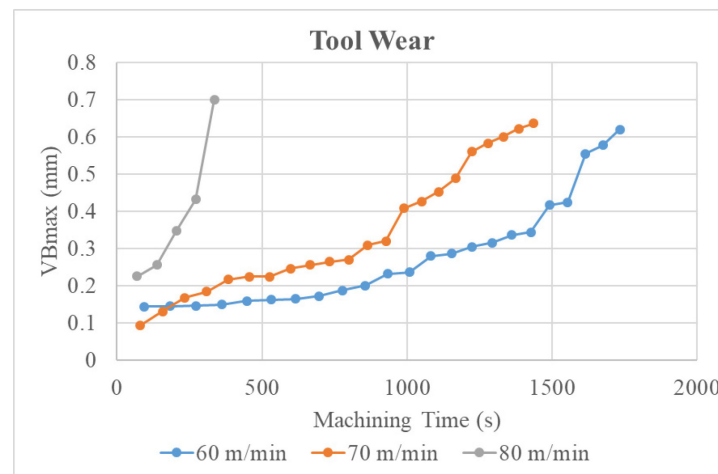


Figure 18. Measured tool flank wear values vs machining time for $v_1 = 60$ m/min, $v_2 = 70$ m/min, $v_3 = 80$ m/min ($f = 0.2$ mm/rev, $d = 0.5$ mm).

On the basis of the experimental results, 60 m/min appears as the most suitable value for maximum cutting speed in dry turning of Ti6Al4V. By setting the cutting speed at 60m/min, the influence of depth of cut or feed rate variations can be observed in Figure 19-20. A notable growth of tool wear rate (3 times faster) is found when increasing depth of cut from $d_1 = 0.5$ mm to $d_2 = 1$ mm and $d_3 = 1.5$ mm as well as when increasing feed rate from $f_2 = 0.25$ mm/rev to $f_3 = 0.3$ mm/rev.

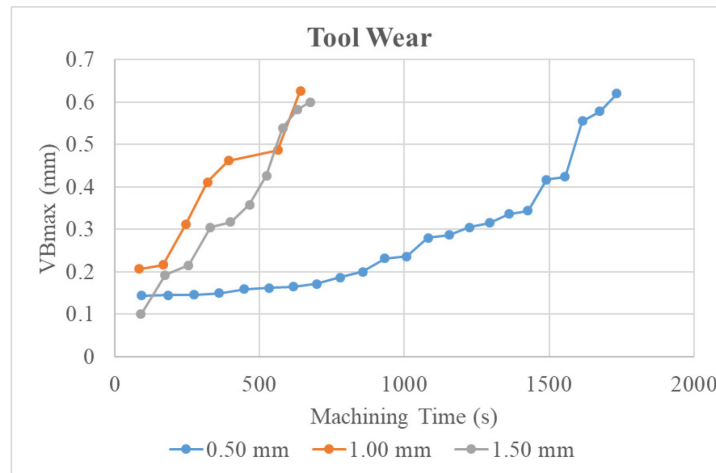


Figure 19. Measured tool flank wear values vs machining time for $d1 = 0.5 \text{ mm}$, $d2 = 1 \text{ mm}$, $d3 = 1.5 \text{ mm}$ ($v = 60 \text{ m/min}$, $f = 0.2 \text{ mm/rev}$).

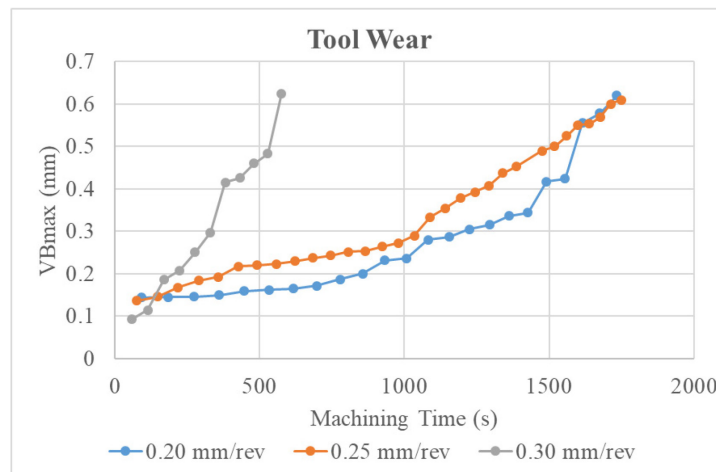


Figure 20. Measured tool flank wear values vs machining time for $f1 = 0.2 \text{ mm/rev}$, $f2 = 0.25 \text{ mm/rev}$, $f3 = 0.3 \text{ mm/rev}$ ($v = 60 \text{ m/min}$, $d = 0.5 \text{ mm}$).

3.4 Signal processing and feature extraction

In this paragraph will show the whole procedure which begins from the segmentation because the sensor signals acquired by the multiple sensor system during the experimental turning tests included head and tail transient portions which do not belong to the actual machining process (Figures 21-23). As these signal portions are not relevant for process monitoring, they had to be removed in order to consider only the signal part consistent with steady state machining (Teti 2015; Teti et al. 2010). On the steady portion will be performed the analysis in order to extract several sensor features and finally will calculate the Pearson coefficients with the aim to highlight the most correlated features. The final result is the constitution of the Sensor Fusion Pattern Vector which will use to feed the cognitive system.

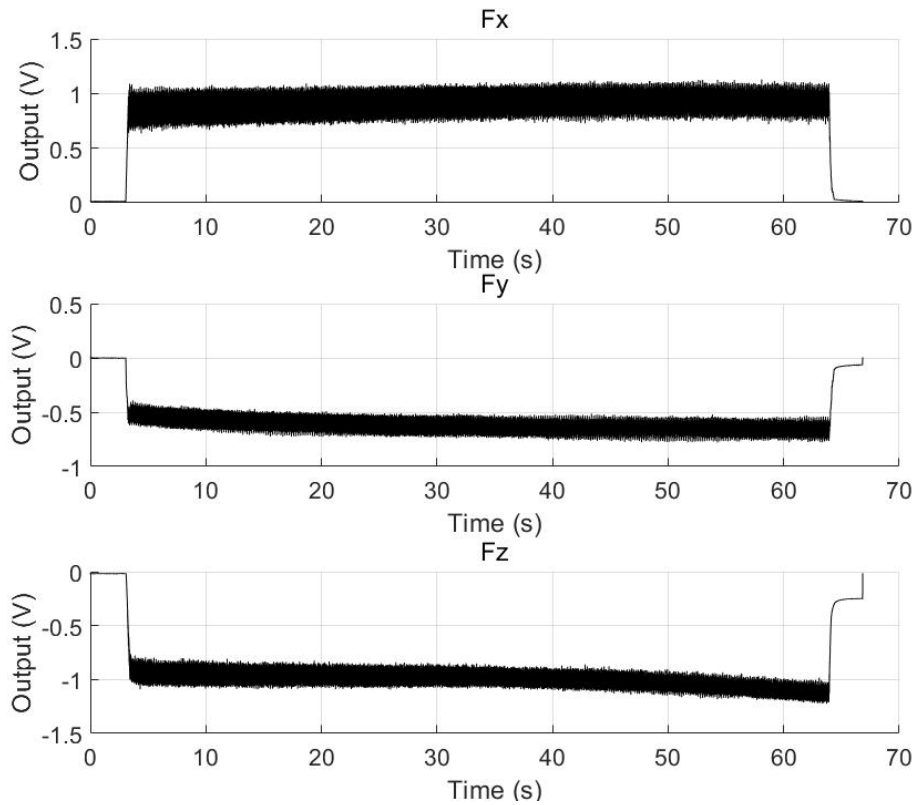


Figure 21. Acquired Force signals.

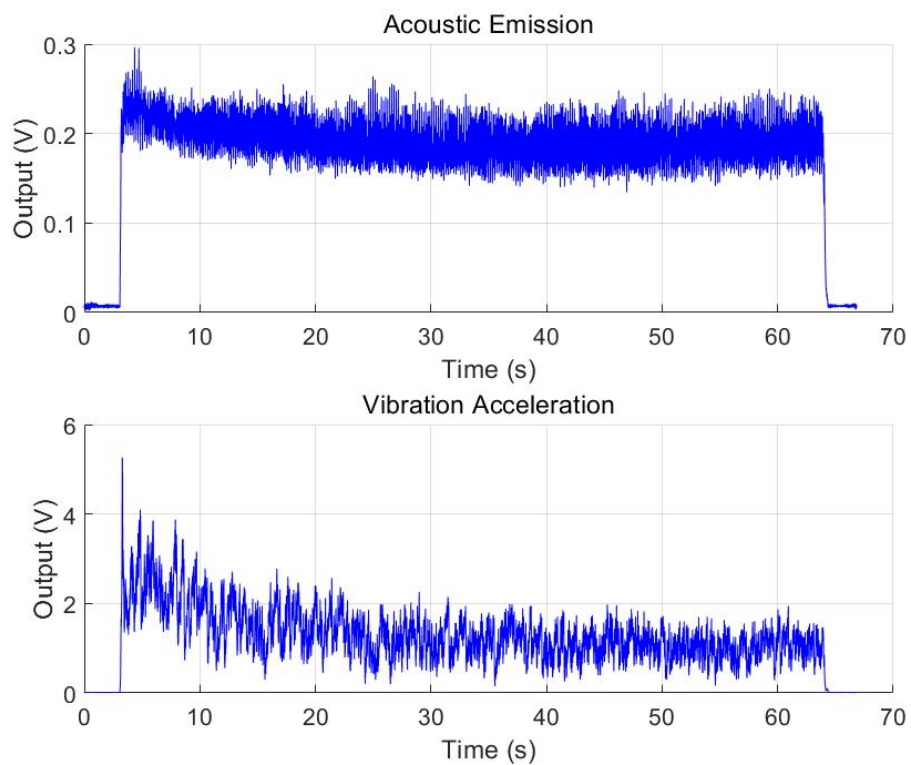


Figure 22. Acquired Acoustic Emission RMS and Vibration Acceleration signals.

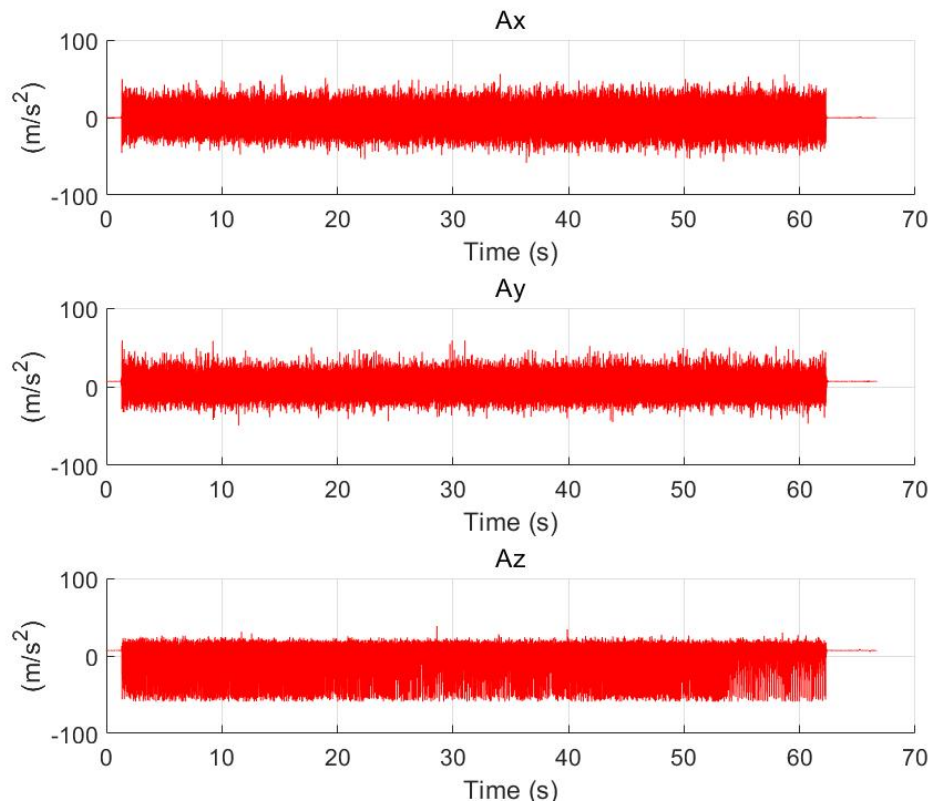


Figure 23. Acquired Acceleration signals.

3.4.1 Signal segmentation and resampling

This signal segmentation procedure was carried out using two different methods for the DAQ board signals (F_x , F_y , F_z and AERMS) and for the vibration acceleration digital sensor signals (A_x , A_y , A_z), respectively.

As regards the DAQ board signals, segmentation was performed on the basis of the F_x signal and synchronically extended to the other signals F_y , F_z and AERMS. The automated segmentation procedure to cut out transient signal portions is based on the calculation of the signal moving average with a fixed subset size of 50 samples to reduce high frequency oscillations. The mean value of the resulting smoother signal is then employed as a threshold to identify the steady signal portion. In particular, considering only the signal portion over this threshold, the slope between consecutive samples is calculated: the first sample with negative slope and the last sample with positive slope are identified as the start and the end of the segmented signal (Figure 24). The segmented signals are shown in Figures 25-26.

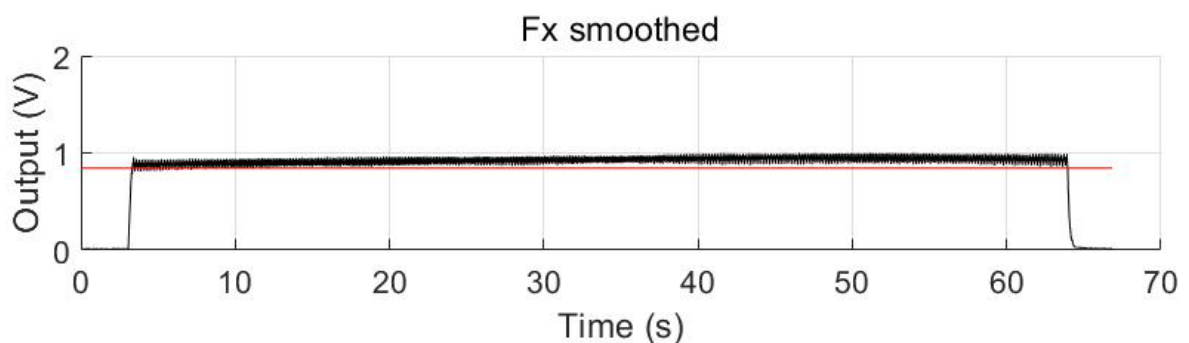


Figure 24. Moving average of F_x cutting force component signal and set threshold (red line).

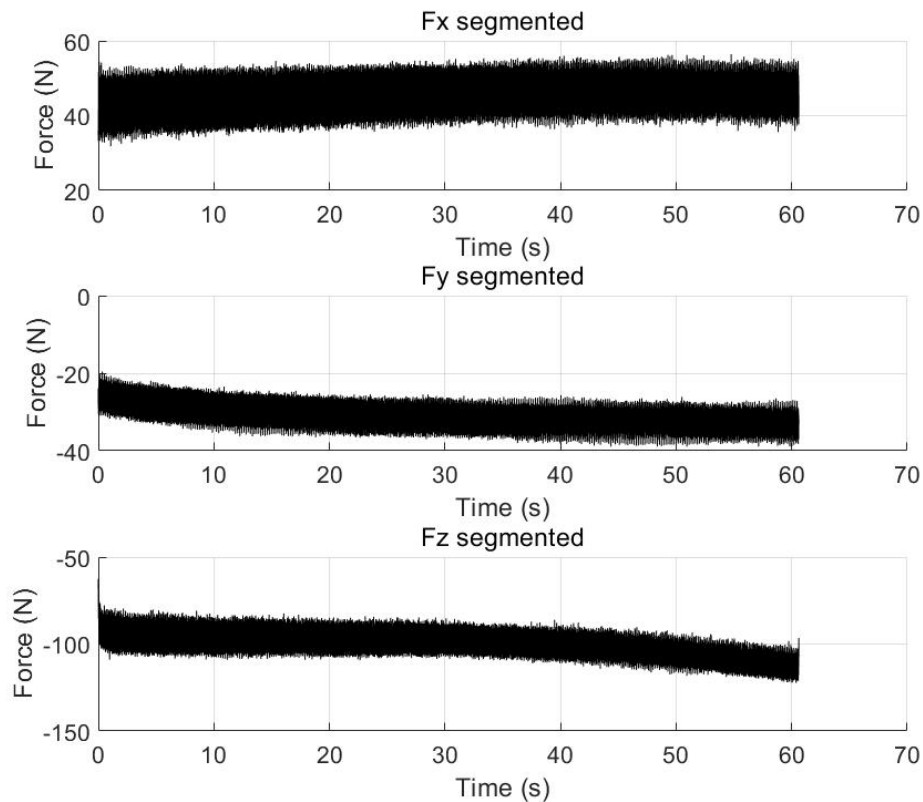


Figure 25. Segmented F_x , F_y , F_z cutting force components signals.

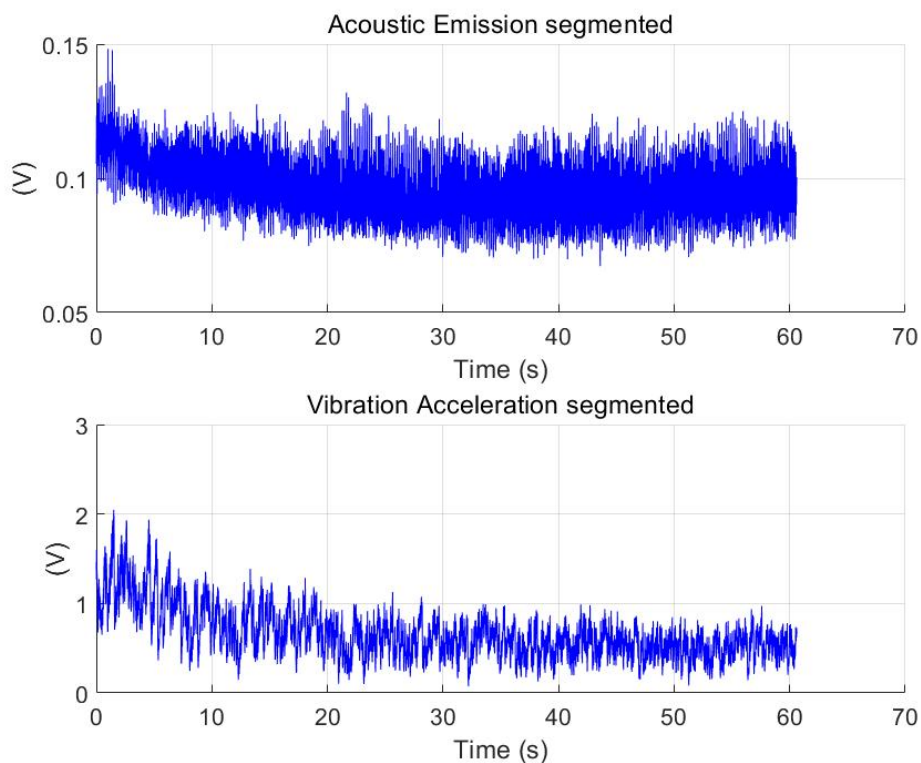


Figure 26. Segmented acoustic emission RMS and vibration acceleration RMS signals.

A different segmentation procedure was applied to the acceleration signals acquired by the digital vibration sensor. Each vibration acceleration component signal (A_x , A_y , A_z) has an offset which depends on its orientation with respect to the gravity acceleration (the sum of the x, y and z offset

values is 9.81 m/s^2). Therefore, the first operation which was carried out is the signals unbiasing, that consists in calculating, for each sensor signal, the average value of the first 100 points in the transient signal portion in order to find the offset value, and then shifting the signals by removing this value. These signals have oscillations around their offset value, so the developed procedure identifies the difference between transient and steady state signal portions by calculating the square of the signal, i.e. the square of the vertical distance of the signal values from the rest state. The first and the last value over the threshold set at 20 m/s^2 are selected as the start and the end of the signal segment consistent with actual machining. Moreover, a resampling of the digital sensor signals to 10 kS/s was necessary. As a matter of fact, the digital vibration acceleration signals were compulsorily acquired with a fixed sampling rate of 3.24 kS/s , whereas the DAQ signals were acquired with a properly chosen sampling rate of 10 kS/s . The final segmented vibration acceleration signals are shown in Figure 27.

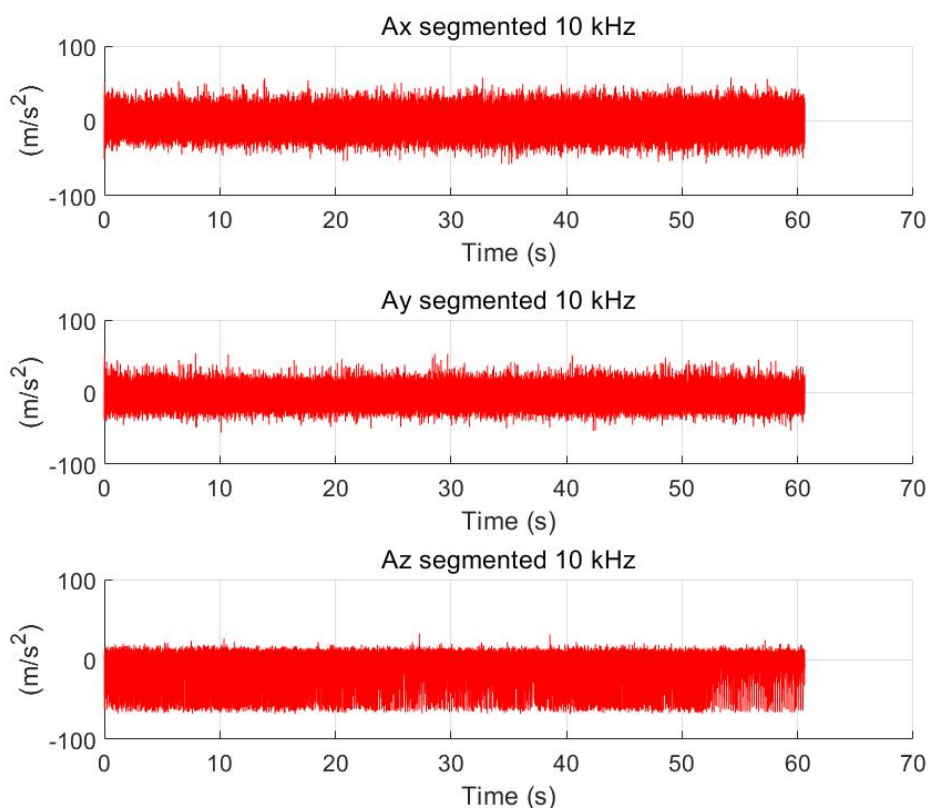


Figure 27. Segmented A_x , A_y and A_z vibration acceleration signals.

3.4.2 Signal feature extraction

Signal pre-processing was carried out to isolate the relevant signal portion with the aim to allow for the subsequent extraction of functional sensor signal features correlated with tool state and/or process condition (Teti et al. 2010).

A statistical approach in the time domain was applied for feature extraction. Among the several statistical signal features that can be extracted from a time domain signal, the following five were taken into consideration: arithmetic mean, variance, skewness and kurtosis (Figure 28).

The extracted sensor signal features can be employed to feed cognitive decision making support systems able to provide a diagnosis on tool wear state. The latter can be used for selecting appropriate corrective actions such as emergency stop of the machine, tool replacement (either automatic or manual) or adaptive change of the process parameters.

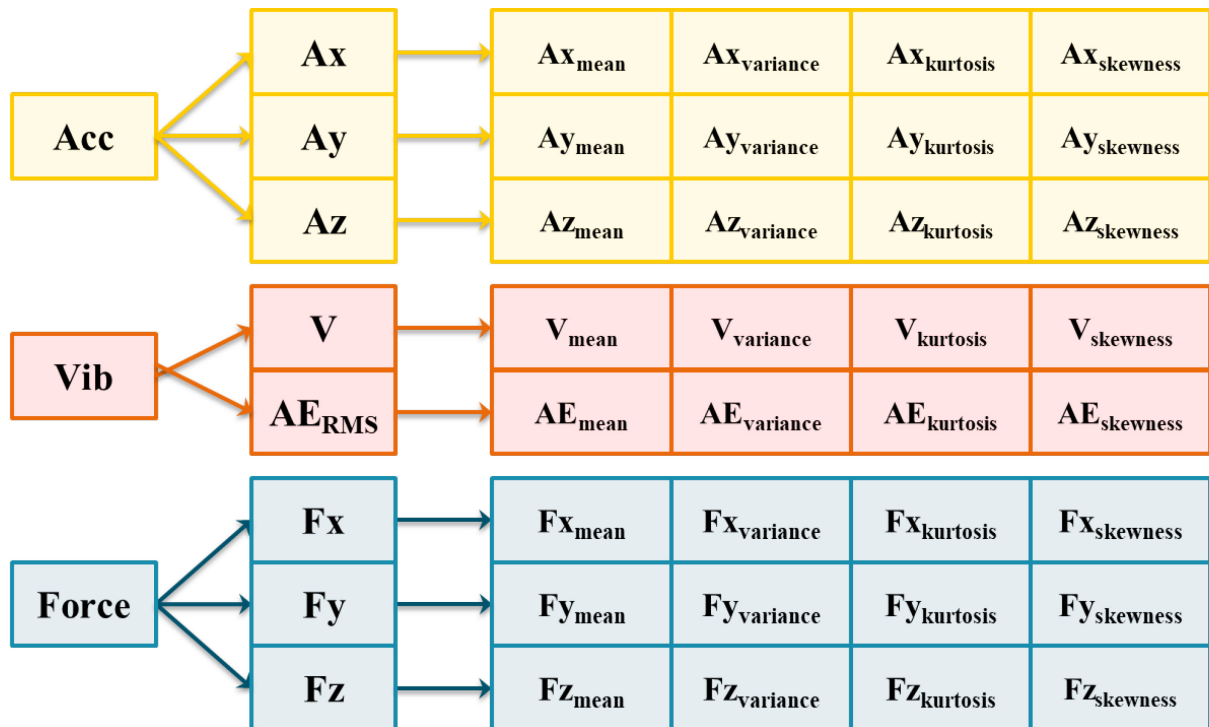


Figure 28. Extracted statistical sensor signal features in time domain.

3.4.3 Signal feature selection

The signal feature extraction procedure generated five features for each acquired signal. This large number of extracted features needs a proper selection method to identify the most relevant features for the tool wear monitoring scope. A statistical approach based on the calculation of the Pearson correlation coefficient was employed to evaluate the correlation between extracted features and tool wear conditions. Considering the Pearson coefficient calculation method and the considerations on the coefficient values described in the paragraph 2.3.3, based on the r value, only 8 out of all the extracted statistical features showed a strong correlation with tool wear (Table 10): Fx average (Fx_{av}), Fy average (Fy_{av}), Fz average (Fz_{av}), AERMS average (AE_{RMSav}), Fx skewness (Fx_{sk}), Fz skewness (Fz_{sk}), Fx kurtosis (Fx_{kurt}), Fz kurtosis (Fz_{kurt}).

Graphical analysis showed that the behaviour of the selected statistical sensor signal features and the behaviour of the tool wear development are very close. Figure 29 illustrates the Fz_{av} feature behaviour for cutting tests at $v = 60\text{m/min}$, $d = 0.5\text{ mm}$ with diverse feed rate values: $f_1 = 0.2\text{ mm/rev}$, $f_2 = 0.25\text{ mm/rev}$, $f_3 = 0.3\text{ mm/rev}$.

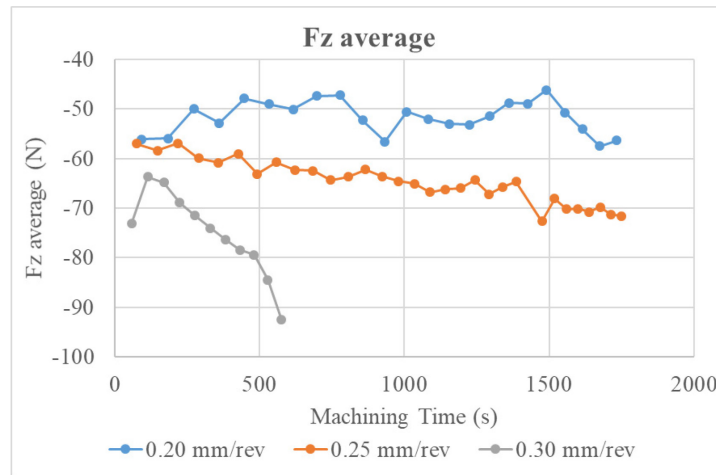


Figure 29. Average of F_z cutting force component signal, $F_{z_{av}}$, vs machining time for $f_1 = 0.2$ mm/rev, $f_2 = 0.25$ mm/rev, $f_3 = 0.3$ mm/rev ($v = 60$ m/min, $d = 0.5$ mm).

3.5 Tool wear curve reconstruction and generation through intelligent methods

The selected statistical features were employed to construct sensor fusion feature pattern vectors (SFPVs) to be correlated with tool wear state through cognitive pattern recognition based on artificial neural networks (ANN) (Teti 2015).

ANN paradigms were developed to accomplish two main objectives: (a) reconstruction of the missing points of a single tool wear curve obtained from several passes under a given turning condition; (b) generation of the entire tool wear curve for a given turning condition based on a training set consisting of sensor signal features and corresponding tool wear values measured for different turning conditions.

In both cases, three-layer cascade-forward backpropagation ANNs using the Levenberg-Marquardt optimization algorithm for training were setup, and an algorithm to train and test different numbers of hidden layer nodes was implemented (Figure 30).

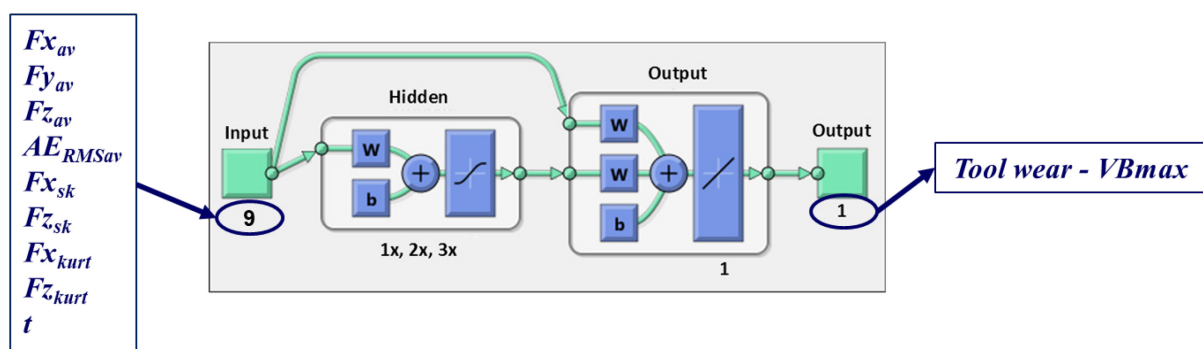


Figure 30. Artificial Neural Network architecture.

3.5.1 Tool wear curve reconstruction

For each turning condition, ANNs were set up in order to reconstruct the complete tool wear curve based on the features extracted from the signal data relative to the consecutive turning passes carried out with the same turning condition.

The ANNs were fed with a set of 9-feature SFPV_a constructed for each turning pass in a full turning test by combining the selected statistical signal features and the corresponding machining time (t), i.e. the time at which the turning pass was terminated.

$$\text{SFPV}_a = [F_{x_{av}}, F_{y_{av}}, F_{z_{av}}, A_{E_{RMS_{av}}}, F_{x_{sk}}, F_{z_{sk}}, F_{x_{kurt}}, F_{z_{kurt}}, t]$$

Each SFPV_a was associated to its matching flank wear value (VB_{max}) to create input-output vectors for ANN learning. For each turning condition, n input-output vectors (n = number of turning passes in a full turning test) were built to form the related ANN training set. ANN cross-validation was performed through the leave-k-out method with k = 1 (Lewandowski 2015).

According to the leave-k-out method, at each step, k = 1 SFPV_a is removed in turn from the original set of n SFPV_a and used for ANN testing while the remaining n-k SFPV_a are used for training. This is repeated for all the n SFPV_a and the overall pattern recognition performance is eventually estimated by combining the n recognition rates obtained.

Diverse configurations of ANNs using different numbers of hidden layer nodes, multiples of the number of input layer nodes (9, 18 and 27 nodes, respectively), were trained and tested to identify the best ANN configuration for the recognition of the maximum tool flank wear land, VB_{max}.

3.5.2 Tool wear curve generation

With the objective to generate the entire tool wear curve for a given turning condition, a different set of features was selected to construct the sensor fusion feature pattern vector SFPV_b to be fed to the ANN. The new SFPV_b is a 12-feature vector constructed by adding to SFPV_a the cutting parameters, i.e. cutting speed, v, feed rate, f, and depth of cut, d.

$$\text{SFPV}_b = [F_{x_{av}}, F_{y_{av}}, F_{z_{av}}, A_{E_{RMS_{av}}}, F_{x_{sk}}, F_{z_{sk}}, F_{x_{kurt}}, F_{z_{kurt}}, t, v, f, d]$$

In this case, a different leave-k-out procedure was applied, with k equal in turn to the number of passes of the turning condition to be tested: this means removing all the SFPV_b and corresponding tool wear values of the given turning condition from the training set. Therefore, the training set consists only of SFPV_b and corresponding tool wear values measured at turning conditions different from the one to be tested. In particular, surrounding cutting conditions were selected for training by fixing two of three cutting parameters and varying the last one. E.g., to generate the tool wear curve for v₁ = 60 m/min, f₁ = 0.25 mm/rev, d₁ = 0.5 mm, the SFPV_b and corresponding tool wear values obtained for v₂ = 60 m/min, f₂ = 0.20 mm/rev, d₂ = 0.5 mm and for v₃ = 60 m/min, f₃ = 0.30 mm/rev, d₃ = 0.5 mm were used to train the ANN.

3.6 Results and discussion

The ANN based pattern recognition performance was estimated in terms of mean squared error, MSE, between the ANN predicted VBmax values and the measured VBmax values.

Table 11 reports the MSE values obtained from the ANN tool wear curve reconstruction for the experimental tests carried out at $v = 60$ m/min with various feed rate and depth of cut values. As it can be observed, very low MSE values between 0.00064 and 0.02275 were attained, providing an accurate tool wear curve reconstruction with ANN output values very close to the measured tool wear values. In most cases, the best performance was obtained with the 9-9-1 ANN configuration. In the other cases, it was obtained with the 9-18-1 ANN configuration (Figure 31).

Cutting Parameters	MSE		
	9 hidden nodes	18 hidden nodes	27 hidden nodes
60 m/min -0.30 mm/rev -1.0 mm	0.00049	0.02098	0.00992
60 m/min -0.30 mm/rev -1.5 mm	0.00225	0.06577	0.02998
60 m/min -0.25 mm/rev -1.0 mm	0.01019	0.02903	0.01160
60 m/min -0.20 mm/rev -1.0 mm	0.00495	0.02128	0.05334
60 m/min -0.30 mm/rev -0.5 mm	0.04696	0.02275	0.02703
60 m/min -0.20 mm/rev -0.5 mm	0.01651	0.01330	0.00524
60 m/min -0.25 mm/rev -0.5 mm	0.00370	0.00064	0.00096
60 m/min -0.20 mm/rev -1.5 mm	0.00518	0.02649	0.01499
60 m/min -0.25 mm/rev -1.5 mm	0.00748	0.04195	0.03017

Table 11. Overall Mean Square Error (MSE) obtained by ANN tool wear reconstruction for all the turning tests carried out at $v = 60$ m/min.

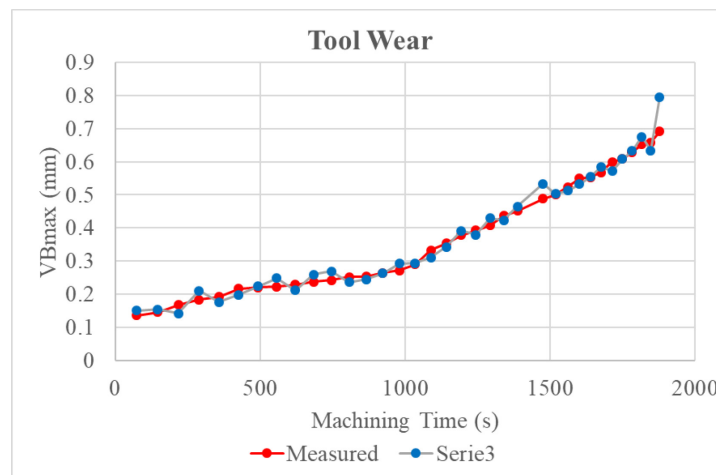


Figure 31. ANN output vs measured VBmax for turning test at $v = 60$ m/min, $f = 0.25$ mm/rev, $d = 0.5$ mm. ANN configuration: 9-18-1. MSE = 0.000639.

As regards the tool wear curve generated by training the ANN with SFPV_b and corresponding tool wear values measured for different turning conditions, slightly higher MSE values between 0.00613 and 0.02683 were obtained, suggesting that this task is more challenging for the ANN. Figure 30 shows the tool wear curve for turning with $v_1 = 60$ m/min, $f_1 = 0.25$ mm/rev, $d_1 = 1.5$, generated by the ANN trained with signal features and corresponding tool wear values for surrounding turning conditions. Although a higher MSE = 0.01373 was obtained in this case, the ANN is still able to satisfactorily provide the tool wear development and identify the critical moment at which the transition of the tool wear curve between second and third tool wear zone occurs (Figure 32).

This allows an accurate diagnosis on tool state that could be reliably implemented on-line. The ANN based diagnosis on tool state can be used for selecting appropriate corrective actions which can be directly fed to the machine tool numerical controller (e.g. for emergency halting or cutting parameters change) or suggested to the machine operator (e.g. for manual tool replacement operations).

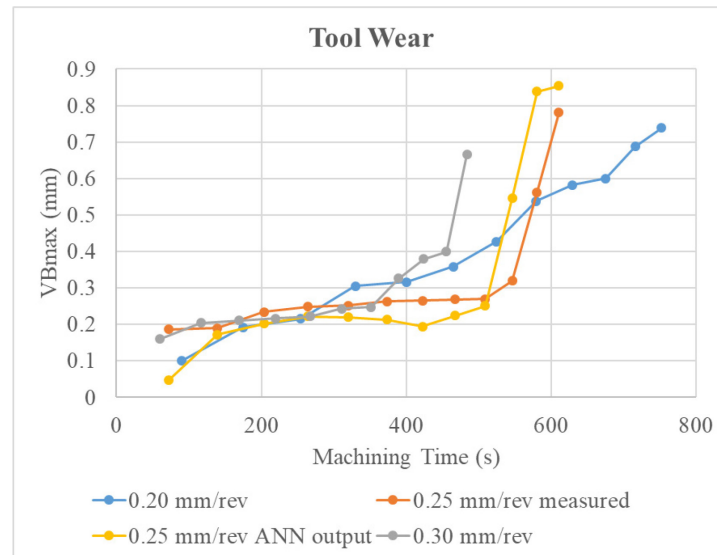


Figure 32. ANN entire tool wear curve generation. The tool wear curve for $v_1 = 60$ m/min, $f_1 = 0.25$ mm/rev, $d_1 = 1.5$ mm is obtained using a training set comprising sensor signal features and corresponding tool wear values for $v_2 = 60$ m/min, $f_2 = 0.20$ mm/rev, $d_2 = 1.5$ mm and $v_3 = 60$ m/min, $f_3 = 0.30$ mm/rev, $d_3 = 1.5$ mm. ANN configuration: 12-24-1. MSE = 0.01373.

An experimental testing campaign of dry turning on Ti6Al4V alloy bars was carried out with the aim to develop a cognitive sensor monitoring procedure for tool wear state diagnosis based on the acquisition and processing of cutting force, acoustic emission and vibration sensor signals.

The experimental tests showed that 70 m/min and 80 m/min cutting speeds result in extremely rapid tool wear and very low machining time and very low material removal per tool life. These phenomena are intensified with increasing feed rate and depth of cut values. Also in the case of $v = 60$ m/min, which appears as most suitable for dry turning of this difficult-to-machine alloy, tool wear monitoring appears necessary to deal with the rapid tool wear development.

The procedure developed for accurate diagnosis of tool wear state involved sensor signal feature extraction, selection and cognitive pattern recognition via ANN.

The latter provided accurate tool wear reconstruction and generation, with ANN output values very close to the measured tool wear values and MSE values < 0.02683 .

This confirms the capability of the developed procedure to reliably carry out a diagnosis on tool wear state, which can be employed to support decision making for appropriate corrective actions on tool replacement, parameters change or process stop, which can be either directly fed to the machine tool numerical controller or suggested to the human operator.

4. Smart sensor monitoring of CFRP/CFRP and Al/CFRP stack drilling

4.1 The framework

The use of new structural materials such as carbon fibre reinforced plastics (CFRP) allows for a substantial weight reduction on aircrafts, which positively affects emissions and management costs through a lower fuel consumption consistent with nowadays environmental requirements (Saoubi et al. 2015), so they are more and more replacing traditional materials and their application is increasing in automotive and aerospace industries.

Due to the difficulties in realizing welding operations or adhesive joints for the assembly of CFRP components, mechanical joining techniques such as riveting are generally employed to realize strong and reliable joints. This is the reason why drilling is the most widespread CFRP machining process in the aeronautical industry. However, the anisotropic nature of the material, the very rapid tool wear caused by the abrasive carbon fibers and the high concentrated efforts and vibrations that may cause damages affecting material integrity, processed surface quality and aspect, make the drilling of CFRP parts a great challenge for manufacturing engineers (Teti 2002; A Caggiano et al. 2017; Zitoune, Krishnaraj, and Collombet 2010; Ho-Cheng and Dharan 1990; Jain and Yang 1994). The drilling process involves two basic motions (El-Hoffy and Abdel-Gawad 2013) (Figure 33):

- The primary (or cutting) motion represents the rotation around the tool axis. The cutting speed is measurable by the following relation:

$$V_t = \frac{\pi * n * D}{1000}$$

where:

D is the bit diameter;

n is the spindle rotation speed.

- The second motion is called the feed motion (V_a). It is obtained from the motion of the tool perpendicular to the work-piece. The feed of the main spindle is calculated as follows:

$$V_a = f_r * n$$

where f_r is the feed per revolution.

The feed rate (f) or forward ratio is the ratio between forward speed Fs and spindle rotation speed:

$$f = \frac{V_a}{n}$$

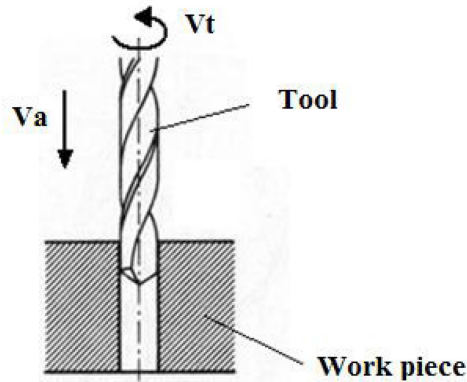


Figure 33. Drilling basic motions.

Due to different orientations of fibres which constitute the laminates of composite materials, they acquire anisotropy and inhomogeneity properties, which make it, light and strong, but also hard to be machined (J. Sheikh-Ahmad and Davim 2011).

Drilling is a particularly hostile operation for composite laminates, because high concentrated efforts and vibrations generated during such processing may cause widespread damages. Such damages cause problems from an aesthetical point of view but it can also compromise finished part mechanical properties.

Although several application of non-traditional machining operations to hole-making of composite laminates, such as laser machining (Herzog et al. 2008) and water-jet machining (Azmir and Ahsan 2009), have been developed, mechanical drilling operations using conventional or special drill bits are primary applications for composite laminates.

With the aim to reduce the tool wear in order to improve the quality of the final product and cut off the costs related to frequent tool changes, some recent studies have been focused on the development of new drill bit geometries (Ko and Chang 2003; Filiz and Burak Ozdoganlar 2010a, 2010b; Hocheng and Tsao 2003; Isbilir and Ghassemieh 2013). Efforts have been also spent for modelling the thrust force during drilling operations, which was found to directly affect the quality of drilled holes (Karpat et al. 2014; López De Lacalle, Rivero, and Lamikiz 2009; Iliescu et al. 2010). To achieve a high productivity, while preserving the integrity of the workpiece during drilling of CFRP components, in-process tool wear state monitoring is crucial. This can be performed by an on-line real-time multiple sensor monitoring procedure (Alessandra Caggiano, Segreto, and Teti 2016).

However the entire replacement of the conventional metallic materials by CFRP laminates is not recommended. First of all, CFRP exhibits low bearing and shear strengths as well as high notch sensitivity. Additionally, the joint strength depends on the laminate configuration. Furthermore, the environmental conditions exert influence on the mechanical behaviour of the joint.

Hence, alternative advanced joining techniques such as bolted structures made of stacked composite laminates and metal alloy sheets have been developed in order to fulfil the material-specific requirements and take advantage of the favourable isotropic behaviour of metal alloys facing the complex stress state of bolt loaded holes (Fink et al. 2010). These stacks can be defined as composite/metal hybrid structures (Jelinek, Schilp, and Reinhart 2015).

As a matter of fact, multi-material components made of composite laminates overlaid on light-weight metal alloy sheets are becoming increasingly employed in the aerospace sector. Airframe industries are increasing the implementation of composite/metal alloy stacks due to their high strength to weight ratio to produce innovative structural configurations for key load-bearing

components, favouring energy saving in the aerospace and automotive industries, and increasing fuel efficiency and cycle life. The use of such multi-material stacks is expanding for structural aerospace applications, especially where high mechanical loads exist such as for aircraft wing and tail-plane components (Castro 2010; Ramulu and Spaulding 2016). Conventional drilling processes using drill bits on CFRP laminates may damage the workpiece through chipping, cracking, delamination and high wear on the cutting tools (Karnik et al. 2008). Several critical defects such as entry/exit delamination, geometric/dimensional errors, internal delamination, fiber pullout, thermal damage have been reported (Dharan and Won 2000). When stacked with metal alloy sheets, the drilling process becomes even more complex, due to the different properties of the stacked materials.

Industrial practice relating to hole production in multilayer composite/metal alloy stacks is often carried out by initially drilling each material element separately followed by temporary assembly of the workpiece laminates/sheets for subsequent deburring and finishing. Despite a reaming operation, difficulties still exist in meeting hole quality requirements as well as productivity issues. The application of ‘single shot’ drilling was proposed as a potential solution; however, the widely different mechanical/physical properties of the different materials involved and their associated machinability characteristics, pose significant challenges.

In general, relatively high cutting speed (150-200m/min) with feed rate < 0.05 mm/rev is recommended for drilling CFRP composites in order to minimise delamination, while low cutting speed (10–30m/min) with moderate feed rate (0.05–0.1mm/rev) is recommended for machining Al alloys. Not surprisingly, there is a lack of knowledge/standards available in the literature with regard to optimal process parameters, tool geometries/materials and cutting environment when machining dissimilar materials stacks (Shyha et al. 2011).

4.1.1 Applications

Three different case studies were investigated with the aim to propose suitable solutions for the problems mentioned before.

In the case study A, experimental CFRP/CFRP stack drilling tests are performed with a traditional twist drill bit, commonly used in the aircraft industry, and an innovative geometry drill bit. The drilling process is monitored through a multiple sensor system able to acquire thrust force and torque signals during the process. Every ten drilled holes, the tool flank wear is measured using an optical device to obtain the tool wear development curve for each drill bit. An artificial neural network for pattern recognition was developed to find correlations between selected sensor signal features extracted in the time domain and tool wear state, in order to realize cognitive tool wear forecast during the CFRP drilling process (Teti 2015; Alessandra Caggiano, Napolitano, and Teti 2017; Teti et al. 2010). The ANN forecast for both drill bits is evaluated in terms of MSE prediction error.

In the case study B, a CFRP laminate was paired with an Aluminium 2024-O sheet in order to create the multi-material stack configuration. It was drilled using a traditional twist drill bit and the process was monitored through the same multiple sensor system mentioned before, also the procedure for tool wear measurement was the same already mentioned. The cognitive system developed consists in an artificial neural network which has the aim to find correlations between selected sensor signal features, extracted in the time and frequency domain, and tool wear state in order to realize cognitive tool wear diagnosis during the CFRP drilling process.

The main aim of the case study C was to reduce the number of the selected features in order to improve the performance of the cognitive system and to give the basis for the next step which is represented by the implementation of these methodologies in a manufacturing cloud based system.

From the acquired sensor signals, multiple sensorial features are extracted to feed artificial neural network-based machine learning paradigms, and an advanced feature extraction methodology based on Principal Component Analysis (PCA) is implemented to perform sensorial features dimensionality reduction. In this way, a smaller number of q features, the principal component scores, able to describe the variance of the sensorial data, are obtained via linear projection of the original d features into a new space with reduced dimensionality q . By feeding artificial neural networks with the PCA features, an accurate diagnosis of tool flank wear is carried out. The following table (Table 12) reports the summary of the three case studies.

Case Study	Stack configuration	Drill bit geometry	Cutting parameters	Acquired signals
A	CFRP/CFRP	Traditional twist drill bit d = 6.35 mm Innovative step drill bit d = 6.35 mm	See Table 14	Thrust Force, Fz Torque, T
B	Al/CFRP	Traditional twist drill bit d = 6.35 mm	See Table 15	Thrust Force, Fz Torque, T
C	CFRP/CFRP	Traditional twist drill bit d = 4.85 mm	See Table 14	Thrust Force, Fz Torque, T Acoustic Emission RMS, AE Vibration Acceleration RMS, V

Table 12. Summary of the experimental setup for drilling case studies.

4.2 Experimental testing campaign

The experimental testing campaign consists of the realization of 60 consecutive drilled holes under different cutting conditions on CFRP/CFRP stacks or the realization of 30 consecutive drilled holes under different cutting conditions on Al/CFRP stacks. During each drilling the sensor signals were acquired using a multiple sensor system installed on the machine and which will show below. After ten consecutive holes an image of the tool flank was taken using an electronic microscope.

4.2.1 Multiple sensor system setup

The multiple sensor monitoring system employed during the experimental drilling tests is composed of the following sensors (Figure 34):

- Force sensor;
- Torque sensor;
- Acoustic Emission (AE) sensor and Vibration Acceleration sensor (only in the case study C).

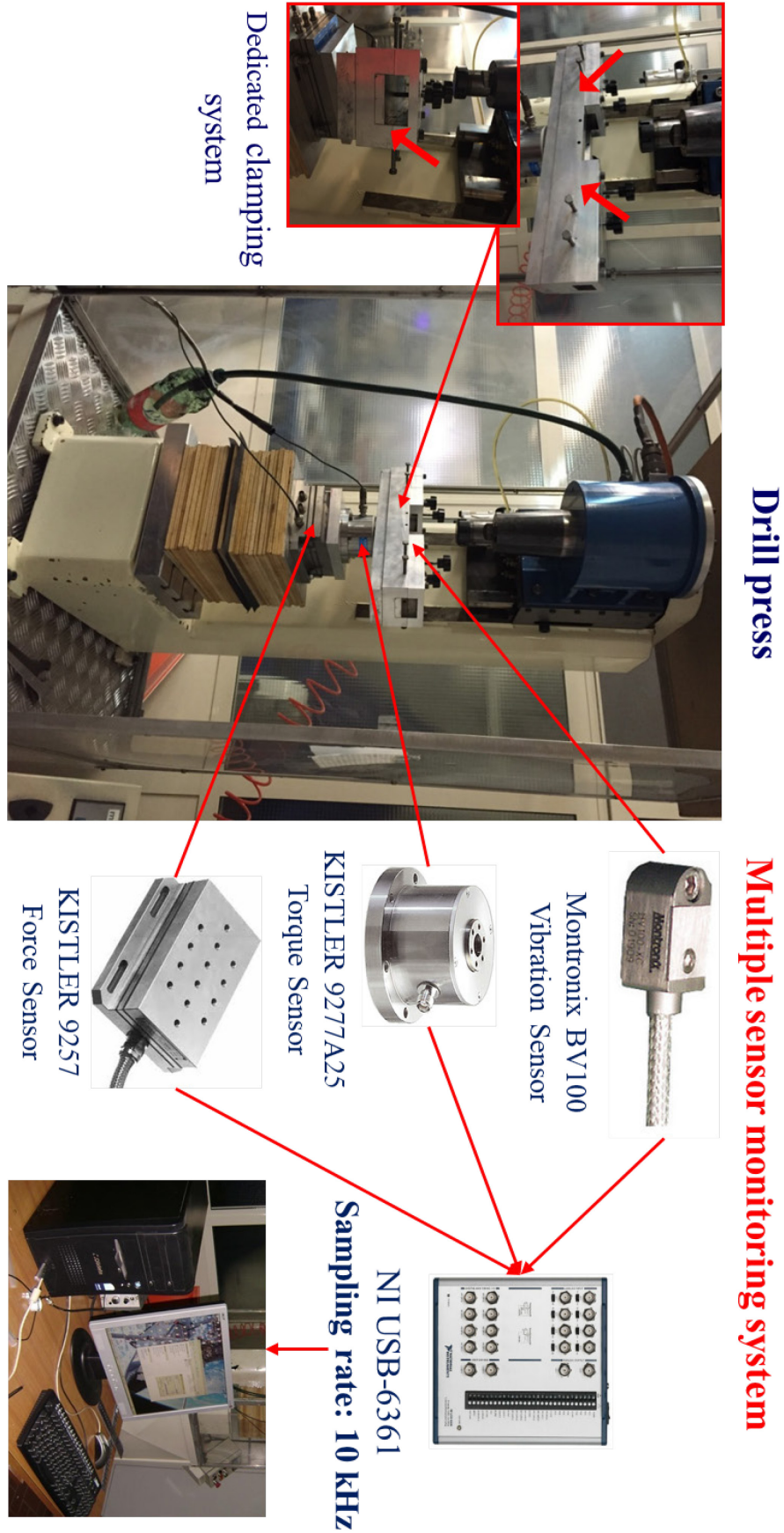


Figure 34. Multiple sensors system for drilling process monitoring setup.

A Kistler 9257 piezoelectric dynamometer was employed to acquire the thrust force along the z-direction, F_z (Figure 35a). The cutting torque about the z axis, T , was acquired using a Kistler 9277A25 piezoelectric dynamometer (Figure 35b).

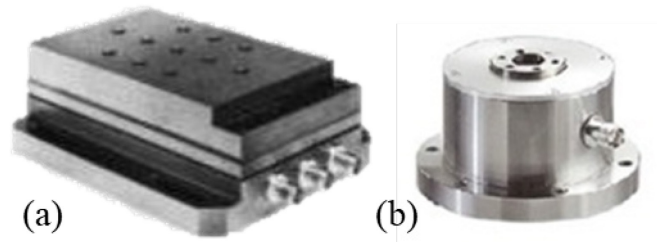


Figure 35. (a) Kistler 9257 piezoelectric dynamometer; (b) Kistler 9277A25 piezoelectric dynamometer.

Two Kistler 5007 amplifiers (Figure 36) were employed for the force and torque signals. The time constant setup was set to “long”. The selected scale in mechanical unit (M.U.) / V was 100. Calibration was necessary for both force and torque after each single drilling test. The transducer sensitivity values to be set are suggested by the technical data sheets of the two piezoelectric dynamometers. As regards force, the values are equal to $-7.5 \text{ pC} / \text{N}$ for the force components along the x and y axes, F_x and F_y , and $-3.5 \text{ pC} / \text{N}$ for the force component along the z axis, F_z , which represents the thrust force of the drilling process. Conversely, the value to be set for the torque component about the z axis, T , is $-2.5 \text{ pC} / \text{Nm}$.



Figure 36. Kistler 5007 amplifiers.

The acoustic emission and vibration acceleration signals were acquired using the Montronix BV100 broadband vibration sensor, provided with two channels to measure both the vibrations and the high frequency acoustic emission (AE) signals. This is the same sensor employed for sensor monitoring

of dry turning process, which was illustrated above (Paragraph 3.2.1), Figure 9 reports the sensor picture and in the Table 5 the specifications of the amplifier are reported.

The setup of the amplifier is shown in Figure 37. It has two channels:

- the yellow on the top (channel 1) is dedicated to the Acceleration signals amplification;
- the red on the bottom (channel 2) is dedicated to the AE signals amplification.

The gain set for Acceleration signals is equal to 2 while the gain set for the AE RMS signals is equal to 10 in order to properly visualize the signals without exceeding the maximum threshold of 10 V imposed by the data acquisition (DAQ) board.

Both the AE and Acceleration signals have been acquired as Root Mean Square (RMS) signals. RMS is a technique used to rectify a RAW signal and convert it to an amplitude envelope, which is easier to view. The rectification process converts all the numbers into positive values rather than positive and negative.

During the experimental tests the RMS conversion time constant was set to $TC1 = \text{short}$, corresponding to a time constant of 0.12 ms. The output low-pass filter cut-off frequency was set to $F3 = \text{high}$ for both channels.

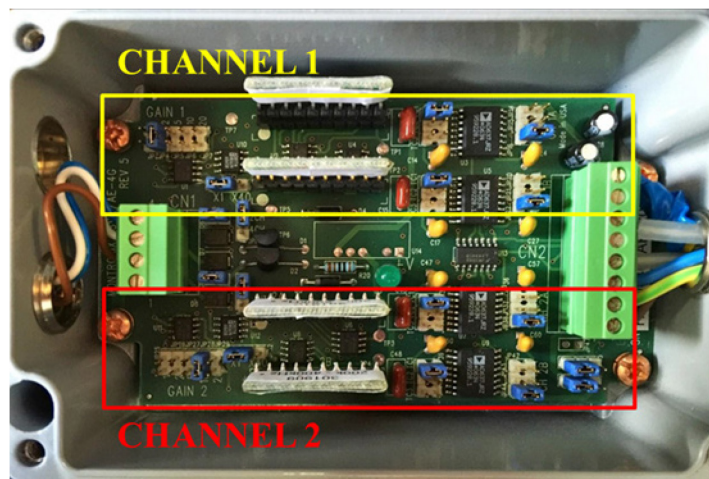


Figure 37. Acoustic Emission and Vibration Acceleration amplifier settings.

The analogue signal from the Thrust Force, cutting Torque, Vibration Acceleration and AERMS sensors were digitized by the National Instruments DAQ device NI USB-6361. It is the same device already mentioned in the Paragraph 3.2.1 (Figure 12), the specifications of the acquisition board are reported in the Table 8. According to the Nyquist-Shannon sampling theorem, the sampling rate was set equal to 10kHz. The data acquisition software used is the NI SignalExpress 2015. The software allows to quickly acquire, analyse and visualize data using the software interface.

4.2.2 Workpiece material

The classification of the composite materials can be made on the basis of multiple criteria. One of the most common classification is according to the type of components used in the realization of the composite material, with particular reference to the type of matrix and the reinforcing fibre type. Since the field of possible applications is mostly influenced by the type of material used for the matrix is commonly used to classify the composite materials according to its characteristics. Due to the excellent physical properties of the final product, the polymer matrix composites, also known as FRP (Fibre Reinforced Plastic), have been widely used in different sectors including aerospace, automotive and civil engineering.

Composite materials can be also distinguished according to the type of reinforcement used. The fibres may be of carbon, glass, steel or aluminium and differ from each other for their mechanical properties (e.g. elastic modulus, breaking strength, specific weight) as well as chemical and electrical properties. It is important to highlight that, with constant Young's modulus, the carbon fibres have a lower density and a resistance six times higher than steel or aluminium.

The most commonly used reinforcing fibres are substantially three: Glass fibres (Fiberglass), Carbon fibres (Carbon fibre) and Aramid fibres (Kevlar).

The Carbon Fibre Reinforced Plastic (CFRP) materials are the widely used composite in aerospace sector mainly for their lightness and resistance (Wilhelm, Commercial, and Company 2001). The advantages of carbon fibres are: high elastic modulus, light weight, high resistance to fatigue and compression, low thermal expansion coefficient, good electrical conductivity, a good resistance to high temperatures (2000°C) in non-oxidizing atmosphere and a good resistance to medium temperatures (400°C) in oxidizing atmosphere. Therefore, the composite materials made up of resin and carbon reinforcements have an excellent combination of low weight, high mechanical strength and high rigidity.

In the last decades there was an increasing percentage of composite materials employed in airplane realization. In general the application of CFRP reduces the overall weight of the airplane, and increases its efficiency and safety, also reducing fuel consumption.

Both the CFRP laminates and the Aluminium alloy, which were employed in different stack configurations, were provided from the industrial partner company Leonardo S.p.A. and belong to real production batches actually employed on the production lines. The setup of the workpiece has the objective to reproduce the real aeronautical industry operating conditions, in which these types of laminates are superimposed and then drilled together to allow the subsequent riveting.

In the case studies A and C the configuration CFRP/CFRP stack under study is composed by two overlaid symmetrical and balanced laminates. Each laminate has a thickness of 5 mm and is made up of 26 prepreg unidirectional plies arranged according to the following stacking sequence $[\pm 45_2/0/90_4/0/90/0_2]_s$. A very thin fiberglass/epoxy ply, reinforced with $0^\circ/90^\circ$ fabric (areal weight 80 g/m²) is laid on the top and bottom of each laminate. The prepreg plies are made of Toray T300 carbon fibres and CYCOM 977-2 epoxy matrix.

Laminates were fabricated by hand layup, vacuum bag moulding (Figure 38a) and autoclave curing (180 min at 180 °C and 6 bar) (Figure 38b).



Figure 38. (a) Vacuum bag moulding; (b) Autoclave.

The surface texture of the laminates on the bag side is very irregular compared to the mould side. Therefore, the two CFRP laminates of each stack were placed with the bag side in contact in order to realize the drilling process in the severest possible conditions (Figure 39).



Figure 39. Laminates profiles and their surface textures.

In the second case study, the Al/CFRP stack configuration proposed is composed by an Aluminium sheet which has a thickness of 2.5 mm and is made of 2024 alloy, and a CFRP laminates which is the same type mentioned above.

Aluminium alloys have strong corrosion resistance characteristics. These alloys are sensitive to high temperatures ranging between 200 and 250°C. An increase in strength takes place when these alloys are exposed at sub-zero temperatures and strength is lost when these alloys are exposed to high temperatures, so they are good low-temperature alloys. These alloys are commonly used in the manufacture of truck wheels, aircraft structures, and screw machine products, scientific instruments, veterinary and orthopaedic braces and equipment, and in rivets. The chemical composition of the Aluminium 2024 alloys and the principal physical, mechanical and thermal properties are outlined in the following tables (Tables 13-14).

Element	Weight (%)
Aluminium, Al	Balanced
Copper, Cu	3.80 - 4.90
Magnesium, Mg	1.20 - 1.80
Manganese, Mn	0.30 - 0.90
Silicon, Si	0.50
Iron, Fe	0.50
Zinc, Zn	0.25
Titanium, Ti	0.15
Chromium, Cr	0.10

Table 13. Chemical composition of the Aluminium 2024 alloy.

Property	Value
Density (g/cm ³)	2.78
Melting point (°C)	510
Tensile strength, ultimate (MPa)	220
Elastic modulus (GPa)	70 - 80
Poisson's ratio	0.33
Thermal expansion in the range 20 - 100 °C (μm/m °C)	22.8
Thermal conductivity at 25°C (W/mK)	193

Table 14. Physical, mechanical and thermal properties of the Aluminium 2024 alloy.

4.2.3 Cutting tool specifications and process parameters

Drilling tools can be divided into different types depending on the processes for which they are designed but the most widely used are the twist-drill bits (Figure 40).

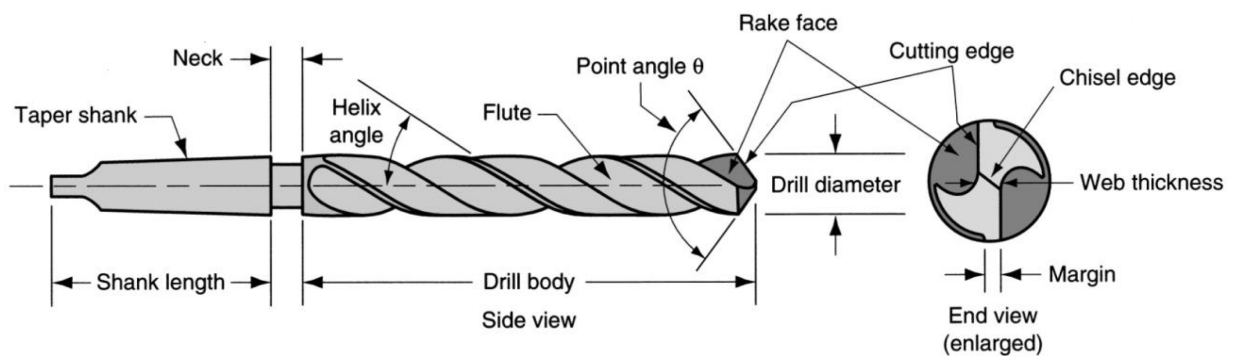


Figure 40. Standard geometry of a twist drill (Mikell P. Groover 2014).

The standard twist drill has two opposite helical grooves. The angle between the spiral flutes and the tool axis is called helix angle, which usually varies between 30° and 35° degrees. The flutes are necessary for the extraction of chips from the hole. Although it is desirable for the flute openings to be large to provide maximum clearance for the chips, the body of the drill must be supported over its length. This support is provided by the web, which is the thickness of the drill between the flutes.

The last part of the body of the twist drill has a conical shape. A typical value for the point angle is 118°. Finally there is the chisel edge. Connected to the chisel edge are two cutting edges (sometimes called lips). The portion of each flute adjacent to the cutting edge acts as the rake face of the tool. The bit is also equipped with margins, which drive the tools into the hole and realizes the finishing of the cylindrical wall. The bit ends, on the other side, with a cylindrical or conical shank, which serves to fix it to the drill spindle.

With the aim to develop a tool with an innovative geometry in order to increase tool life and productivity by reducing the tool wear rate, in the case study A a step drill with innovative geometry was employed. The latter is a 2-flute 6.35 mm diameter with 120° point angle and 20° helix angle made of tungsten carbide (WC) (Figure 41a). In order to have benchmark data in terms of sensor signal features and tool wear, a traditional tool, i.e. a 2-flute 6.35 mm diameter with 125° point angle and 30° helix angle tungsten carbide twist drill (Figure 41b), was also employed.

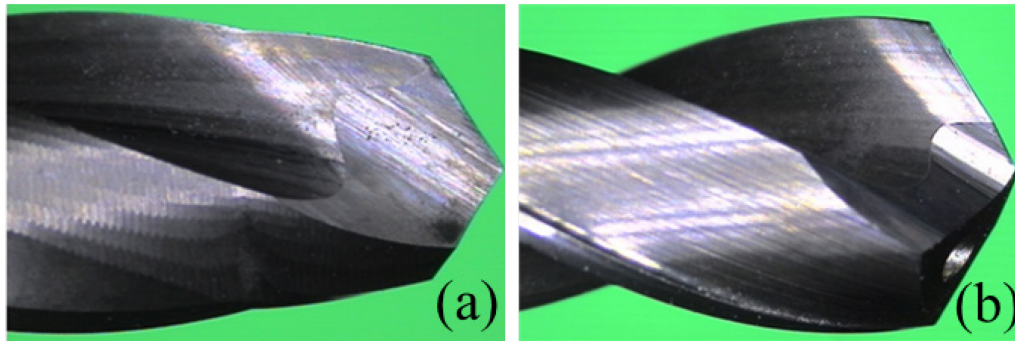


Figure 41. (a) Innovative step drill bit. (b) Traditional twist drill bit.

The same tool, traditional twist drill bit with 6.35 mm diameter was employed in the case study B to carry out drilling operations on Al/CFRP stacks, instead in the case study C the tools employed have a diameter of 4.85 mm and are a scaled model of the traditional twist drill bit already described. Different cutting parameters were adopted for the experimental drilling tests to study the drill bit behaviour under diverse cutting conditions. In the case studies A and C were selected 4 combinations of feed and spindle speed in order to investigate different situations for CFRP/CFRP drilling which requires low spindle speeds and high feed, which is the best condition to avoid the repeated cut of the same carbon fibres, but one of the objectives was to find the best compromise in order to increase the productivity in terms of holes made in the same time (Table 15).

In the case study B, as mentioned before, the main difficulty was to obtain the best compromise for cutting conditions because the drilling process of Aluminium alloys requires relatively high spindle speeds and low feed. The cutting parameters tested are reported in the Table 16. A CNC drilling centre was used for the experimental drilling tests.

Test no.	T1	T2	T3	T4
Spindle speed (rpm)	2700	6000	6000	7500
Feed (mm/rev)	0.11	0.15	0.20	0.20

Table 15. Experimental testing conditions for case studies A and C.

Feed (mm/rev)	Spindle speed (rpm)		
	3000	4500	6000
0.05	X	X	X
0.10	X	X	O
0.15	X	X	O

Table 16. Experimental testing conditions for case study B.

4.3 Tool wear measurement and wear curve construction

The use of a specific cutting tool influences both the quality and the cost of the machined parts. The tool must guarantee the following two properties:

- Material removal action;
- Adequate surface finishing achievement.

One of the main limits during drilling of polymer matrix composites with conventional twist drills such as high speed steel, is the excessive tool wear which are subjected to such tools.

In fact, while a tip of high speed steel can be used for drilling hundreds of holes in carbon steel before completely wear out, the same tool, drilling composite materials is able to drill less than ten holes.

The tool wear, i.e. the progressive removal of material from the tools surface, is linked to the combined effect of high temperature, chemical characteristics of the material and high stresses to which the tool and workpiece are subjected during machining.

The wear mechanisms can be classified as below:

- Wear by abrasion: produced by the sliding of a hard and rough surface on a softer one;
- Wear for bond: originated by the high contact pressures between chip and tool which causes welds between the surfaces in contact;
- Wear by diffusion: produced by the migration of atoms through the tool-chip interface.

The combined effect of mechanical and thermal stresses can cause both chipping, i.e. removal of metal particles near the cutting edge due to impacts or excessive pressures, and plastic deformation due to high temperatures in the cutting zone.

The mechanisms of tool wear can occur on both tool flank (flank wear) and tool crater (crater wear), the two most widely parameters used for tool wear measurement (Figure 42). However flank wear is most commonly used for wear monitoring due to their trend during machining (J. Sheikh-Ahmad and Davim 2011).

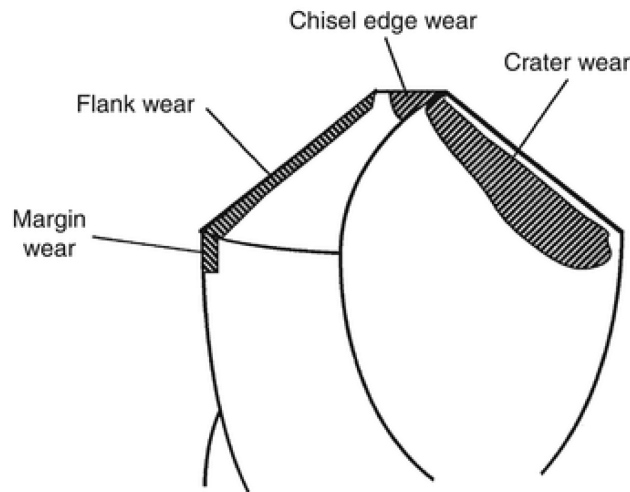


Figure 42. Schematic representation of twist drill (Stephenson and Agapiou 2006).

The first one is the result of a friction between the machined surface of the workpiece and the tool flank. Flank wear appears in the form of so-called wear land and is measured by the width of this wear land, VB. Cutting forces increase significantly with flank wear. The second one is the result of the action of the chip sliding on the tool surface. In Figure 43 the tool wear as a function of cutting time is reported (wear curve). Crater wear follows almost the same growth curve.

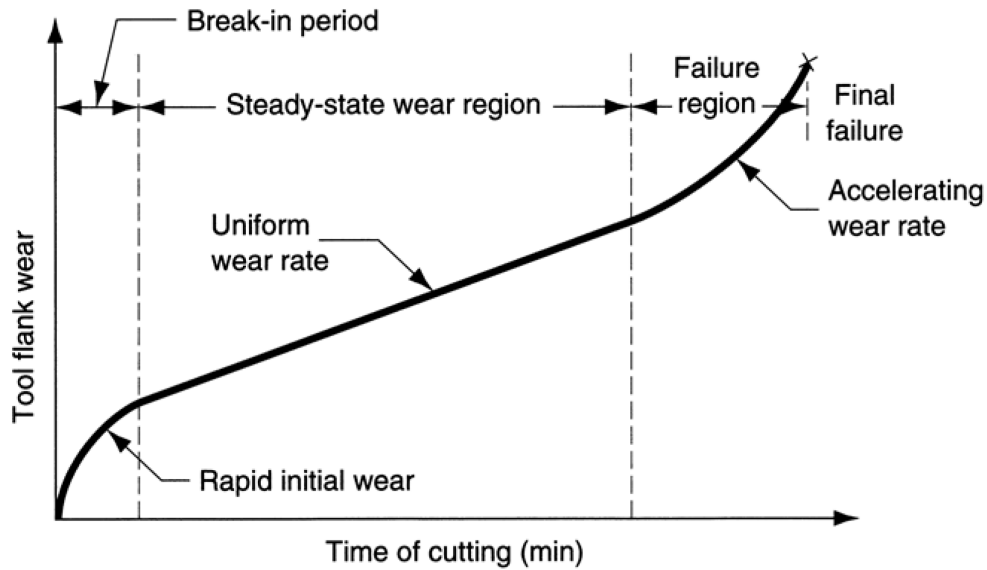


Figure 43. Tool wear as a function of cutting time (Marinov 2004).

As cutting proceeds, the amount of tool wear increases gradually. The tool wear must be lower than a certain limit in order to avoid tool failure, this value is known as tool life (generally in the steady state wear region) and it depends on the operating conditions. The duration of the life of the tool T is defined generally by imposing a limit to the value VB . When this limit is exceeded, the tool must be changed.

Parameters, which affect the rate of tool wear are: cutting conditions (cutting speed V , feed f , depth of cut d), cutting tool geometry (tool orthogonal rake angle), properties of work material.

From these parameters, cutting speed is the most important one. As cutting speed is increased, wear rate increases, so the same wear criterion is reached in less time, i.e. tool life decreases with cutting speed (Figure 44).

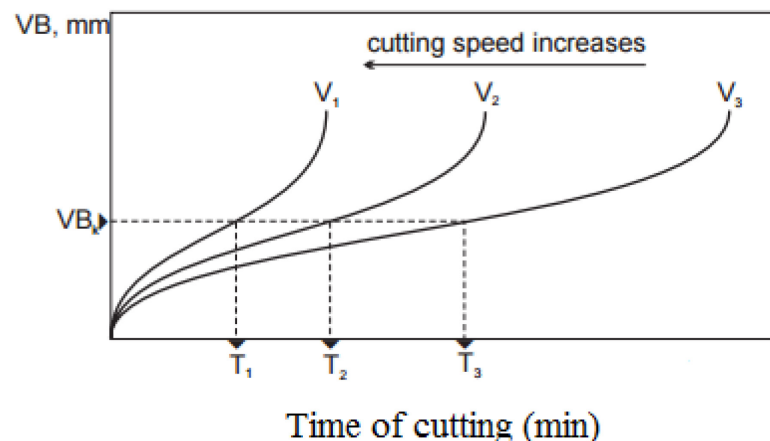


Figure 44. Effect of cutting speed on tool wear and tool life for three cutting speeds.

In general, the tool life can be expressed as:

- a function of the dimensional tolerances permitted on the workpiece;
- as a function of the tolerances of surface roughness of the workpiece;
- as a function of a given parameter for the quality of the holes;
- as a function of the limit fixed for the tool wear.

The most widely used parameter for the monitoring of the tool wear during drilling operations is the flank wear, according to the literature (Park et al. 2011; Zitoune, El Mansori, and Krishnaraj 2013; Zitoune, Krishnaraj, and Collombet 2010). Although it is not possible to do an exact comparison of the two drill bit types due to their different geometries, the flank wear was measured for both of them and used to assess the behaviour of the two different drill bits during the drilling process.

The tool wear measurement operations were carried out during the drilling tests: every 10 holes, a magnified picture of the cutting lip was acquired through an optical measuring machine (Tesa Visio V-200) to measure the flank wear (Figures 45-47).

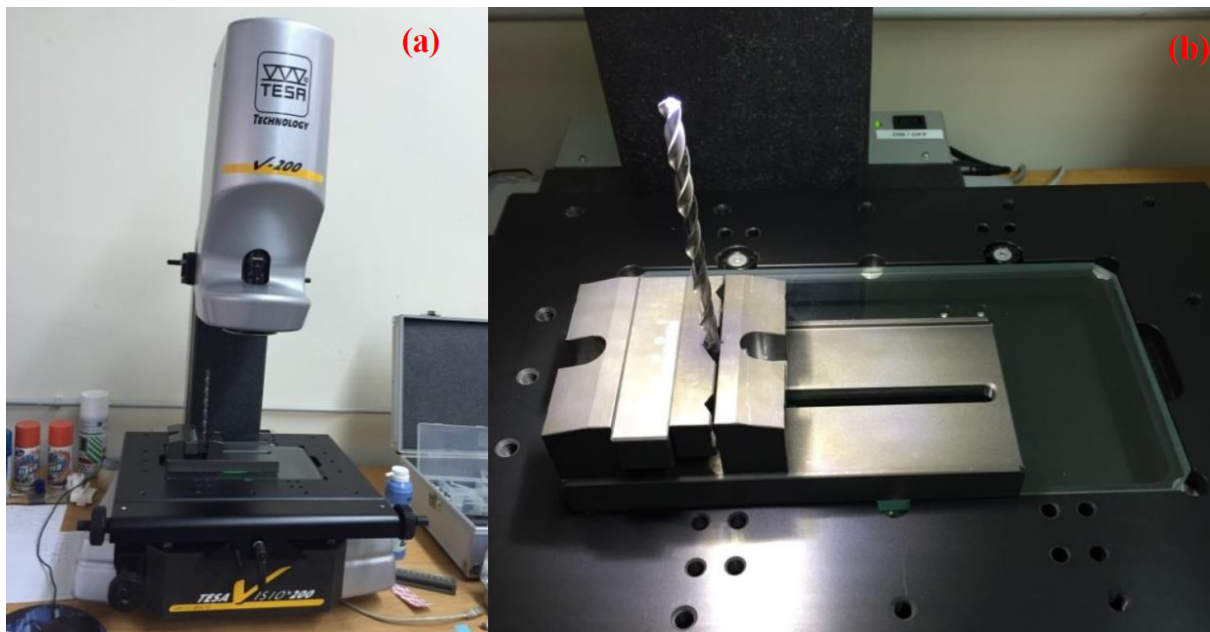


Figure 45. (a) Tesa Visio V-200 optical microscope, (b) clamping system.

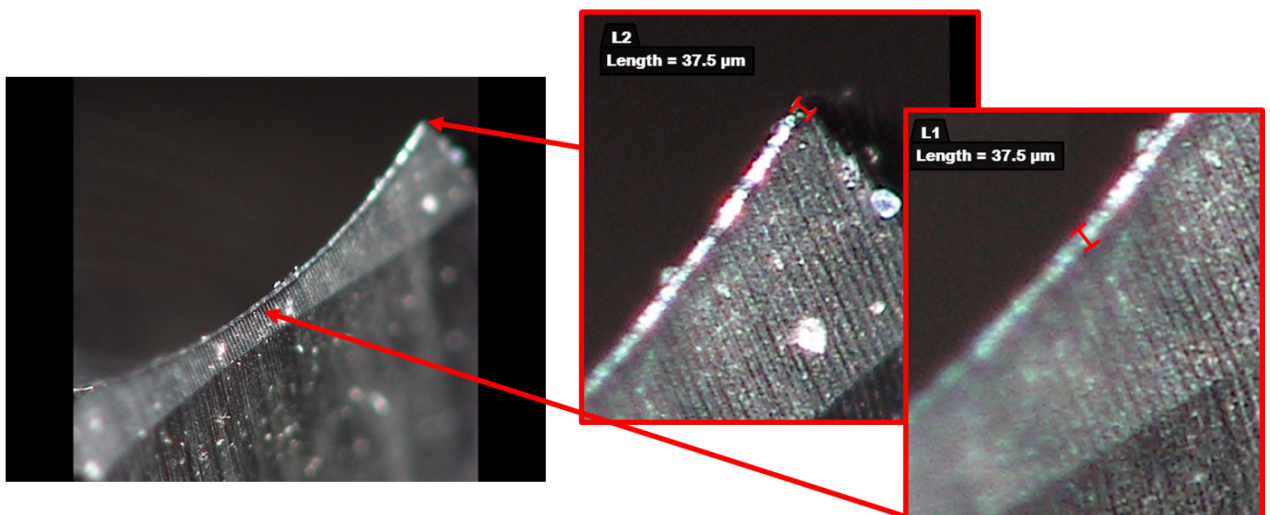


Figure 46. VB max and VB tool wear measurement on innovative drill bit.

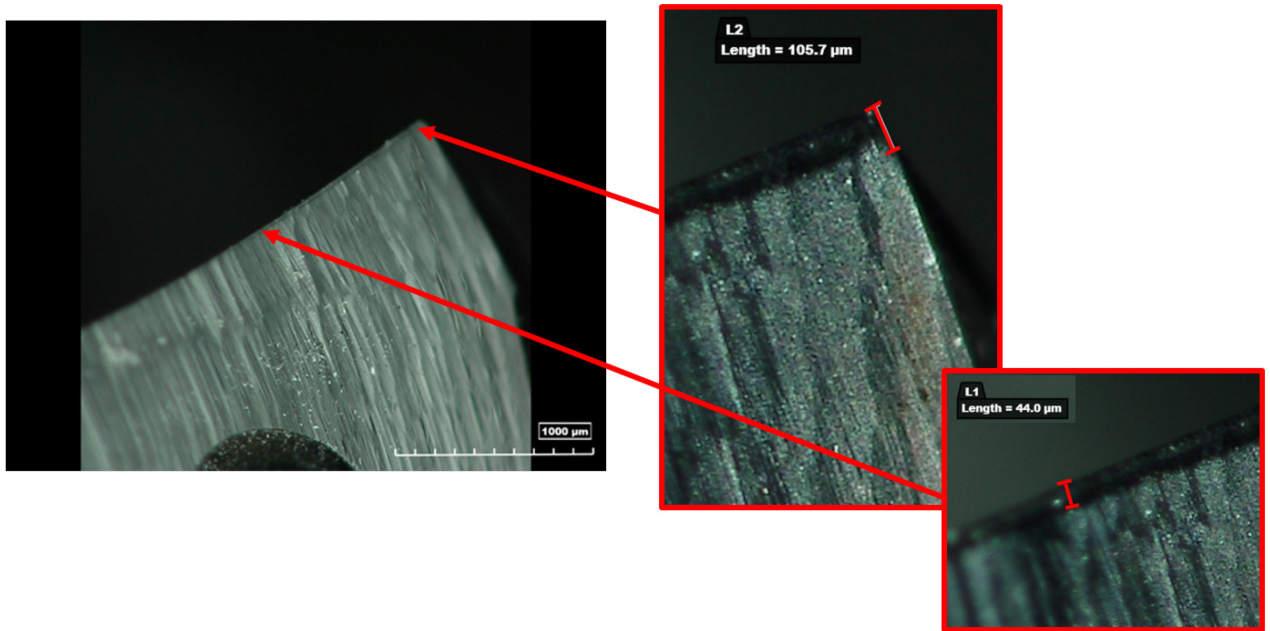


Figure 47. VB max and VB tool wear measurement on traditional drill bit.

In order to make the measuring process repeatable, the drill bits were notched to identify the left and the right side and were fixed on a dedicated clamping device. The flank wear measurement, VB (mm), was taken at $1/6$ of the tool diameter, in accordance with the procedure proposed in (Dolinšek, Šuštaršič, and Kopač 2001; Sousa et al. 2014; J. Y. Sheikh-Ahmad and Davim 2012; A Caggiano et al. 2017) (Figure 48). The measurement was carried out on both left and right cutting lips obtaining 12 VB values for each drilling condition, i.e. one for each cutting lip. By calculating the average of the two VB values, 6 VB mean values were finally obtained. The latter values were used to describe the tool wear development.

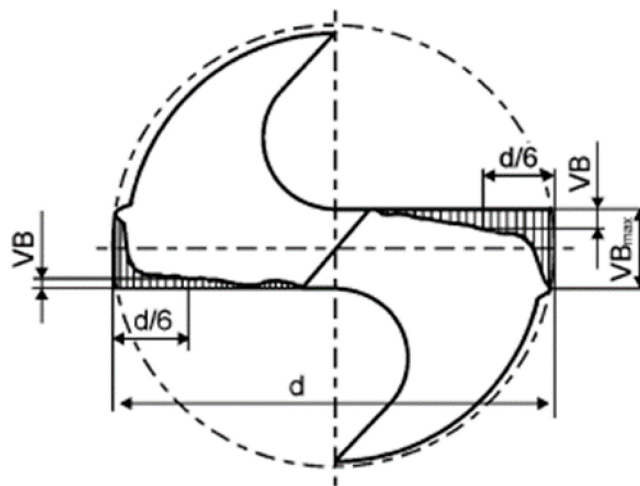


Figure 48. Tool wear measurement scheme for drill bits (Dolinšek, Šuštaršič, and Kopač 2001).

A 3rd order polynomial interpolation of the VB values was applied to construct the tool wear curves to be used for finding correlations between the statistical sensor signal features and the flank tool wear (Figures 49-50).

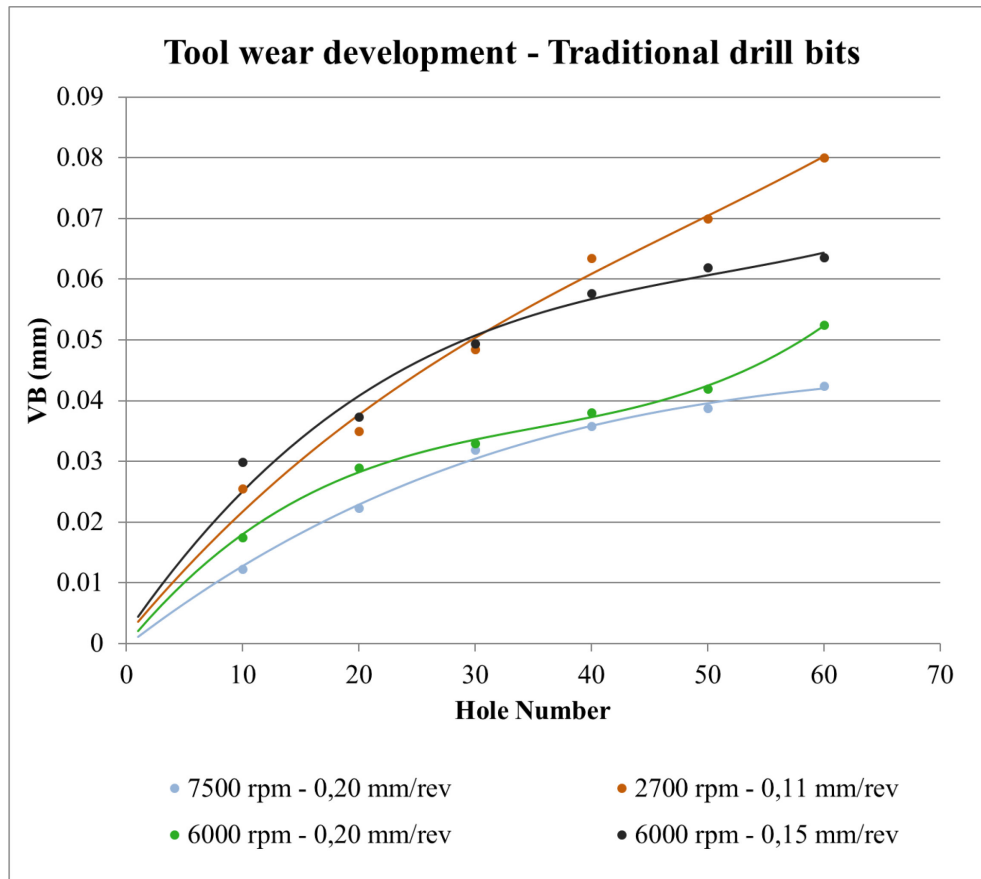


Figure 49. Tool wear values and interpolated curves. Traditional drill bits.

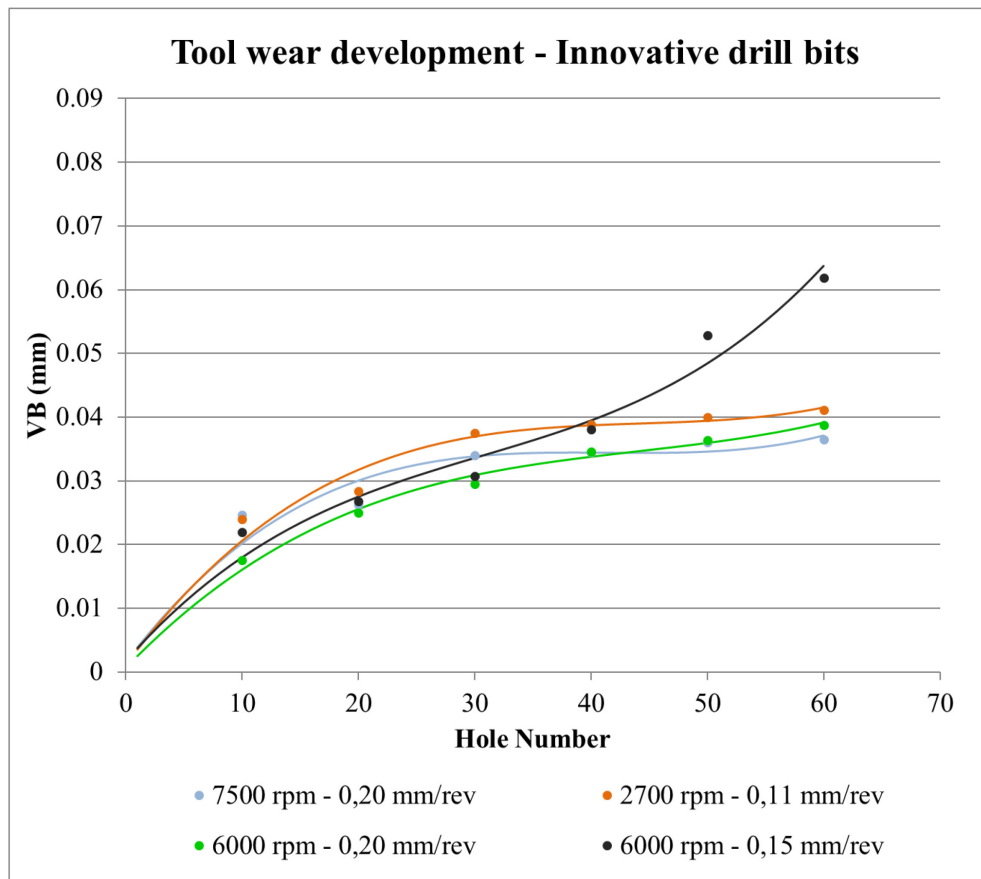


Figure 50. Tool wear values and interpolated curves. Innovative drill bits.

4.4 Signal processing and feature extraction

In this paragraph the whole procedure which was applied for signal analysis is reported. It begins from the segmentation made on the raw signals (Figures 51-54). Once the steady portion of the signals are taken will be performed the analysis in order to extract several sensor features and finally will calculate the Spearman coefficients with the aim to highlight the most correlated features. The final result is the constitution of the Sensor Fusion Pattern Vector which will use to feed the cognitive system.

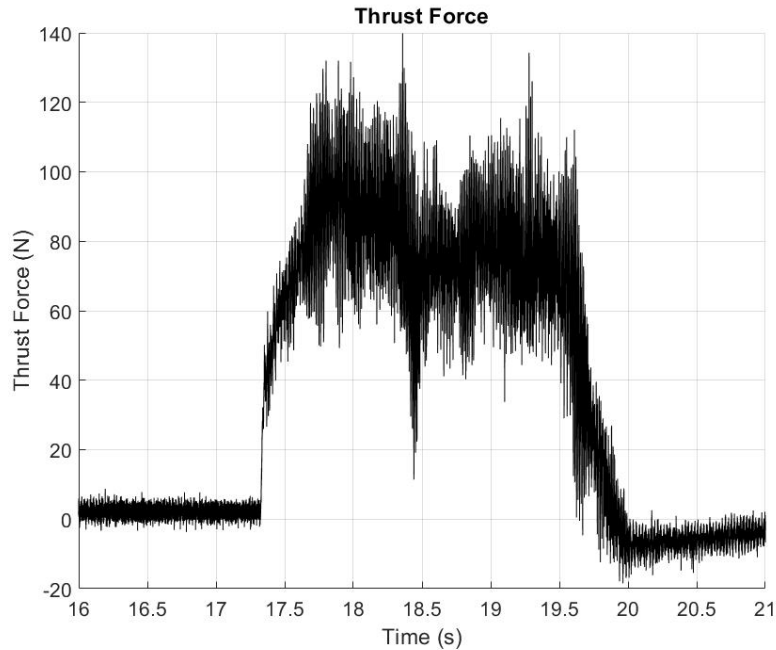


Figure 51. Acquired Thrust Force signal.

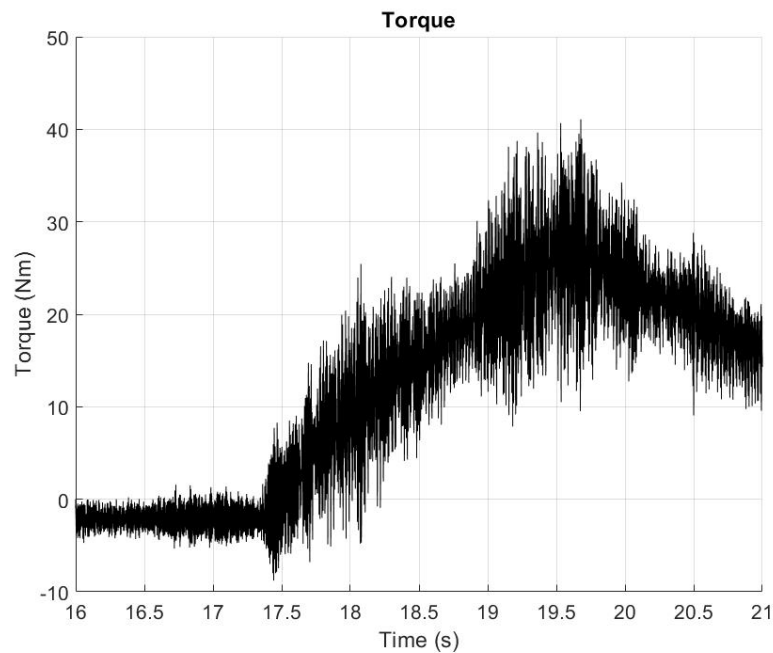


Figure 52. Acquired Torque signal.

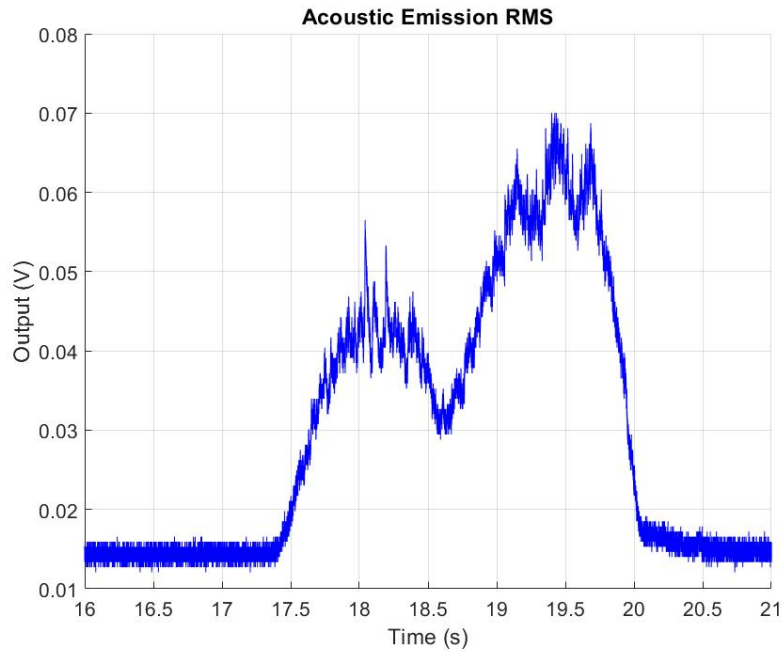


Figure 53. Acquired Acoustic emission RMS signal.

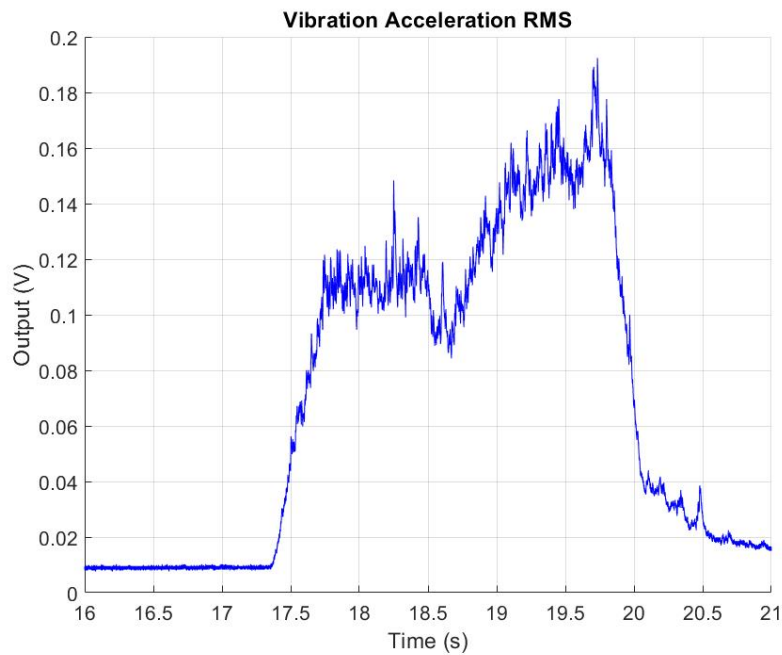


Figure 54. Acquired Vibration Acceleration signal.

4.4.1 Signal segmentation

The signal segmentation procedure was performed on the basis of the thrust force signal and synchronically extended to the torque signal. The automated segmentation procedure to cut out transient signal portions is based on the identification of the machining start point and the machining end point. In order to do that, a smoothing filter based on moving average 150-points window was applied, the objective of the filtering is to remove the high frequency oscillations in order to obtain a signal more linear to be analysed (Figure 55).

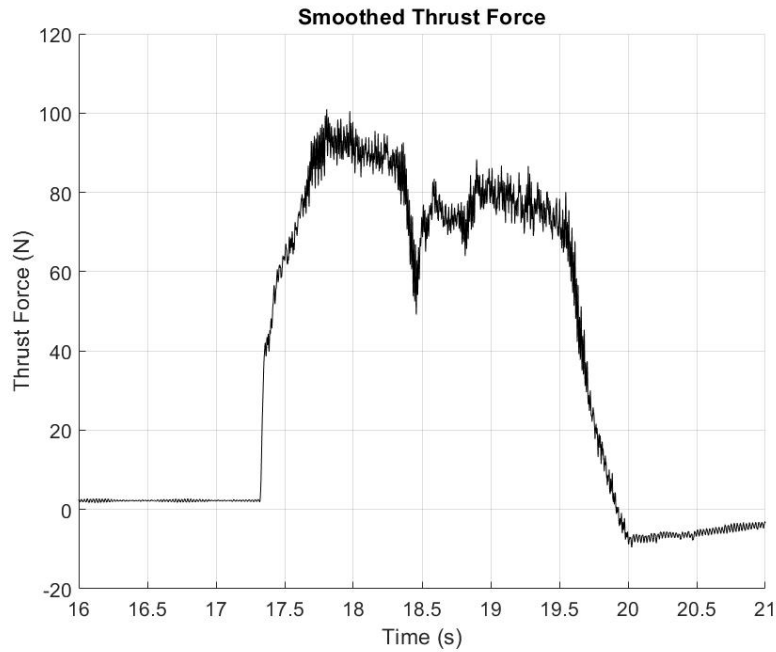


Figure 55. Filtered Thrust Force signal.

Once this signal is available it is possible to highlight the signal level corresponding to the transient portion, the first point over this level becomes the start machining point, the last point over this level becomes the end machining point and they are reported on the acquired signal (Figure 56) in order to obtain the segmented signals (Figures 57-60).

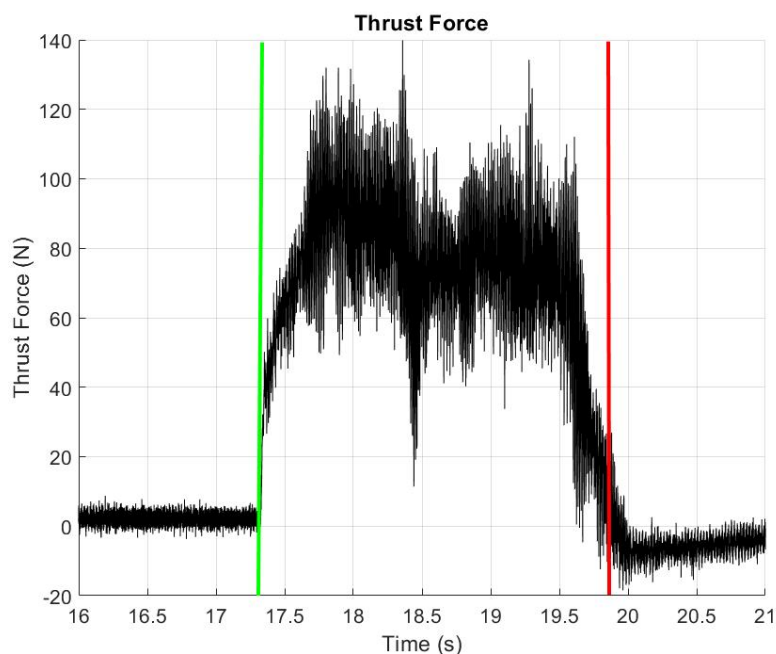


Figure 56. Start point and end point on the acquired Thrust Force signal.

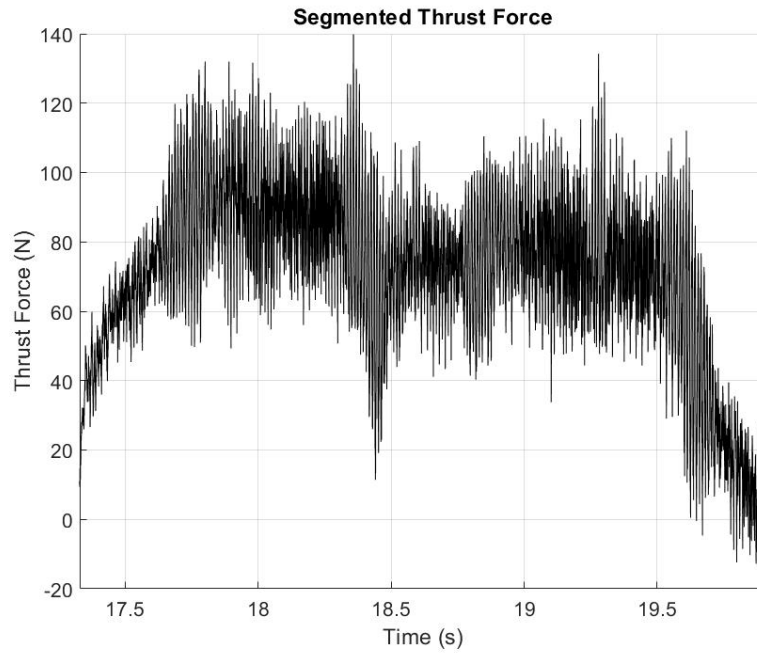


Figure 57. Segmented Thrust Force signal.

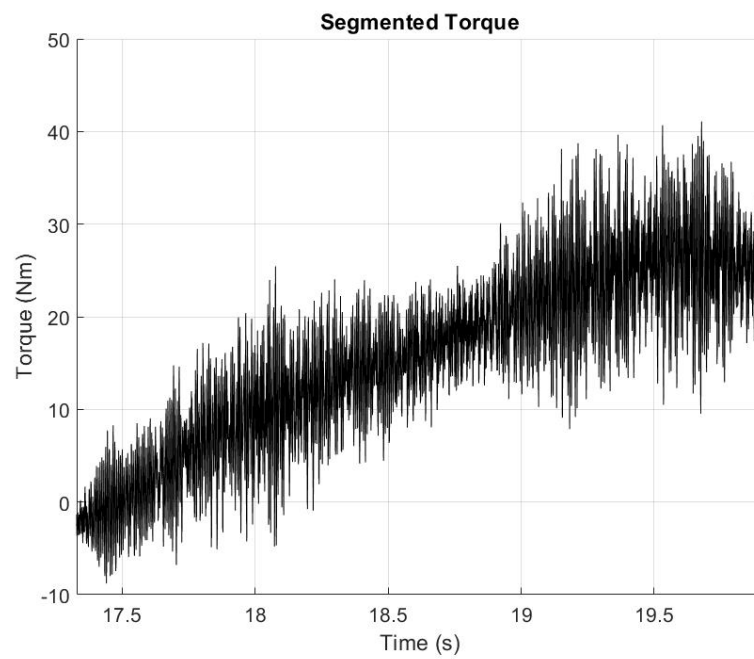


Figure 58. Segmented Torque signal.

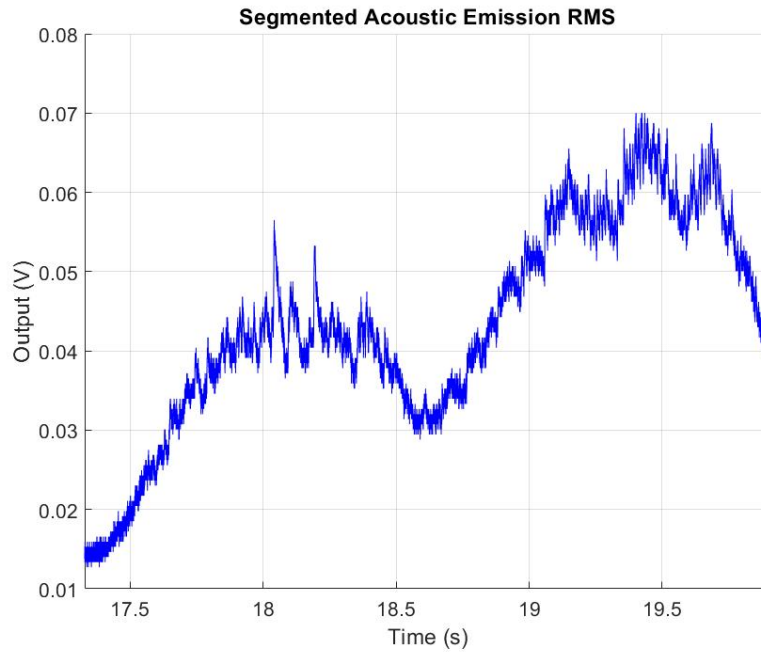


Figure 59. Segmented Acoustic Emission RMS signal.

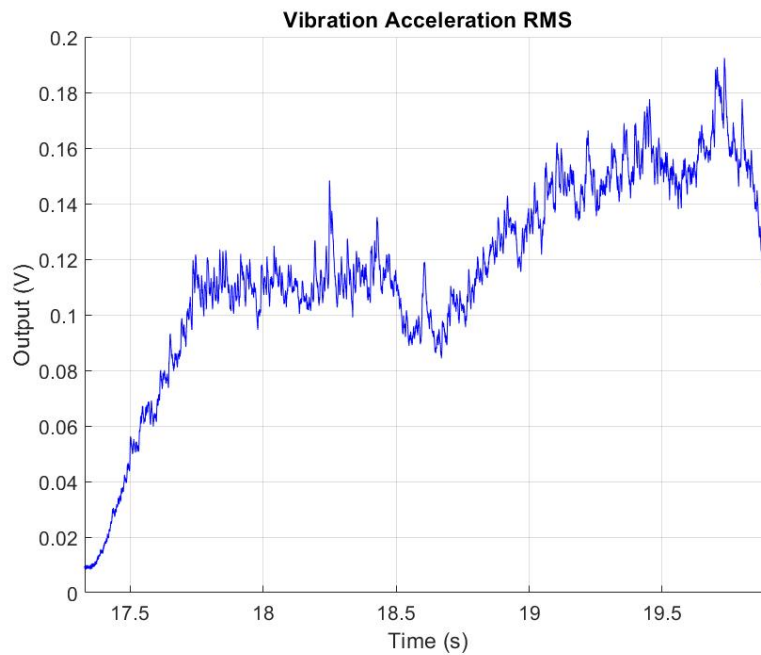


Figure 60. Segmented Vibration Acceleration RMS signal.

4.4.2 Signal features extraction

The isolation of the relevant signal segment allows to perform the extraction of functional sensor signal features that may be correlated with tool state evaluated in terms of flank wear VB. Advanced signal processing, based on signal conditioning, feature extraction and data fusion, was applied to the multiple sensor signals acquired through the monitoring system.

The features were extracted in the time domain for the three case studies, moreover for the case study B also the features in the frequency domain were extracted.

4.4.2.1 Time domain features

The extraction in the time domain was performed using a conventional statistical approach.

Signal analysis in the time domain was performed to extract a number of conventional statistical features from each dataset. The following statistical features were extracted (Figures 61-62) (Binsaeid et al. 2009; Teti et al. 2010):

- Arithmetic Mean: The mean of amplitude values of data signal. It represents the central value of a discrete set of numbers;
- Variance: The variance of amplitude values. It measures how far a set of numbers is spread out;
- Kurtosis: Fourth central moment. It is a measure of the “peakedness” of the probability distribution of the signal raw data;
- Skewness: The 3rd central moment. It is a measure of the asymmetry of the probability distribution of the signal raw data;

The above described features have been plotted for each operating condition and for all the 60 drilled holes. The following figures report, as an example, the values of the statistical features related to the thrust force as a function of the number of drilled holes (Figures 63-66). From a simple visual examination, the values of some of the statistical features seem to increase with increasing number of holes.

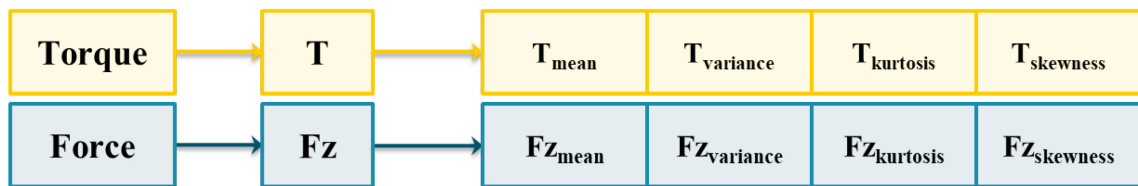


Figure 61. Sensor signal extracted features in the case study A.

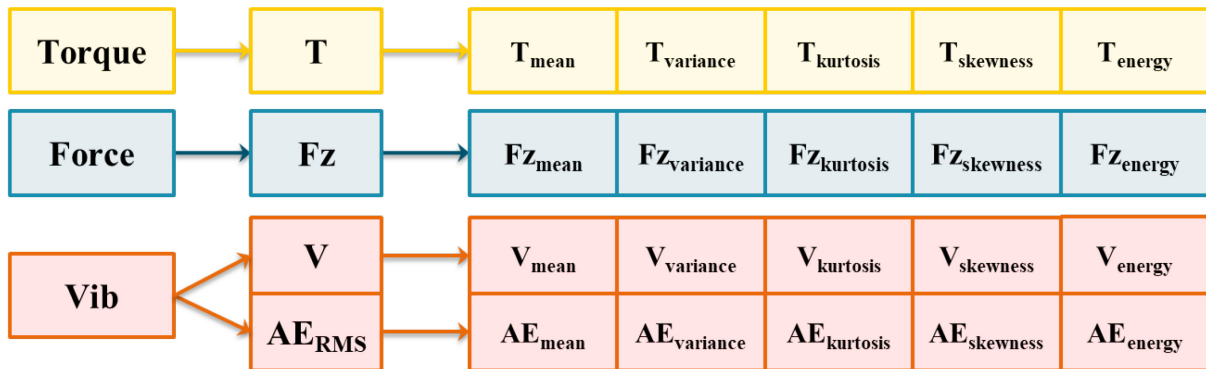


Figure 62. Sensor signal extracted features in the case study C.

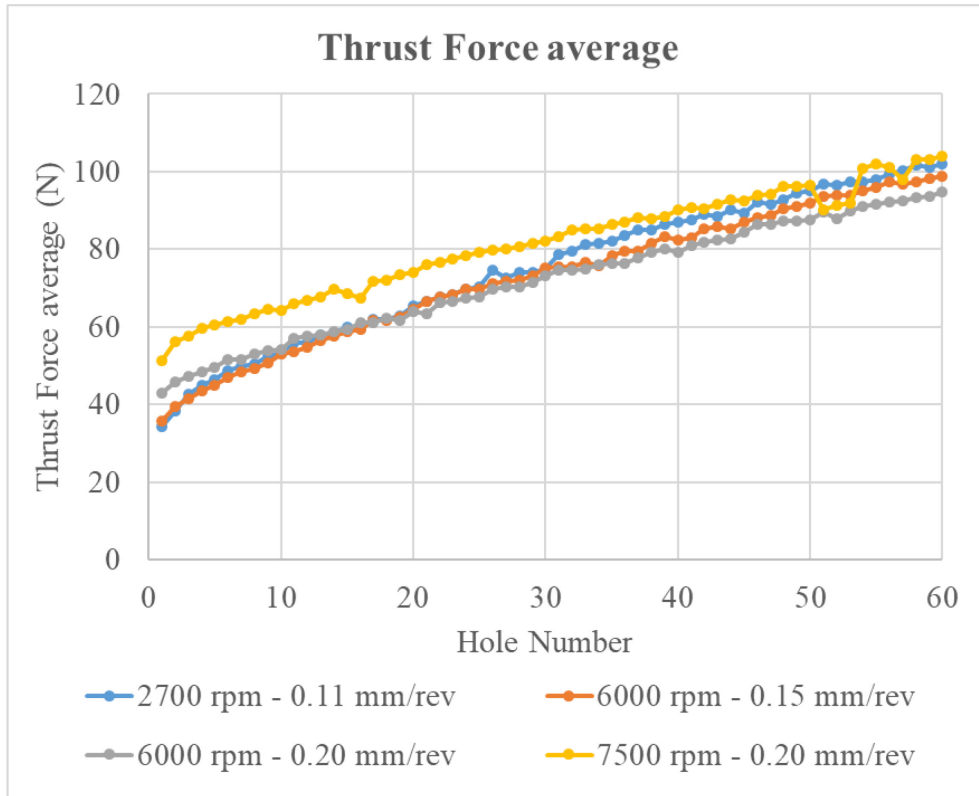


Figure 63. Thrust Force Average for traditional twist drill bit $d = 4.85$ mm.

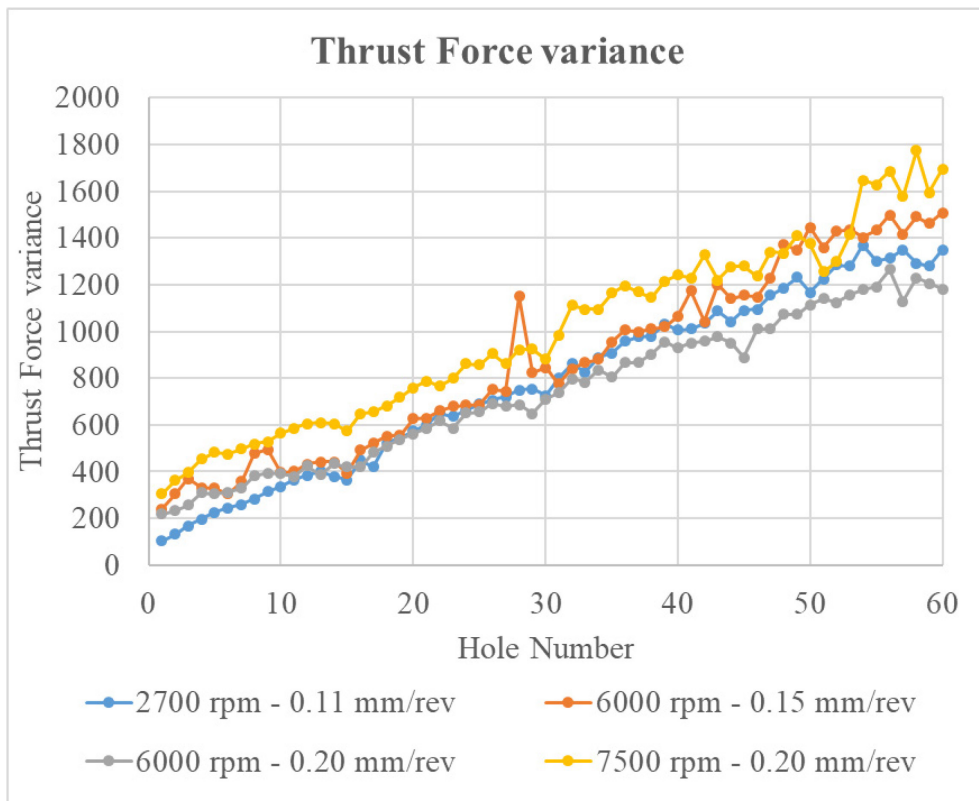


Figure 64. Thrust Force Variance for traditional twist drill bit $d = 4.85$ mm.

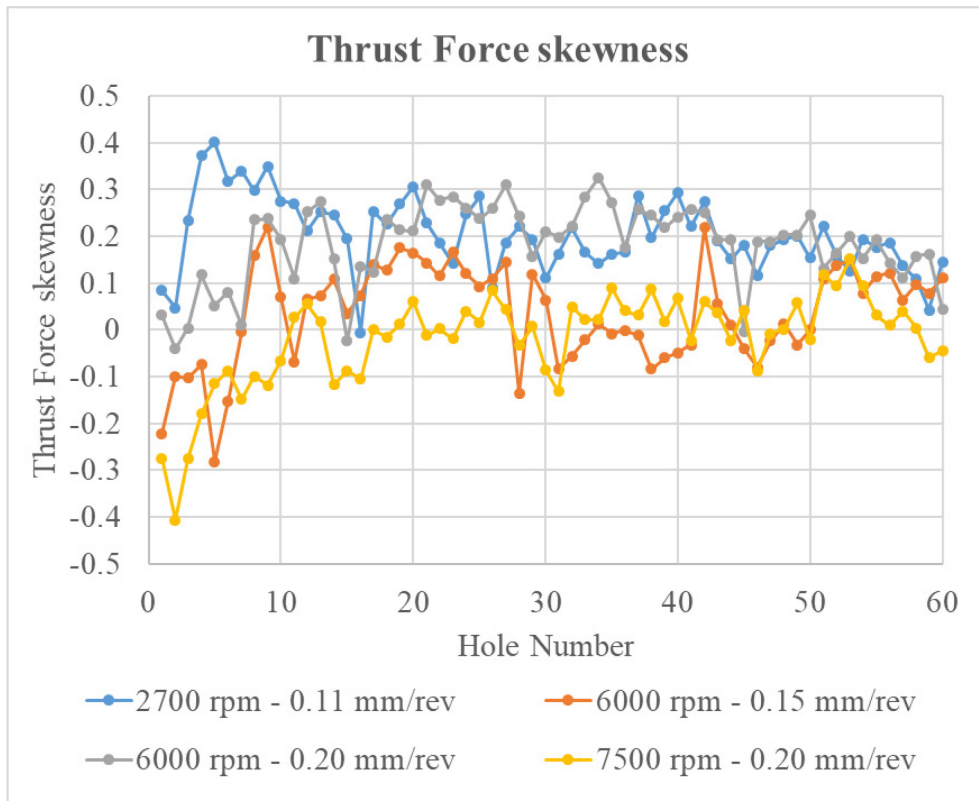


Figure 65. Thrust Force Skewness for traditional twist drill bit $d = 4.85$ mm.

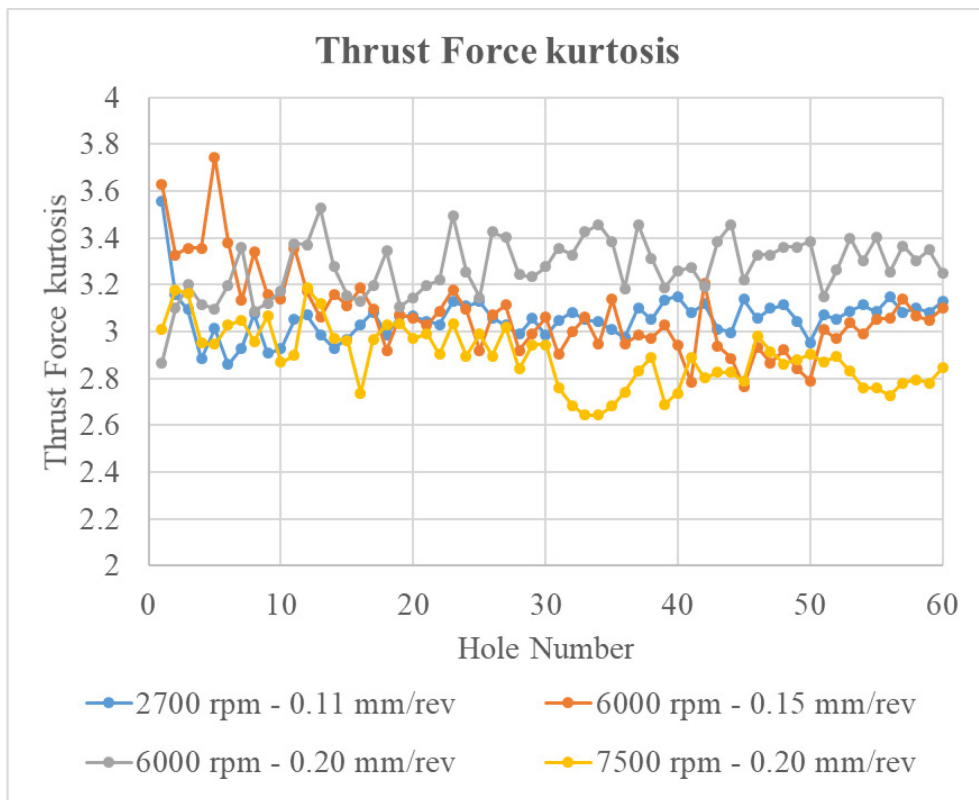


Figure 66. Thrust Force Kurtosis for traditional twist drill bit $d = 4.85$ mm.

4.4.2.2 Frequency domain features

The objective of the frequency domain analysis is to investigate the influence of the multi-layer laminate with different fibres orientations on drilling process.

The acquired signals are highly scattered this behaviour is mainly related to the anisotropic nature of the CFRP laminates.

Different cutting modes can be identified based on the angle formed between the cutting edge and the carbon fibers, also known as fiber cutting angle. In CFRP drilling, the fibre cutting angle varies continuously during a drill revolution and the loading varies accordingly as it depends on the cutting edge geometry and on the cutting modes (Figure 67).

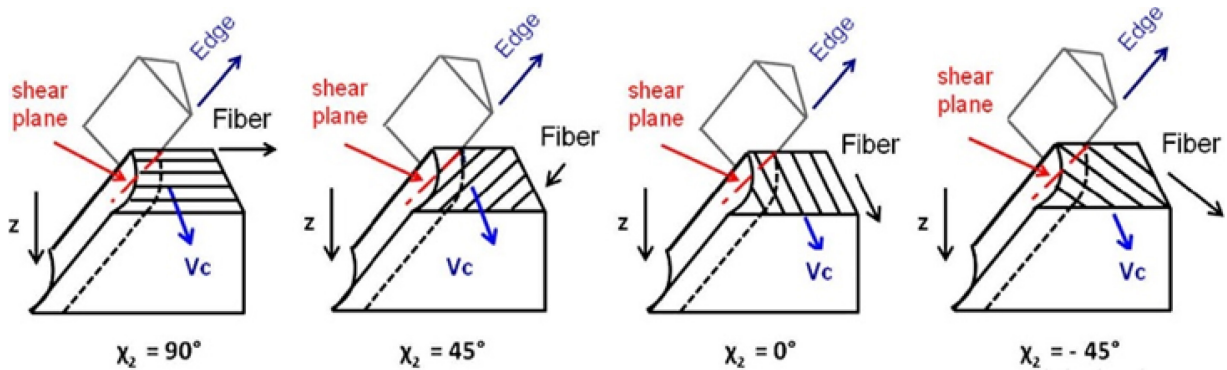


Figure 67. Fibre cutting angle variations during CFRP drilling.

The case of multidirectional CFRP drilling is even more complex: not only the fiber cutting angle varies during the drill rotation, but also different cutting modes occur at the same time along the cutting edge, according to the diverse fiber orientations of the multiple plies simultaneously cut by the drill cutting edge (Figure 68).

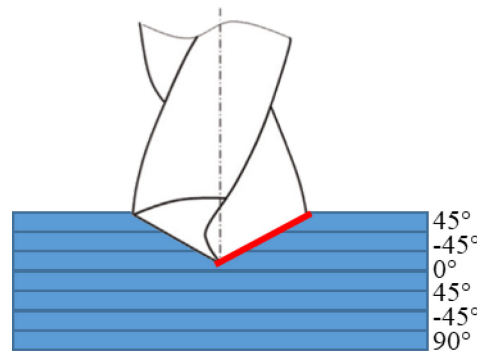


Figure 68. Diverse fiber orientations simultaneously along the cutting edge.

The high amplitude oscillations that can be observed in the signals acquired during stack drilling of multidirectional CFRP laminates are the sum of multiple waves having a phase difference depending on the different orientations of the fibers (e.g. 0° , 45° , 90° , -45°) and amplitude related to the number of plies with same fiber orientations simultaneously cut by the drill cutting edge.

In order to complete the signals analysis, a number of frequency domain features were calculated using the fast Fourier Transform (FFT). More specifically there is a relationship between the peaks obtained in the FFT and the influence of fibre cutting angle during the drilling process. Using the MATLAB function `fft`, the discrete Fourier Transform was calculated for each signal type: Force (Figure 69), Torque. The `fft` function was used to convert the signal to the frequency domain.

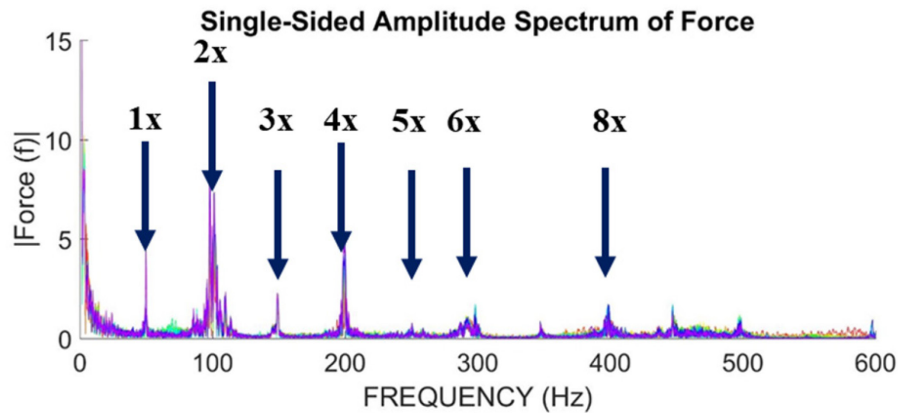


Figure 69. Single-Sided Amplitude Spectrum of the Thrust Force signals acquired in drilling tests at 3000 rpm, 0.15 mm/rev.

This Single-Sided Amplitude Spectrum of Force highlights the presence of some peaks corresponding to different frequency values. Therefore, the peak analysis was conducted to investigate the evolution of the peak values with increasing number of holes. In particular, the frequency peaks corresponding to 1, 2, 3, 4, 5, 6 and 8 times the revolution frequency of the drill bit proved to be relevant for the sensor signals.

Figure 70 shows the values of the peaks at 50, 100, 150, 200, 300 and 400 Hz as a function of the number of holes for the experimental test performed at 3000 rpm and 0.15 mm/rev (the revolution frequency in this case is equal to $3000 \text{ rpm} / 60 = 50 \text{ Hz}$). It can be observed that the amplitude of some of the peaks seem to increase with increasing number of holes.

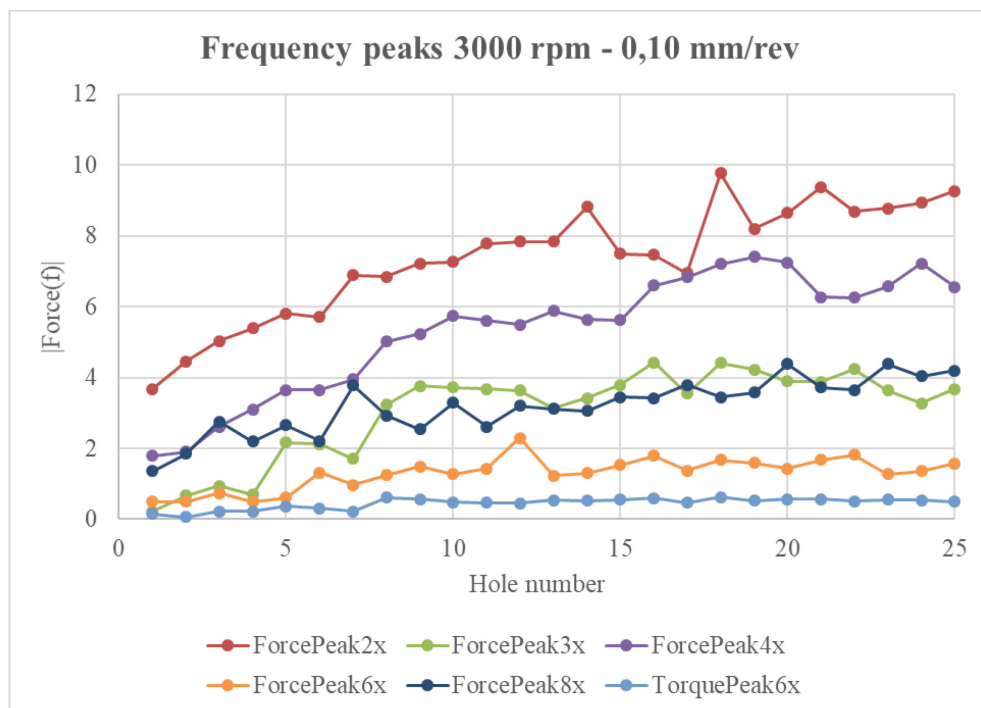


Figure 70. Evolution of peaks detected in frequency domain using discrete Fourier Transform (3000 rpm – 0.15 mm/rev).

The frequency analysis results particularly interesting in the case study B because in this case is possible to differentiate two parts for each signal. As can be seen in the Figure 71 the first portion

of the segmented thrust force signal is related to the drilling of the Aluminium sheet instead the second portion is related to the drilling of the CFRP laminate. By separating these two signal portion is possible to obtain an augmented number of extracted features which can provide important information about the whole drilling process on hybrid stacks an also about the effects and the weight of each single portion during drilling. The sensor signal features extracted in the second case study by doing the time domain analysis on the whole process and on the single signal portion, and extracted performing the frequency domain analysis are reported in the following figure (Figure 72).

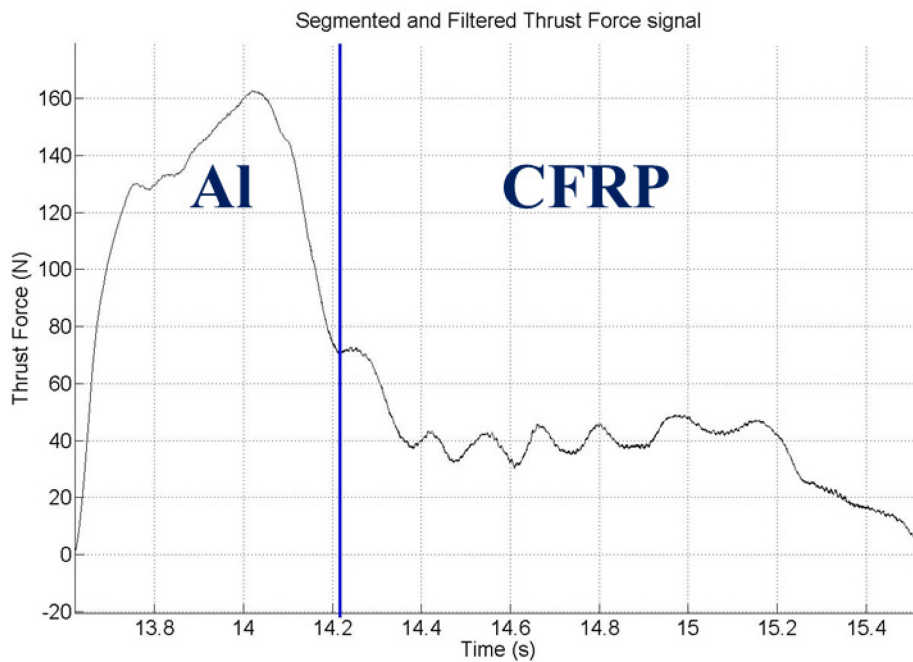


Figure 71. Segmented and filtered thrust force signal with separation line for Aluminium drilling portion and CFRP drilling portion.

4.4.3 Signal features selection

The signal feature extraction procedure generated four features for each acquired signal. In order to identify the most relevant features for tool wear monitoring scope a proper selection method has to be used. For all the three case studies a statistical approach based on the calculation of the Spearman correlation coefficient was employed to evaluate the correlation between the extracted features and the corresponding tool wear values.

Based on the coefficient values, in the case study A only 5 out of all the extracted features showed a strong correlation with tool wear:

- thrust force average ($F_{z,avg}$),
- torque average (T_{avg}),
- thrust force variance ($F_{z,var}$),
- torque variance (T_{var}),
- thrust force kurtosis ($F_{z,kurt}$).

The selected statistical features were employed to construct, for each drilling condition, 60 sensor fusion feature pattern vectors (SFPVs), i.e. one for each drilled hole. Each SFPV was built by combining the selected statistical signal features and the corresponding hole number, n . The resulting SFPV is:

$$SFPV_A = [F_{z,avg}, T_{avg}, F_{z,var}, T_{var}, F_{z,kurt}, n];$$

In the case study C, based on the coefficient values, 8 features showed a strong correlation with the tool wear:

- thrust force average ($F_{z,avg}$),
- torque average (T_{avg}),
- thrust force variance ($F_{z,var}$),
- torque variance (T_{var}),
- acoustic emission variance ($AE_{RMS,var}$),
- torque skewness (T_{ske}),
- acoustic emission skewness ($AE_{RMS,sk}$),
- acoustic emission kurtosis ($AE_{RMS,kur}$).

Sensor fusion is realized by combining features from sensor signals of different nature to construct Feature Pattern Vectors (FPVs) that can be fed to cognitive paradigms for pattern recognition and decision making.

In the case study B any SFPV was constructed but was performed an investigation on the diverse methods which were proposed. The result is represented by a list of features having a strong correlation (Table 17). It can be observed the presence of statistical features in the time domain extracted from the overall signal (orange cells), from the Aluminium signal portion (blue cells) and from the CFRP signal portion (green cells), and also features extracted from the frequency domain analysis (yellow cells).

Feature	Spearman coefficient value
FZ _{avCFRP}	0,97
FZ _{av}	0,97
FZ _{avAl}	0,95
FZ _{varAl}	0,94
FZ _{avCFRP}	0,93
FZ _{peak2x}	0,92
FZ _{peak2xCFRP}	0,91
T _{avCFRP}	0,85
T _{av}	0,82
FZ _{peak4x}	0,77
FZ _{peak4xCFRP}	0,77

Table 17. List of most correlated features (case study B).

4.4.3.1 Feature dimensionality reduction

In machine learning, it is essential to reduce the feature set dimensionality to simplify modelling, decrease the problem complexity and reduce the training time. Simpler models are also more robust on small datasets and are less affected by variance due to noise or outliers. However, to avoid loss of information, suitable techniques of feature selection (to select a subset of significant features) and feature extraction (to generate a lower number of new features from the initial ones) are required (Bishop 1995; Alpaydin 2014).

In the case study C, feature set dimensionality reduction was performed on the sensor signal features by using an initial supervised feature selection method to cut off irrelevant features followed by an unsupervised feature extraction method based on linear projection via Principal Components Analysis (PCA) to combine the relevant features into fewer new features.

The initial features selection based on the Spearman coefficient calculation of the statistical features extracted in the time domain was illustrated above. So using the filter method for feature selection, the number of features was initially cut from 20 to 8 features by removing those which did not exhibit a robust correlation with tool wear.

With the aim to further decrease the number of features and hence reduce the feature set dimensionality without going through any loss of information, a feature extraction method based on linear projection via Principal Components Analysis (PCA) was adopted (Joliffe 2002; Bishop 1995; Alpaydin 2014). PCA consists in an unsupervised linear projection allowing to perform a mapping from the input vectors x in the original d -dimensional space to new vectors z in the q -dimensional space (with $q < d$), with minimum loss of information. In practice, PCA identifies new variables along new directions, namely the principal components, that are linear combinations of the original variables. PCA is an unsupervised technique since it does not utilize the output data.

The criterion to be maximized is the variance. The principal components are computed as the normalized eigenvectors of the covariance matrix of the original variables and ranked according to how much of the variation existing in the data they comprehend. The first principal component, PC1, is the eigenvector of the covariance matrix of the input sample with the largest eigenvalue, that is the direction along which the samples show the largest variation. The second principal component, PC2, is the direction, uncorrelated to the first component, with the largest eigenvalue, and so on. The positions of each observation in this new coordinate system of principal components are called scores and are linear combinations of the original variables and the relative weights.

Given a set of data vectors in a d -dimensional space, if the first q eigenvalues have significantly larger values than the remaining $d-q$ eigenvalues, it means that the data can be represented to a relatively high accuracy by projection onto the first q eigenvectors. If the dimensions are highly

correlated, there will be few eigenvectors with large eigenvalues, hence q will be much smaller than d and a notable dimensionality reduction may be achieved. If the dimensions are not correlated, q will be as large as d and PCA is not helpful.

In this case study, PCA was applied via Singular Value Decomposition (SVD), which is a computationally efficient method for determining principal components. Through linear projection from the $d = 8$ original statistical features, $d = 8$ principal components were generated (named PC1, ..., PC8).

To decide the suitable size of q ($q < d$) allowing for feature reduction without loss of important information, visual analysis through the scree graph technique was employed. The scree graph is the plot of variance explained (i.e. the eigenvalues of the covariance matrix of x) as a function of the number of eigenvectors (i.e. the principal components). When the plot takes a bend displaying an “elbow”, it indicates that adding another eigenvector does not considerably increase the variance explained. Figure 73 shows the scree plot reporting the variance explained as a function of the principal components for all the drilling tests. The plot elbows suggest that a number of $q = 2$ components is sufficient to describe the variance of the data. Hence, for all the drilling tests, the first 2 principal components were selected to be used for machine learning.

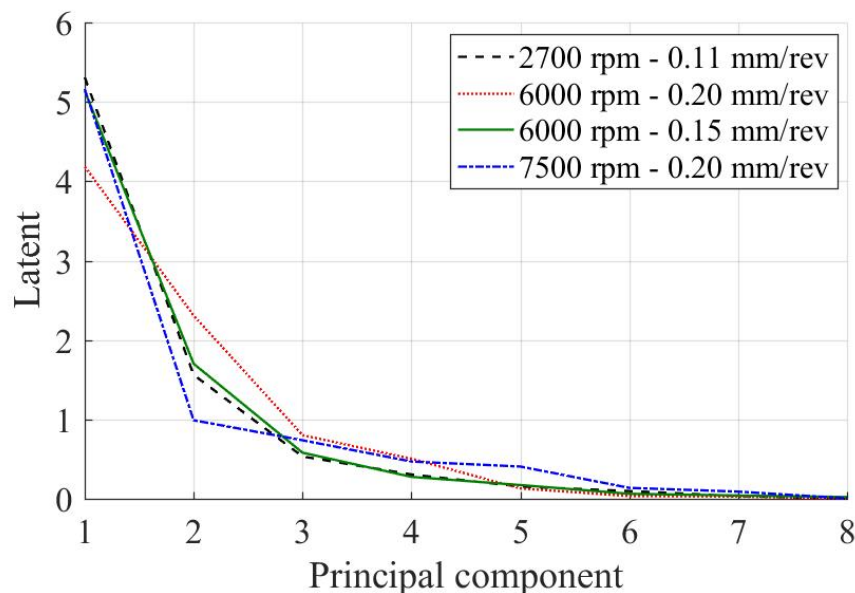


Figure 73. Scree plot reporting the variance explained as a function of the principal components for all the drilling tests.

Specifically, the scores, i.e. the representations of the original data in the principal component space, corresponding to the first 2 principal components were used as input for machine learning. The principal components scores are sensor fusion features, as they are linear combinations of the original features extracted from the multiple sensor signals of different nature (in this case force, torque and acoustic emission).

In this way, a significant dimensionality reduction by one order of magnitude was achieved, decreasing the number of required features from the initial 20 statistical features to 8 features via statistical correlation and finally to 2 features via PCA. Irrelevant features were cut off and the significant ones were combined to retain important information.

In practice, each of the 4 experimental tests in Table 12 was initially represented by a set of $n = 60$ data vectors (where $n = 60$ is the number of holes) in a 20-dimensional space ($d = 20$ features for

each hole). After the implementation of the PCA method, the data set for each experimental test was drastically reduced to a set of $n = 60$ vectors in a smaller 2-dimensional space ($q = 2$ principal components for each hole n).

Graphical analysis of the first principal component scores plotted together with the corresponding tool wear value, VB, shows that the behaviour with increasing hole number is in agreement with tool wear development. Figure 74 illustrates the PC1 scores and the tool wear values for the drilling test carried out at $v = 6000$ rpm and $f = 0.15$ mm/rev.

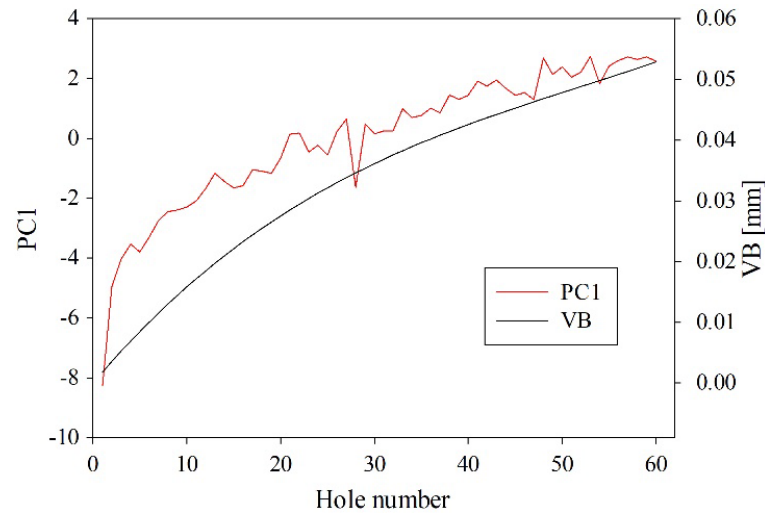


Figure 74. Scores of the first principal component, PC1, and measured tool wear values, VB, vs hole no. for test T3 ($v = 6000$ rpm, $f = 0.15$ mm/rev).

4.5 Tool wear curve reconstruction through intelligent methods

In the case study B the investigation ends with the evaluation of the signal features correlation. In the other two cases, for each situation, a cognitive decision-making support system able to provide a diagnosis on tool wear state can be fed with the selected sensor signal features. These systems allow to select the appropriate corrective actions such as emergency stop of the machine, tool replacement or adaptive change of the process parameters.

The SFPVs should be correlated with tool wear state through cognitive pattern recognition based on three-layer cascade-forward backpropagation artificial neural networks (ANN) using the Levenberg-Marquardt training algorithm (Teti 2015).

Each SFPV was associated to its matching flank wear value (VB) to create input-output vectors for ANN learning (Figure 75). For each drilling condition, 60 input-output vectors (i.e. one for each drilled hole) were built to form the related set for ANN training and testing according to the procedure described below (Paragraph 4.6).

The final aim is to perform tool wear forecast based on a training set consisting of the first $m < 60$ input-output vectors.

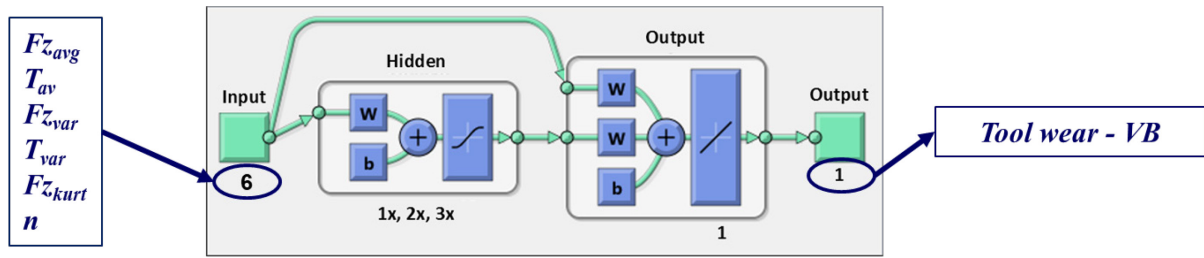


Figure 75. ANN architecture proposed in the case study A.

To evaluate the capability of the ANN procedure to correctly forecast the upcoming tool wear values based on a limited number of initial training input-output vectors and determine the minimum number of vectors necessary to obtain a reliable tool wear forecast, the number, m , of input-output vectors used for ANN training was regularly incremented by steps of 10 from $m = 20$ to $m = 50$.

For each m value, the following procedure for tool wear forecast was adopted. Initially, a training set made of the first m input-output vectors is employed for ANN training, and the prediction of the $m+1$ tool wear value is performed by the ANN. Then, the predicted tool wear value is associated to the corresponding SFPV to build the $m+1$ input-output vector, which is added to the initial training set. The incremented training set is used to train the ANN again and to predict the $m+2$ tool wear value. This procedure is repeated over and over until the total number of 60 holes is reached.

The overall pattern recognition performance for a given m value is eventually estimated by combining all the recognition rates obtained through the described recursive procedure.

In the case study C the two selected PCA features, PC1 and PC2, were employed to construct sensor fusion feature pattern vectors (SFPVs) to be fed to the ANN for pattern recognition.

For each hole a 3-feature SFPV was built by combining the first two PCA features with the hole number, n :

$$\text{SFPV}_C = [\text{PC1}, \text{PC2}, n].$$

Where n is the specific hole number. In this way, for each drilling test of Table 12, a learning set consisting of a number of $i = 60$ SFPVs, equal to the number of holes, was set up.

Supervised machine learning was implemented for each drilling test by associating each 3-feature SFPV to the corresponding flank wear value, VB.

Three-layer cascade-forward backpropagation ANNs were built with a number of input layer nodes equal to 3, that is the number of input features of each SFPV, and varying the numbers of hidden layer nodes between 3, 6, and 9 nodes, i.e. 1x, 2x and 3x the number of input layer nodes, with the objective to find the best ANN configuration providing the highest performance rate. The output layer had a number of nodes equal to 1, corresponding to the tool wear value, VB.

The Levenberg-Marquardt optimization algorithm was chosen for ANN training. ANN cross-validation was performed through the leave- k -out method with $k = 1$ (Lewandowski 2015) (Figure 76). According to the leave- k -out method, at each step, $k = 1$ SFPV was removed in turn from the original set of n SFPVs and used for ANN testing while the remaining $n-k$ SFPVs were used for training. This procedure was repeated for all the n SFPVs and the overall pattern recognition performance was eventually estimated by aggregating the n recognition rates obtained.

The final aim is to estimate the tool wear through cognitive pattern recognition based on the input PCA features extracted from the sensor signals, a machine learning model based on artificial neural networks (ANN) was developed.

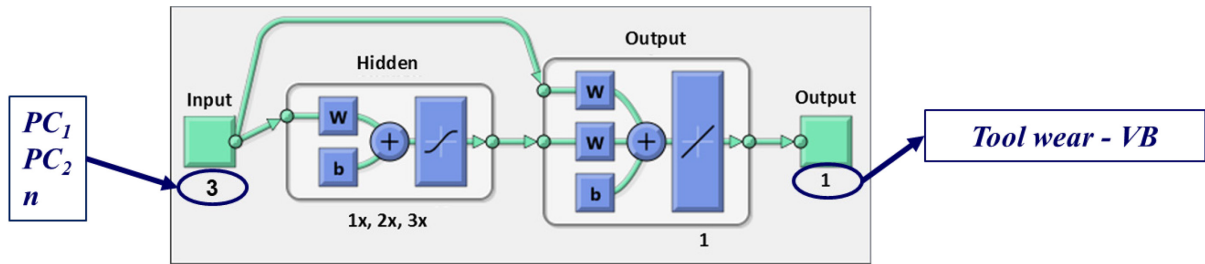


Figure 76. ANN architecture proposed in the case study C.

4.6 Results and discussion

4.6.1 Tool wear forecast in drilling

The recognition performance is measured in terms of root mean squared error (RMSE) values, i.e. the sample standard deviation of the differences between the ANN predicted tool wear values and the measured tool wear values.

As regards the experimental tests with the traditional drill bits, Figure 77 shows, for each drilling condition, the performance of the ANN forecast obtained by varying the number, m , of input-output vectors used for training. It can be observed that, overall, the prediction performance improves by increasing m . This is due to the fact that, by enlarging the number of input-output vectors used for training the ANN, the latter is able to perform a better forecast of future tool wear values.

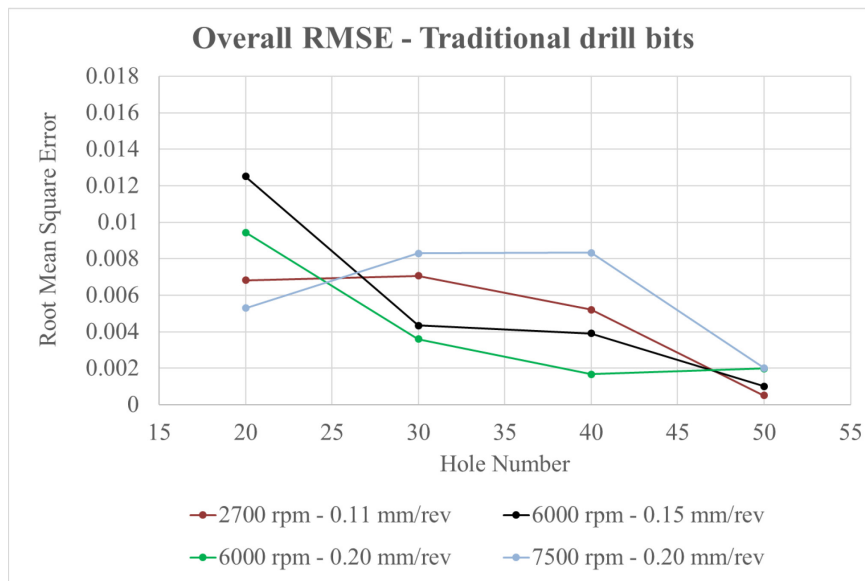


Figure 77. RMSE prediction performance of the ANN trained with diverse numbers, m , of SFPVs for the tests with traditional drill bits.

Figure 78 shows the same performance for the experimental tests with the innovative drill bits. Also in this case, overall, the prediction performance significantly improves by increasing the number of input-output vectors used for training the ANN.

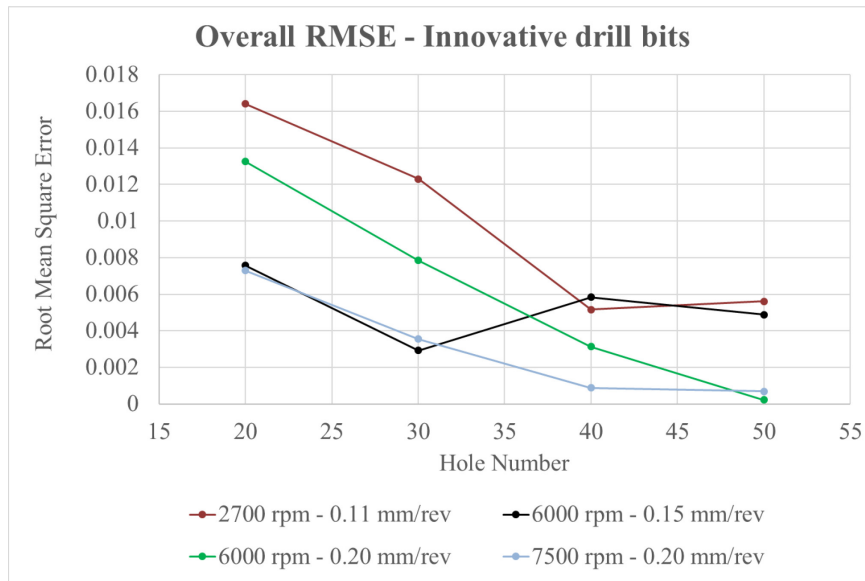


Figure 78. RMSE prediction performance of the ANN trained with diverse numbers, m , of SFPVs for the tests with innovative drill bits.

The best and the worst ANN prediction performances were found for the innovative drill bits.

In the worst case, i.e. the experimental drilling test at 2700 rpm and 0.11 mm/rev, a maximum RMSE of 0.0164 for $m = 20$ and of 0.0056 for $m = 50$ were obtained. Figure 79 shows the tool wear curves predicted by the ANN for this condition, where a couple of outliers, corresponding to holes no. 51 and 52, are visible in the ANN prediction curves.

In the best case, i.e. the experimental drilling test at 6000 rpm and 0.20 mm/rev, a minimum RMSE of 0.00023 for $m = 50$ was obtained. Figure 76 shows the tool wear curves predicted by the ANN for this case. The final curve corresponding to $m = 50$ is practically overlaid to the measured tool wear curve, meaning that the ANN is capable to accurately forecast the upcoming 10 tool wear values.

In both the cases illustrated in Figures 79-80, as well as in the other tests with the traditional drill bits, a similar behaviour is observable for the forecasts with increasing m values: in particular, the first forecasts tend to overestimate the tool wear value, while the subsequent forecasts gradually move towards the measured tool wear curve. Since the forecast error consists of an overestimation of tool wear, the decision-making system for identifying the time for tool change based on this ANN procedure is able to operate in a safe manner.

The satisfactory ANN prediction performance also in the case of the innovative drill bits is encouraging considering the more complex drill bit geometry, involving different areas of tool wear development, for which neither a standard tool wear measurement procedure nor standard parameters exist. Therefore, the prediction tasks can be regarded as more challenging for the ANN.

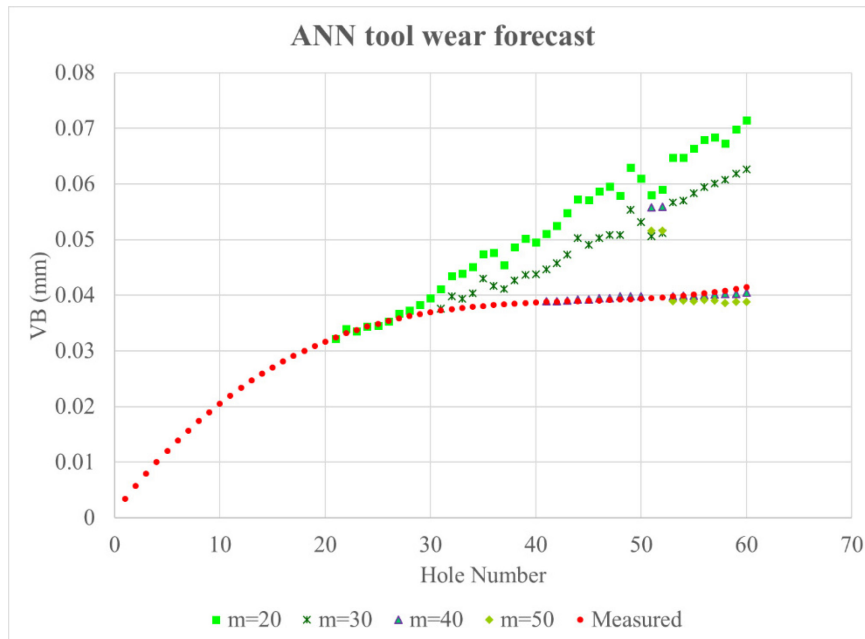


Figure 79. Worst case ANN forecast: experimental tests at 2700 rpm – 0.11 mm/rev with innovative drill bit.

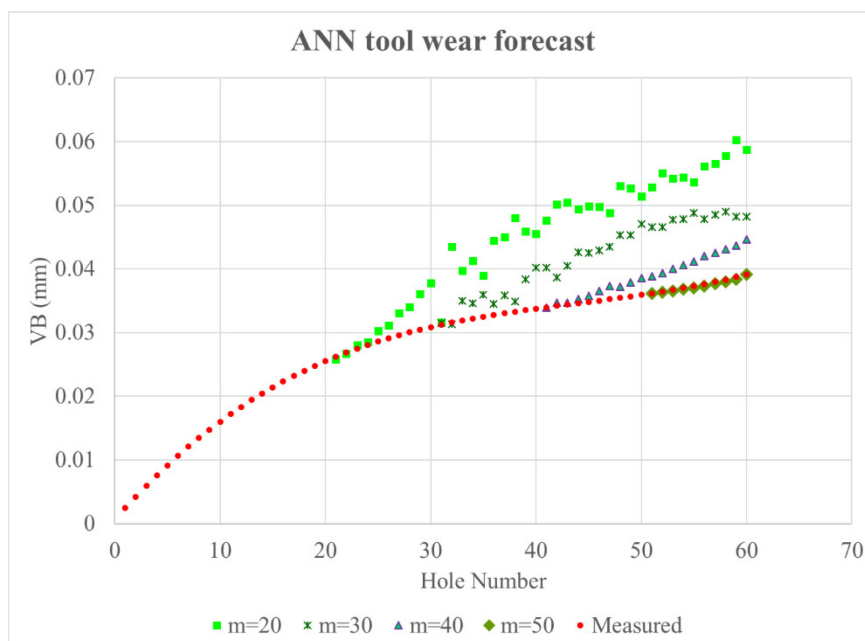


Figure 80. Best case ANN forecast: experimental tests at 6000 rpm – 0.20 mm/rev with innovative drill bit.

A multiple sensor monitoring procedure based on cognitive pattern recognition was developed to perform tool wear forecast in drilling of CFRP/CFRP stack.

Experimental drilling tests under diverse drilling conditions employing a multiple sensor system able to acquire thrust force and torque signals during drilling were performed with two different tool types: a traditional twist drill bit and an innovative geometry step drill bit. The tool flank wear was measured using an optical device to obtain the tool wear curve for each drill bit under the tested drilling conditions.

The final goal of the research work was to perform the forecast of tool wear values based on the information coming from the acquired sensor signals during drilling. To this aim, an artificial neural network paradigm for pattern recognition was implemented to perform the tool wear forecast by

detecting correlations between selected statistical sensor signal features extracted in the time domain and tool wear state.

To evaluate the capability of the ANN procedure, the number, m , of input-output vectors used for ANN training was regularly incremented by steps of 10 from $m = 20$ to $m = 50$.

In both the tests with the traditional and the innovative drill bits, a similar behaviour was observed, where the forecasts with $m < 40$ tend to visibly overestimate the tool wear value, while the subsequent forecasts with $m \geq 40$ gradually move towards the measured tool wear curve.

Although the prediction tasks can be regarded as more challenging for the ANN in the case of the innovative drill bits, which have a more complex geometry and tool wear development, the ANN performance was largely satisfactory, showing very low prediction errors (reaching a minimum RMSE = 0.00023 and a maximum RMSE = 0.0164).

The decision-making system for identifying the end of the tool useful life based on this ANN procedure can operate in a safe manner. The multiple sensor monitoring procedure can be usefully employed for on-line tool condition monitoring aimed at the implementation of a condition-based tool replacement strategy instead of a time-based one.

4.6.2 Feature dimensionality reduction

The tool wear diagnosis performance achieved by the different ANN architectures was estimated in terms of root mean squared error, RMSE, between the VB values predicted by the ANN and the measured VB values.

$$RMSE = \sqrt{\frac{\sum_{i=1}^n (VB_{ANN} - VB_{meas})^2}{n}}$$

Table 18 reports the RMSE values obtained by the ANNs for tool wear estimation of all the experimental turning tests. It can be observed that very low RMSE values, between 2.86E-05 and 2.17E-03, were achieved for all the experimental tests. These low values indicate that the ANN output values are very close to the measured flank wear values, therefore the ANN provided an accurate tool wear diagnosis. Table 18 also shows the influence of the varying number of hidden layer nodes: in most cases, the best performance was obtained with a lower number of hidden nodes, namely with the 3-3-1 configuration. In Figure 81, the ANN predicted VB values are reported vs the measured VB values for the test carried out at $v = 6000$ rpm, $f = 0.15$ mm/rev. In the graph, the diagonal line indicates the perfect condition in which the measured VB and the predicted VB coincide: the minimal dispersion of values around this line allows to graphically evaluate the ANN tool wear prediction performance, which shows to be very accurate.

Cutting Parameters	RMSE		
	3 nodes	6 nodes	9 nodes
2700 rpm - 0.11 mm/rev	8.95E-05	1.34E-04	1.78E-04
6000 rpm - 0.15 mm/rev	4.09E-04	2.17E-03	9.19E-04
6000 rpm - 0.20 mm/rev	1.18E-04	3.23E-04	4.78E-05
7500 rpm - 0.20 mm/rev	2.86E-05	1.73E-04	7.76E-05

Table 18. Overall Root Mean Square Error (RMSE) obtained by ANN tool wear estimation for all the drilling tests.

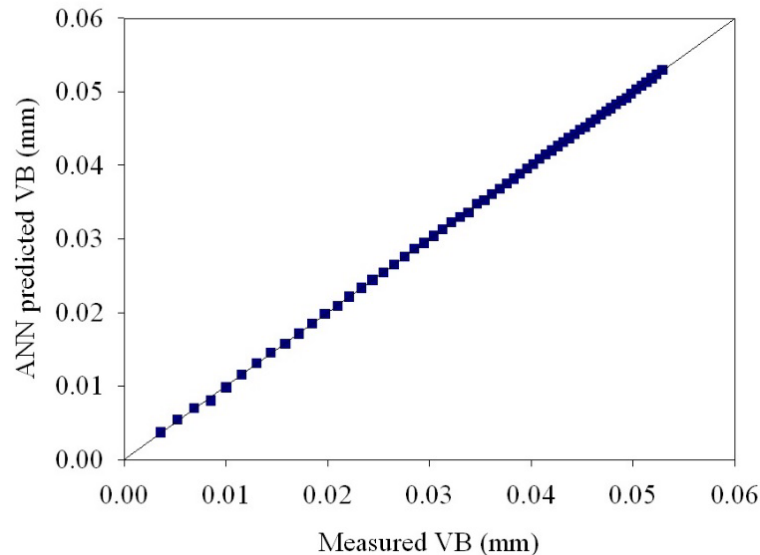


Figure 81. Regression plot between ANN predicted and measured VB for test $v = 6000$ rpm, $f = 0.15$ mm/rev. ANN configuration: 3-3-1. RMSE = $4.09E-04$.

With the aim to monitor the tool conditions during drilling of carbon fiber reinforced plastic laminates, a machine learning procedure based on the acquisition and processing of thrust force, torque, acoustic emission and vibration sensor signals during drilling was implemented.

The acquired sensor signals were processed to extract multiple sensorial features ($d = 20$ features) via conventional statistical technique to feed machine learning paradigms based on artificial neural networks for tool wear diagnosis based on pattern recognition. To reduce the large dimensionality of the sensorial features, a methodology based on a supervised feature selection method to cut off irrelevant features followed by an unsupervised feature extraction method based on Principal Components Analysis (PCA) was implemented.

PCA permitted to identify a lower number of features ($q = 2$ features), namely the principal component scores, obtained via linear projection of the original d features into a new space with reduced dimensionality $q = 2$, that showed to be adequate for describing the variance of the data. The extracted principal components scores represent sensor fusion features, being linear combinations of the original features extracted from the multiple sensor signals of different nature. By feeding machine learning algorithms based on artificial neural networks with the PCA features, a very accurate diagnosis of tool wear (flank wear, VB) was achieved, with ANN predicted values very close to the measured tool wear values and root mean squared error always $< 2.17E-03$.

The accurate diagnosis of tool wear achieved via the machine learning procedure presented in this work can be effectively implemented on-line to monitor the tool conditions during drilling of CFRP stack laminates allowing for the actuation of more efficient tool replacement strategies based on the actual tool conditions.

The features set dimensionality reduction realised using the PCA based methodology allowed to improve the efficiency of the machine learning procedure, by lowering the complexity of the modelling and drastically reducing the number of useful data to be stored by one order of magnitude (from 20 features to 2 features for each drilled hole).

5. Summary and future developments

In this research work, different methodologies for smart monitoring of machining processes, with particular reference to difficult-to-cut materials, were proposed.

The development of smart monitoring procedures in manufacturing can significantly increase productivity and reduce production costs, enhance the performance of manufacturing processes in the perspective of zero defect manufacturing and support the reliable automation of manufacturing systems via smart system adaptation. Monitoring of manufacturing processes has several scopes.

The proposed methodologies presented in this thesis, developed in the framework of different case studies, were aimed at tool condition monitoring (TCM) with the objective to allow for a more efficient condition-based tool replacement strategy to optimally exploit the tool life.

The smart monitoring procedures were based on the acquisition and processing of multiple sensor signals (e.g. force, torque, acoustic emission, vibration, etc.) during the machining process with the aim to extract multiple sensorial features to construct sensor fusion pattern vectors (SFPVs) to feed machine learning paradigms. In particular, artificial neural networks for pattern recognition were constructed to find correlations between the SFPVs and the tool wear state, with the final aim to forecast the tool wear values during machining based on the sensor signal features.

In order to apply the sensor fusion technology, different multiple sensor system setups were proposed due to the diverse nature of the processes to be monitored, i.e. turning of Ti6Al4V and drilling of CFRP and hybrid Al/CFRP stacks.

Moreover, different configurations for the machine learning paradigms based on artificial neural networks were studied due to the different compositions of the sensor fusion pattern vectors and due to the different objectives which had to be detected. The proposed configurations proved to be suitable to perform a real time analysis of the tool condition in terms of tool flank wear diagnosis and also to perform a forecast of tool wear conditions.

Because the set of relevant features which were selected to construct the SFPVs was very large, a method for features set dimensionality reduction was applied using a PCA based methodology. It allowed to decrease the set of most relevant features from 8 to 2 and then allowed to improve the robustness and the reliability of the machine learning procedure.

The very low artificial neural network prediction error values, measured in terms of MSE and RMSE, confirmed the capability of the developed procedures to reliably carry out a diagnosis and forecast on tool wear state, which can be employed to support decision making for appropriate corrective actions on tool replacement, parameters change or process stop, which can be either directly fed to the machine tool numerical controller or suggested to the human operator.

Although the results were very promising, it is worth mentioning that they cannot be generalized to different cutting conditions (i.e. materials, tools, cutting parameters, etc.) and different machining processes. Therefore, the future developments of this research work involve different objectives.

One of the objectives is the study of other machining conditions for the presented case studies, including the investigation of different machining parameters, using the same setups proposed in this thesis.

The second objective is the implementation of the smart sensor monitoring systems in other machining processes such as milling, through the design of a new system setup and dedicated sensor monitoring procedures.

Concerning the machining of composite materials stacks or hybrid stacks, the main industrial sector of reference for the manufacturing of these multi-material products is the aerospace industry;

however, a further future development could be the application of the results of this research and innovation action to other industrial sectors like automotive, naval, sporting goods industries that make increasing use of low-weight high-strength advanced materials.

An important future development in the Industry 4.0 framework is related to data volume reduction, which is a main goal in modern manufacturing industry, where huge amounts of data are increasingly collected and utilised. The progressive improvements in signal analysis and features selection offers a good starting point in the field of big data analytics within the Industry 4.0 perspective.

Finally, an interesting development in the Industry 4.0 framework is represented by the implementation of the multiple sensor systems and the correlate methodologies in a cloud manufacturing system. Due to the wide discussion about this topic, the paragraph below is dedicated to the description of this idea.

5.1 Cloud manufacturing approach

In the presented smart TCM applications, the monitoring system collects the sensor signal selected features in order to feed the cognitive decision-making support systems based on pattern recognition techniques for the final diagnosis that can be used to suggest or execute appropriate adaptive/corrective actions. Many of the TCM approaches presented in the literature employ multiple sensors and advanced signal processing techniques that require the local availability of high-level computational resources, storage capability, interoperability and user skills (Krzysztof Jemielniak et al. 2012; Boud and Gindy 2008; G. Wang et al. 2014; Teti 2015; Teti et al. 2010; K Jemielniak and Arrazola 2008). Such requirements may represent barriers to the online implementation of such approaches in industry. Hence, the possibility to realise the remote and timely acquisition, distribution and utilisation of data from manufacturing processes is extremely interesting for the realisation of innovative monitoring procedures (L. Monostori et al. 2016). In this direction, the new paradigms such as Industry 4.0, Internet of Things and cloud manufacturing represent key enablers to overcome the traditional barriers of TCM applications and achieve objectives such as increased use of sensors, interoperability, cloud-hosted analysis and wider technology acceptance by operators (G. Byrne et al. 2016).

The implementation of the proposed monitoring systems in a cloud manufacturing framework represents a remarkable advancement for smart process monitoring, allowing to exploit the cloud capabilities in order to offer real-time diagnosis on tool conditions according to a service-oriented approach. The introduction of the sensors and of the networked communication into the factory strongly supports smart in-process diagnosis as well as the timely activation of adaptive actions based on actual process conditions (Gao et al. 2015). These actions include human interventions and proper commands directly fed to the machine tool numerical control, improving the robustness and adaptability of processes and systems.

The diagnosis on tool conditions could benefit from the cloud infrastructure in terms of enhanced computational capability, which improves the execution efficiency of the diagnosis and enables more robust decision-making due to large information and knowledge sharing available in the cloud.

Bibliography

- Abellan-Nebot, Jose Vicente, and Fernando Romero Subirón. 2010. "A Review of Machining Monitoring Systems Based on Artificial Intelligence Process Models." *International Journal of Advanced Manufacturing Technology* 47 (1–4): 237–57. <https://doi.org/10.1007/s00170-009-2191-8>.
- Abouelatta, O B, and J Mádł. 2001. "Surface Roughness Prediction Based on Cutting Parameters and Tool Vibrations in Turning Operations." *Journal of Materials Processing Technology* 118: 269–77.
- Abu-Mahfouz, Issam. 2003. "Drilling Wear Detection and Classification Using Vibration Signals and Artificial Neural Network." *International Journal of Machine Tools and Manufacture* 43 (7): 707–20. [https://doi.org/10.1016/S0890-6955\(03\)00023-3](https://doi.org/10.1016/S0890-6955(03)00023-3).
- Abu-zahra, Nidal H, and Gang Yu. 2000. "Analytical Model for Tool Wear Monitoring in Turning Operations Using Ultrasound Waves." *International Journal of Machine Tools and Manufacture* 40 (11): 1619–35.
- Achiche, Sofiane, Marek Balazinski, Luc Baron, and Krzysztof Jemielniak. 2002. "Tool Wear Monitoring Using Genetically-Generated Fuzzy Knowledge Bases." *Engineering Applications of Artificial Intelligence* 15 (3–4): 303–14.
- Ahn, J H, Y F Shen, H Y Kim, H D Jeong, and K K Cho. 2001. "Development of a Sensor Information Integrated Expert System for Optimizing Die Polishing." *Robotics and Computer-Integrated Manufacturing* 17 (4): 269–76.
- Al-Habaibeh, A, and N Gindy. 2000. "A New Approach for Systematic Design of Condition Monitoring Systems for Milling Processes." *Journal of Materials Processing Technology* 107 (1–3): 243–51.
- Alpaydin, E. 2014. *Introduction to Machine Learning*. Edited by MIT Press. USA.
- Altintas, Y, and S S Park. 2004. "Dynamic Compensation of Spindle-Integrated Force Sensors." *CIRP Annals - Manufacturing Technology* 53 (1): 7–10.
- Andreasen, J L, and L De Chiffre. 1998. "Automatic System for Elaboration of Chip Breaking Diagrams." *CIRP Annals - Manufacturing Technology* 47 (1): 35.
- Arrazola, P J, I Arriola, M A Davies, A L Cooke, and B S Dutterer. 2008. "The Effect of Machinability on Thermal Fields in Orthogonal Cutting of AISI 4140 Steel." *CIRP Annals - Manufacturing Technology* 57: 65–68. <https://doi.org/10.1016/j.cirp.2008.03.139>.
- Axinte, A, Deepak R Natarajan, and Nabil N Z Gindy. 2005. "An Approach to Use an Array of Three Acoustic Emission Sensors to Locate Uneven Events in Machining — Part 1 : Method and Validation." *International Journal of Machine Tools and Manufacture* 45 (14): 1605–13. <https://doi.org/10.1016/j.ijmachtools.2005.02.005>.
- Axinte, D A. 2007. "An Experimental Analysis of Damped Coupled Vibrations in Broaching." *International Journal of Machine Tools and Manufacture* 47 (14): 2182–88. <https://doi.org/10.1016/j.ijmachtools.2007.04.006>.
- Axinte, D, F Boud, J Penny, N Gindy, and D Williams. 2005. "Broaching of Ti-6-4 - Detection

- of Workpiece Surface Anomalies on Dovetail Slots through Process Monitoring.” *CIRP Annals - Manufacturing Technology* 54 (1): 87–90.
- Axinte, Dragos A. 2006. “Approach into the Use of Probabilistic Neural Networks for Automated Classification of Tool Malfunctions in Broaching.” *International Journal of Machine Tools and Manufacture* 46 (12–13): 1445–48. <https://doi.org/10.1016/j.ijmachtools.2005.09.017>.
- Axinte, Dragos A, and Nabil Gindy. 2003. “Tool Condition Monitoring in Broaching.” *Wear* 254: 370–82. [https://doi.org/10.1016/S0043-1648\(03\)00003-6](https://doi.org/10.1016/S0043-1648(03)00003-6).
- Axinte, Dragos, Nabil Gindy, Kate Fox, and Iker Unanue. 2004. “Process Monitoring to Assist the Workpiece Surface Quality in Machining.” *International Journal of Machine Tools and Manufacture* 44: 1091–1108. <https://doi.org/10.1016/j.ijmachtools.2004.02.020>.
- Azmir, M. A., and A. K. Ahsan. 2009. “A Study of Abrasive Water Jet Machining Process on Glass/Epoxy Composite Laminate.” *Journal of Materials Processing Technology* 209 (20): 6168–73. <https://doi.org/10.1016/j.jmatprotec.2009.08.011>.
- Azouzi, R, and M Guillot. 1997. “On-Line Prediction of Surface Finish and Dimensional Deviation in Turning Using Neural Network Based Sensor Fusion.” *International Journal of Machine Tools and Manufacture* 37 (9): 1201–17.
- Balazinski, Marek, and Krzysztof Jemielniak. 1998. “Tool Conditions Monitoring Using Fuzzy Decision Support System.” *CIRP International Conference on Automatic Supervision, Monitoring and Adaptive Control in Manufacturing*, 115–22.
- Balsamo, Vittorio, Alessandra Caggiano, Krzysztof Jemielniak, Joanna Kossakowska, Miroslaw Nejman, and Roberto Teti. 2016. “Multi Sensor Signal Processing for Catastrophic Tool Failure Detection in Turning.” *Procedia CIRP* 41: 939–44. <https://doi.org/10.1016/j.procir.2016.01.010>.
- Bhattacharyya, P, D Sengupta, and S Mukhopadhyay. 2007. “Cutting Force-Based Real-Time Estimation of Tool Wear in Face Milling Using a Combination of Signal Processing Techniques.” *Mechanical Systems and Signal Processing* 21 (6): 2665–83. <https://doi.org/10.1016/j.ymsp.2007.01.004>.
- Bhuiyan, M. S H, I. A. Choudhury, and M. Dahari. 2014. “Monitoring the Tool Wear, Surface Roughness and Chip Formation Occurrences Using Multiple Sensors in Turning.” *Journal of Manufacturing Systems* 33 (4): 476–87. <https://doi.org/10.1016/j.jmsy.2014.04.005>.
- Biermann, Dirk, Marko Kirschner, Klaus Pantke, Wolfgang Tillmann, and Jan Herper. 2013. “Surface & Coatings Technology New Coating Systems for Temperature Monitoring in Turning Processes.” *Surface & Coatings Technology* 215: 376–80. <https://doi.org/10.1016/j.surfcoat.2012.08.086>.
- Binsaeid, Sultan, Shihab Asfour, Sohyung Cho, and Arzu Onar. 2009. “Machine Ensemble Approach for Simultaneous Detection of Transient and Gradual Abnormalities in End Milling Using Multisensor Fusion.” *Journal of Materials Processing Technology* 209: 4728–38. <https://doi.org/10.1016/j.jmatprotec.2008.11.038>.
- Bishop, Christopher M. 1995. *Neural Networks for Pattern Recognition*.
- Boud, F., and N. N.Z. Gindy. 2008. “Application of Multi-Sensor Signals for Monitoring

- Tool/Workpiece Condition in Broaching.” *International Journal of Computer Integrated Manufacturing* 21 (6): 715–29. <https://doi.org/10.1080/09511920701233357>.
- Brophy, B, K Kelly, and G Byrne. 2002. “AI-Based Condition Monitoring of the Drilling Process.” *Journal of Materials Processing Technology* 124 (3): 305–10.
- Bukkapatnam, Satish T S, Soundar R T Kumara, and Akhlesh Lakhtakia. 2000. “Fractal Estimation of Flank Wear.” *Journal of Dynamic Systems, Measurement and Control, Transactions of the ASME* 122 (1): 89–94.
- Bukkapatnam, Satish T S, Soundar R T Kumara, Akhlesh Lakhtakia, and Parthasarathy Srinivasan. 2002. “The Neighborhood Method and Its Coupling with the Wavelet Method for Signal Separation of Chaotic Signals.” *Signal Processing* 82 (10): 1351–74.
- Byrne, G., E. Ahearne, M. Cotterell, B. Mullany, G. E. O’Donnell, and F. Sammler. 2016. “High Performance Cutting (HPC) in the New Era of Digital Manufacturing - A Roadmap.” *Procedia CIRP* 46: 1–6. <https://doi.org/10.1016/j.procir.2016.05.038>.
- Byrne, G, D Dornfeld, I Inasaki, G Ketteler, W Konig, and R Teti. 1995. “Tool Condition Monitoring (TCM) - The Status of Research and Industrial Application.” *CIRP Annals - Manufacturing Technology* 44 (2): 541–67.
- Byrne, G I, D I Dornfeld, and B Denkena. 2003. “Advancing Cutting Technology.” *CIRP Annals - Manufacturing Technology* 52 (2): 483–507.
- Byrne, G, and G O’ Donnell. 2007. “An Integrated Force Sensor Solution for Process Monitoring of Drilling Operations.” *CIRP Annals - Manufacturing Technology* 56 (1): 89–92. <https://doi.org/10.1016/j.cirp.2007.05.023>.
- Caggiano, A, P Centobelli, L Nele, and R Teti. 2017. “Multiple Sensor Monitoring in Drilling of CFRP/CFRP Stacks for Cognitive Tool Wear Prediction and Product Quality Assessment.” *Procedia CIRP* 2017 62: 3–8. <https://doi.org/10.1016/j.procir.2017.03.047>.
- Caggiano, Alessandra. 2018. “Cloud-Based Manufacturing Process Monitoring for Smart Diagnosis Services.” *International Journal of Computer Integrated Manufacturing* 31 (7): 612–23. <https://doi.org/10.1080/0951192X.2018.1425552>.
- Caggiano, Alessandra, Francesco Napolitano, and Roberto Teti. 2017. “Dry Turning of Ti6Al4V: Tool Wear Curve Reconstruction Based on Cognitive Sensor Monitoring.” *Procedia CIRP* 62: 209–14. <https://doi.org/10.1016/j.procir.2017.03.046>.
- Caggiano, Alessandra, Roberto Perez, Tiziana Segreto, Roberto Teti, and Paul Xirouchakis. 2016. “Advanced Sensor Signal Feature Extraction and Pattern Recognition for Wire EDM Process Monitoring.” *Procedia CIRP* 42: 34–39. <https://doi.org/10.1016/j.procir.2016.02.181>.
- Caggiano, Alessandra, Tiziana Segreto, and Roberto Teti. 2016. “Cloud Manufacturing Framework for Smart Monitoring of Machining.” *Procedia CIRP* 55: 248–53. <https://doi.org/10.1016/j.procir.2016.08.049>.
- Carolan, T, S Kidd, D Hand, S Wilcox, P Wilkinson, J Barton, J D C Jones, and R Reuben. 1997a. “Acoustic Emission Monitoring of Tool Wear during the Face Milling of Steels and Aluminium Alloys Using a Fibre Optic Sensor. Part 1: Energy Analysis.” *Proceedings of the Institution of Mechanical Engineers, Part B: Journal of Engineering Manufacture*

- 211 (4): 209–309.
- . 1997b. “Acoustic Emission Monitoring of Tool Wear during the Face Milling of Steels and Aluminium Alloys Using a Fibre Optic Sensor. Part 1: Frequency Analysis.” *Proceedings of the Institution of Mechanical Engineers, Part B: Journal of Engineering Manufacture* 211 (4): 311–19.
- Castro, Gabriel. 2010. “Drilling Carbon Fiber Reinforced Plastic and Titanium Stacks,” no. May. <https://doi.org/10.1017/CBO9781107415324.004>.
- Chang, Hun-keun, Jin-hyun Kim, Il Hae, Dong Young, and Dong Chul. 2007. “In-Process Surface Roughness Prediction Using Displacement Signals from Spindle Motion.” *International Journal of Machine Tools and Manufacture* 47: 1021–26. <https://doi.org/10.1016/j.ijmachtools.2006.07.004>.
- Che-Haron, C. H. 2001. “Tool Life and Surface Integrity in Turning Titanium Alloy.” *Journal of Materials Processing Technology* 118 (1–3): 231–37. [https://doi.org/10.1016/S0924-0136\(01\)00926-8](https://doi.org/10.1016/S0924-0136(01)00926-8).
- Che-Haron, C. H., and A. Jawaid. 2005. “The Effect of Machining on Surface Integrity of Titanium Alloy Ti-6% Al-4% V.” *Journal of Materials Processing Technology* 166 (2): 188–92. <https://doi.org/10.1016/j.jmatprotec.2004.08.012>.
- Chen, Lienjing, P Bende, P Renton, U T C Fuel Cells, A United Technologies Company, and South Windsor. 2002. “Integrated Virtual Manufacturing Systems for Process Optimisation and Monitoring.” *CIRP Annals* 51 (1): 409–12.
- Choudhury, S K, V K Jain, and Ch V V Rama Rao. 1999. “On-Line Monitoring of Tool Wear in Turning Using a Neural Network.” *International Journal of Machine Tools and Manufacture* 39 (3): 489–504.
- Chungchoo, C., and D. Saini. 2002. “On-Line Tool Wear Estimation in CNC Turning Operations Using Fuzzy Neural Network Model.” *International Journal of Machine Tools and Manufacture* 42 (1): 29–40. [https://doi.org/10.1016/S0890-6955\(01\)00096-7](https://doi.org/10.1016/S0890-6955(01)00096-7).
- Daisuke, Hiratsu, and Nagao Tomoharu. 2001. “2-D Artificial Cellular Neural Network and Its Application to Chase Game.” *IEEJ Transactions on Electronics, Information and Systems* 6: 1071–79.
- Daubechies, Ingrid. 1990. “The Wavelet Transform , Time-Frequency Localization and Signal Analysis.” *IEEE Transactions on Information Theory* 36 (5): 961–1005.
- Davies, M A, T Ueda, R M’Saoubi, B Mullany, and A L Cooke. 2007. “On The Measurement of Temperature in Material Removal Processes.” *CIRP Annals - Manufacturing Technology* 56 (2): 581–604. <https://doi.org/10.1016/j.cirp.2007.10.009>.
- Dey, S, and J A Ñ Stori. 2005. “A Bayesian Network Approach to Root Cause Diagnosis of Process Variations” 45: 75–91. <https://doi.org/10.1016/j.ijmachtools.2004.06.018>.
- Dharan, C. K.H., and M. S. Won. 2000. “Machining Parameters for an Intelligent Machining System for Composite Laminates.” *International Journal of Machine Tools and Manufacture* 40 (3): 415–26. [https://doi.org/10.1016/S0890-6955\(99\)00065-6](https://doi.org/10.1016/S0890-6955(99)00065-6).
- Diaz, Nancy, Moneer Helu, Andrew Jarvis, Stefan Tönissen, David Dornfeld, and Ralf Schlosser. 2009. “Strategies for Minimum Energy Operation for Precision Machining.”

- The Proceedings of MTTRF 2009 Annual Meeting*. <https://doi.org/10.1007/978-3-642-19692-8>.
- Dimla, D Senior. 2000. "Sensor Signals for Tool-Wear Monitoring in Metal Cutting Operations — a Review of Methods." *International Journal of Machine Tools and Manufacture* 40 (8): 1073–98.
- Dimla, DE, and PM Lister. 2000. "On-Line Metal Cutting Tool Condition Monitoring. I : Force and Vibration Analyses." *International Journal of Machine Tools and Manufacture* 40 (5): 739–68.
- Dolinšek, Slavko, Borivoj Šuštaršič, and Janez Kopač. 2001. "Wear Mechanisms of Cutting Tools in High-Speed Cutting Processes." *Wear* 250–251 (1–12): 349–56. [https://doi.org/10.1016/S0043-1648\(01\)00620-2](https://doi.org/10.1016/S0043-1648(01)00620-2).
- Donachie, M J Jr. 1983. *Titanium and Titanium Alloys*. Edited by Metals Park American Society for Metals. Ohio.
- . 1988. *Titanium – A Technical Guide*. Edited by Metals Park American Society for Metals. Ohio.
- Dong, Jianfei, K V R Subrahmanyam, Yoke San Wong, Geok Soon Hong, and A R Mohanty. 2006. "Bayesian-Inference-Based Neural Networks for Tool Wear Estimation." *International Journal of Advanced Manufacturing Technology* 30 (9–10): 797–807. <https://doi.org/10.1007/s00170-005-0124-8>.
- Duda, O., and P.E. Hart. 1973. *Pattern Classification and Scene Analysis*. Edited by New York: John Wiley and Sons.
- Duflou, Joost R., John W. Sutherland, David Dornfeld, Christoph Herrmann, Jack Jeswiet, Sami Kara, Michael Hauschild, and Karel Kellens. 2012. "Towards Energy and Resource Efficient Manufacturing: A Processes and Systems Approach." *CIRP Annals - Manufacturing Technology* 61 (2): 587–609. <https://doi.org/10.1016/j.cirp.2012.05.002>.
- Dweiri, F., M. Al-Jarrah, and H. Al-Wedyan. 2003. "Fuzzy Surface Roughness Modeling of CNC down Milling of Aluminic-79." *Journal of Materials Processing Technology* 133 (3): 266–75. [https://doi.org/10.1016/S0924-0136\(02\)00847-6](https://doi.org/10.1016/S0924-0136(02)00847-6).
- El-Hoffy, and Hassan Abdel-Gawad. 2013. *Fundamentals of Machining Processes : Conventional and Nonconventional Processes*.
- Ezugwu, E.O., and Z.M. Wang. 1997. "Titanium Alloys and Their Machinability-a Review." *Journal of Materials Processing Technology* 68 (3): 262–74. [https://doi.org/10.1016/S0924-0136\(96\)00030-1](https://doi.org/10.1016/S0924-0136(96)00030-1).
- Filiz, Sinan, and O Burak Ozdoganlar. 2010a. "A Model for Bending , Torsional , and Axial Vibrations of Micro- and Macro-Drills Including Actual Drill Geometry — Part I : Model Development and Numerical." *Journal of Manufacturing Science and Engineering, Transactions of the ASME* 132: 1–8. <https://doi.org/10.1115/1.4001720>.
- . 2010b. "A Model for Bending , Torsional , and Axial Vibrations of Micro- and Macro-Drills Including Actual Drill Geometry — Part II : Model Validation and Application." *Journal of Manufacturing Science and Engineering, Transactions of the ASME* 132. <https://doi.org/10.1115/1.4001721>.

- Fink, A., P. P. Camanho, J. M. Andrés, E. Pfeiffer, and A. Obst. 2010. "Hybrid CFRP/Titanium Bolted Joints: Performance Assessment and Application to a Spacecraft Payload Adaptor." *Composites Science and Technology* 70 (2): 305–17. <https://doi.org/10.1016/j.compscitech.2009.11.002>.
- Gandarias, E, S Dimov, D T Pham, A Ivanov, K Popov, R Lizarralde, and P J Arrazola. 2006. "New Methods for Tool Failure Detection in Micro-Milling." *Proceedings of IMechE* 220 (2): 137–44.
- Gao, R., L. Wang, R. Teti, D. Dornfeld, S. Kumara, M. Mori, and M. Helu. 2015. "Cloud-Enabled Prognosis for Manufacturing." *CIRP Annals - Manufacturing Technology* 64 (2): 749–72. <https://doi.org/10.1016/j.cirp.2015.05.011>.
- Ghosh, N, Y B Ravi, A Patra, S Mukhopadhyay, S Paul, A R Mohanty, and A B Chattopadhyay. 2007. "Estimation of Tool Wear during CNC Milling Using Neural Network-Based Sensor Fusion." *Mechanical Systems and Signal Processing* 21 (1): 466–79. <https://doi.org/10.1016/j.ymsp.2005.10.010>.
- Ginting, A., and M. Nouari. 2009. "Surface Integrity of Dry Machined Titanium Alloys." *International Journal of Machine Tools and Manufacture* 49 (3–4): 325–32. <https://doi.org/10.1016/j.ijmactools.2008.10.011>.
- Govekar, E, J Gradisek, and I Grabec. 2000. "Analysis of Acoustic Emission Signals and Monitoring of Machining Processes." *Ultrasonics* 38: 598–603.
- Grzesik, W, and P Bernat. 1998. "An Investigation of the Cutting Process for Chip Breaking Monitoring in Turning of Steels." *Journal of Manufacturing Science and Engineering, Transactions of the ASME* 120 (3): 555–62.
- Gu, Shuxin, Jun Ni, and Jingxia Yuan. 2002. "Non-Stationary Signal Analysis and Transient Machining Process Condition Monitoring." *International Journal of Machine Tools and Manufacture* 42 (1): 41–51.
- Guo, Y B, and S C Ammula. 2005. "Real-Time Acoustic Emission Monitoring for Surface Damage in Hard Machining." *International Journal of Machine Tools and Manufacture* 45: 1622–27. <https://doi.org/10.1016/j.ijmactools.2005.02.007>.
- Halgamuge, S K, and M Glesner. 1994. "Neural Networks in Designing Fuzzy Systems for Real World Applications." *Fuzzy Sets and Systems* 65 (1): 1–12.
- Hauke, J, and T Kossowski. 2011. "Comparison of Values of Pearson's and Spearman's Correlation Coefficients on the Same Sets of Data." *Quaestiones Geographicae* 30: 87–93.
- Herrmann, Christoph, and Sebastian Thiede. 2009. "Process Chain Simulation to Foster Energy Efficiency in Manufacturing." *CIRP Journal of Manufacturing Science and Technology* 1 (4): 221–29. <https://doi.org/10.1016/j.cirpj.2009.06.005>.
- Herzog, Dirk, Peter Jaeschke, Oliver Meier, and Heinz Haferkamp. 2008. "Investigations on the Thermal Effect Caused by Laser Cutting with Respect to Static Strength of CFRP." *International Journal of Machine Tools and Manufacture* 48 (12–13): 1464–73. <https://doi.org/10.1016/j.ijmactools.2008.04.007>.
- Ho-Cheng, H., and C. K. H. Dharan. 1990. "Delamination During Drilling in Composite

- Laminates.” *Journal of Engineering for Industry*. <https://doi.org/10.1115/1.2899580>.
- Hocheng, H, and C C Tsao. 2003. “Comprehensive Analysis of Delamination in Drilling of Composite Materials with Various Drill Bits.” *Journal of Materials Processing Technology* 140 (1–3): 335–39. [https://doi.org/10.1016/S0924-0136\(03\)00749-0](https://doi.org/10.1016/S0924-0136(03)00749-0).
- Hong, G S, M Rahman, and Q Zhou. 1996. “Using Neural Network for Tool Condition Monitoring Based on Wavelet Decomposition.” *International Journal of Machine Tools and Manufacture* 36 (5): 551–66.
- Hu, Shaohua, Fei Liu, Yan He, and Tong Hu. 2012. “An On-Line Approach for Energy Efficiency Monitoring of Machine Tools.” *Journal of Cleaner Production* 27: 133–40. <https://doi.org/10.1016/j.jclepro.2012.01.013>.
- Huang, B, and J C Chen. 2003. “An In-Process Neural Network-Based Surface Roughness Prediction (INN-SRP) System Using a Dynamometer in End Milling Operations.” *International Journal of Advanced Manufacturing Technology* 21 (5): 339–47.
- Hundt, W, D Leuenberger, F Rehsteiner, and P Gygax. 1994. “An Approach to Monitoring of the Grinding Process Using Acoustic Emission (AE) Technique.” *CIRP Annals - Manufacturing Technology* 43 (1): 295–98.
- Hutton, D V, and F Hu. 1999. “Acoustic Emission Monitoring of Tool Wear in End-Milling Using Time-Domain Averaging.” *Journal of Manufacturing Science and Engineering, Transactions of the ASME* 121 (1): 8–12.
- Iliescu, D., D. Gehin, M. E. Gutierrez, and F. Girot. 2010. “Modeling and Tool Wear in Drilling of CFRP.” *International Journal of Machine Tools and Manufacture* 50 (2): 204–13. <https://doi.org/10.1016/j.ijmachtools.2009.10.004>.
- Inasaki, Ichiro. 1998. “Application of Acoustic Emission Sensor for Monitoring Machining Processes.” *Ultrasonics* 36: 273–81.
- Isbilir, Ozden, and Elaheh Ghassemieh. 2013. “Numerical Investigation of the Effects of Drill Geometry on Drilling Induced Delamination of Carbon Fiber Reinforced Composites.” *Composite Structures* 105: 126–33. <https://doi.org/10.1016/j.compstruct.2013.04.026>.
- Jain, S, and D C H Yang. 1994. “Delamination-Free Drilling of Composite Laminates.” *Journal of Engineering for Industry-Transactions of the Asme*. <https://doi.org/Doi10.1115/1.2902131>.
- Jardine, Andrew K.S., Daming Lin, and Dragan Banjevic. 2006. “A Review on Machinery Diagnostics and Prognostics Implementing Condition-Based Maintenance.” *Mechanical Systems and Signal Processing* 20 (7): 1483–1510. <https://doi.org/10.1016/j.ymsp.2005.09.012>.
- Jelinek, Michael, Johannes Schilp, and Gunther Reinhart. 2015. “Optimised Parameter Sets for Thermographic Inspection of CFRP Metal Hybrid Components.” *Procedia CIRP* 37: 218–24. <https://doi.org/10.1016/j.procir.2015.08.044>.
- Jemielniak, K. 1998. “Catastrophic Tool Failure Detection Based on Acoustic Emission Signal Analysis.” *CIRP Annals - Manufacturing Technology* 47 (1): 31–34.
- Jemielniak, K, and P J Arrazola. 2008. “Application of AE and Cutting Force Signals in Tool Condition Monitoring in Micro-Milling.” *CIRP Journal of Manufacturing Science and*

- Technology* 1 (2): 97–102. <https://doi.org/10.1016/j.cirpj.2008.09.007>.
- Jemielniak, K, S Bombin, and P X Aristimuno. 2008. “Tool Condition Monitoring in Micromilling Based on Hierarchical Integration of Signal Measures.” *CIRP Annals - Manufacturing Technology* 57 (1): 121–24. <https://doi.org/10.1016/j.cirp.2008.03.053>.
- Jemielniak, Krzysztof. 2000. “Some Aspects of AE Application in Tool Condition Monitoring.” *Ultrasonics* 38 (1): 604–8.
- . 2001. “Some Aspects of Acoustic Emission Signal Pre-Processing.” *Journal of Materials Processing Technology* 109 (3): 242–47.
- Jemielniak, Krzysztof, and Sebastian Bombinski. 2006. “Hierarchical Strategies in Tool Wear Monitoring.” *Proceedings of the Institution of Mechanical Engineers, Part B: Journal of Engineering Manufacture* 220 (3): 375–81.
- Jemielniak, Krzysztof, Leszek Kwiatkowski, and Pawel Wrzosek. 1998. “Diagnosis of Tool Wear Based on Cutting Forces and Acoustic Emission Measures as Inputs to a Neural Network.” *Journal of Intelligent Manufacturing* 9 (5): 447–55.
- Jemielniak, Krzysztof, Tomasz Urbański, Joanna Kossakowska, and Sebastian Bombiński. 2012. “Tool Condition Monitoring Based on Numerous Signal Features.” *International Journal of Advanced Manufacturing Technology* 59 (1–4): 73–81. <https://doi.org/10.1007/s00170-011-3504-2>.
- Joliffe, I T. 2002. “Principal Component Analysis.” In *Encyclopedia of Statistics in Behavioral Science*, 30–487.
- Jun, Martin B, O Burak Ozdoganlar, Richard E Devor, Shiv G Kapoor, Andreas Kirchheim, and Georges Schaffner. 2002. “Evaluation of a Spindle-Based Force Sensor for Monitoring and Fault Diagnosis of Machining Operations.” *International Journal of Machine Tools and Manufacture* 42 (6): 741–51.
- Kamarthi, S V, S R T Kumara, and P H Cohen. 2000. “Flank Wear Estimation in Turning Through Wavelet Representation of Acoustic Emission Signals.” *Journal of Manufacturing Science and Engineering, Transactions of the ASME* 122 (1): 12–19.
- Kamarthi, S V, and S Pittner. 1997. “FOURIER AND WAVELET TRANSFORM FOR FLANK WEAR ESTIMATION — A COMPARISON.” *Mechanical Systems and Signal Processing* 11 (6): 791–809.
- Kannan, T. Deepan Bharathi, G. Rajesh kannan, B. Suresh Kumar, and N. Baskar. 2014. “Application of Artificial Neural Network Modeling for Machining Parameters Optimization in Drilling Operation.” *Procedia Materials Science*. <https://doi.org/10.1016/j.mspro.2014.07.433>.
- Kannatey-Asibu Jr, E, and D A Dornfeld. 1982. “A Study of Tool Wear Using Statistical Analysis of Metal-Cutting Acoustic Emission.” *Wear* 76 (2): 247–61.
- Karnik, S. R., V. N. Gaitonde, J. Campos Rubio, A. Esteves Correia, A. M. Abrão, and J. Paulo Davim. 2008. “Delamination Analysis in High Speed Drilling of Carbon Fiber Reinforced Plastics (CFRP) Using Artificial Neural Network Model.” *Materials and Design* 29 (9): 1768–76. <https://doi.org/10.1016/j.matdes.2008.03.014>.
- Karpat, Y., O. Bahtiyar, B. Değer, and Bilgin Kaftanoğlu. 2014. “A Mechanistic Approach to

- Investigate Drilling of UD-CFRP Laminates with PCD Drills.” *CIRP Annals - Manufacturing Technology* 63 (1): 81–84. <https://doi.org/10.1016/j.cirp.2014.03.077>.
- Karpuschewski, B, M Wehmeier, and I Inasaki. 2000. “Grinding Monitoring System Based on Power and Acoustic Emission Sensors.” *CIRP Annals - Manufacturing Technology* 49 (1): 235–40.
- Kim, H Y, J H Ahn, S H Kim, and S Takata. 2002. “Real-Time Drill Wear Estimation Based on Spindle Motor Power.” *Journal of Materials Processing Technology* 124 (3): 267–73.
- Kim, Hwa-young, and Jung-hwan Ahn. 2002. “Chip Disposal State Monitoring in Drilling Using Neural Network Based Spindle Motor Power Sensing.” *International Journal of Machine Tools and Manufacture* 42 (10): 1113–19.
- Kim, Jeong-du, and Dong-sik Kim. 1997. “Development of a Combined-Type Tool Piezo-Film Accelerometer for an Ultra-Precision Lathe.” *Journal of Materials Processing Technology* 71 (3): 360–66.
- Klir, George J, and Tina Folger. 1988. *Fuzzy Sets, Uncertainty, and Information*. Edited by Engelwood-Cliffs: Prentice-Hall.
- Klocke, Fritz, Guido Wirtz, and Drazen Veselovac. 2009. “Design Approach for Adaptive Axial Force Control in Gun Drilling.” *ASME International Mechanical Engineering Congress and Exposition* 11: 583–88.
- Ko, S L, and J E Chang. 2003. “Development of Drill Geometry for Burr Minimization In Drilling.” *CIRP Annals* 52 (1): 45–48.
- Kohonen, Teuvo. 1988. *Self-Organization and Associative Memory*. Edited by Berlin: Springer-Verlag Berlin Heidelberg. <https://doi.org/10.1007/978-3-662-00784-6>.
- . 1997. “Exploration of Very Large Databases by Self-Organizing Maps.” *Proceedings of International Conference on Neural Networks (ICNN'97)*, 1–6.
- Korkut, Ihsan. 2003. “A Dynamometer Design and Its Construction for Milling Operation.” *Materials and Design* 24 (8): 631–37. <https://doi.org/10.1016/S0261-3069>.
- Kuljanic, E, G Totis, and M Æ Sortino. 2009. “Development of an Intelligent Multisensor Chatter Detection System in Milling.” *Mechanical Systems and Signal Processing* 23 (5): 1704–18. <https://doi.org/10.1016/j.ymsp.2009.01.003>.
- Kunpeng, Zhu, Wong Yoke San, and Hong Geok Soon. 2012. “Signal Processing for Tool Condition Monitoring: From Wavelet Analysis to Sparse Decomposition.” In *Mechatronics and Manufacturing Engineering: Research and Development*, 115–57. <https://doi.org/10.1016/B978-0-85709-150-5.50004-2>.
- Kurada, S, and C Bradley. 1997. “A Review of Machine Vision Sensors for Tool Condition Monitoring.” *Computers in Industry* 34 (1): 55–72.
- Kwak, Jae-seob. 2006. “Application of Wavelet Transform Technique to Detect Tool Failure in Turning Operations.” *International Journal of Advanced Manufacturing Technology* 28 (11–12): 1078–83. <https://doi.org/10.1007/s00170-004-2476-x>.
- Kwak, Jae-seob, and Ji-bok Song. 2001. “Trouble Diagnosis of the Grinding Process by Using Acoustic Emission Signals.” *International Journal of Machine Tools and Manufacture* 41:

- 899–913.
- Lee, Jay. 1995. “Machine Performance Monitoring and Proactive Maintenance in Computer-Integrated Manufacturing: Review and Perspective.” *International Journal of Computer Integrated Manufacturing*. <https://doi.org/10.1080/09511929508944664>.
- Lee, JM, DK Choi, J Kim, and CM Chu. 1995. “Real-Time Tool Breakage Monitoring For.” *CIRP Annals* 44 (1): 59–62.
- Lewandowski, Clare M. 2015. *Pattern Classification Neuro-Fuzzy Methods and Their Comparison. The Effects of Brief Mindfulness Intervention on Acute Pain Experience: An Examination of Individual Difference*. <https://doi.org/10.1017/CBO9781107415324.004>.
- Li, B H, L Zhang, S L Wang, F Tao, J W Cao, X D Jiang, X Song, and X D Chai. 2010. “Cloud Manufacturing: A New Service-Oriented Networked Manufacturing Model.” *Computer Integrated Manufacturing Systems, CIMS* 16 (1): 1–7. <https://doi.org/10.1017/CBO9781107415324.004>.
- Li, Xiaoli. 2002. “A Brief Review : Acoustic Emission Method for Tool Wear Monitoring during Turning.” *International Journal of Machine Tools and Manufacture* 42: 157–65.
- Li, Xiaoli, Shen Dong, and Zhejun Yuan. 1999. “Discrete Wavelet Transform for Tool Breakage Monitoring.” *International Journal of Machine Tools and Manufacture* 39 (12): 1935–44.
- Li, Xiaoli, Gaoxiang Ouyang, and Zhenhu Liang. 2008. “Complexity Measure of Motor Current Signals for Tool Flute Breakage Detection in End Milling.” *International Journal of Machine Tools and Manufacture* 48 (3–4): 371–79. <https://doi.org/10.1016/j.ijmachtools.2007.09.008>.
- Lin, S. C., and C. J. Ting. 1996. “Drill Wear Monitoring Using Neural Networks.” *International Journal of Machine Tools and Manufacture*. [https://doi.org/10.1016/0890-6955\(95\)00059-3](https://doi.org/10.1016/0890-6955(95)00059-3).
- Liu, Changqing, Yingguang Li, and Weiming Shen. 2014. “A Wavelet-Based Characteristic Vector Construction Method for Machining Condition Monitoring.” *IEEE International Conference on Automation Science and Engineering*, 304–8.
- Lo, Ship Peng. 2003. “An Adaptive-Network Based Fuzzy Inference System for Prediction of Workpiece Surface Roughness in End Milling.” *Journal of Materials Processing Technology* 142 (3): 665–75. [https://doi.org/10.1016/S0924-0136\(03\)00687-3](https://doi.org/10.1016/S0924-0136(03)00687-3).
- López De Lacalle, Luis Norberto, Asun Rivero, and Aitzol Lamikiz. 2009. “Mechanistic Model for Drills with Double Point-Angle Edges.” *International Journal of Advanced Manufacturing Technology* 40 (5–6): 447–57. <https://doi.org/10.1007/s00170-007-1362-8>.
- Mali, Rahul, M. T. Telsang, and T. V.K. Gupta. 2017. “Real Time Tool Wear Condition Monitoring in Hard Turning of Inconel 718 Using Sensor Fusion System.” *Materials Today: Proceedings* 4 (8): 8605–12. <https://doi.org/10.1016/j.matpr.2017.07.208>.
- Mallat, Stephane G. 1989. “A Theory for Multiresolution Signal Decomposition : The Wavelet Representation.” *IEEE Transactions on Pattern Analysis and Machine Intelligence* 11 (7): 674–93.
- Mannan, M A, Ashraf A Kassim, and Ma Jing. 2000. “Application of Image and Sound

- Analysis Techniques to Monitor the Condition of Cutting Tools.” *Pattern Recognition Letters* 21 (11): 969–79.
- Marinescu, Iulian, and Dragos Axinte. 2009. “A Time – Frequency Acoustic Emission-Based Monitoring Technique to Identify Workpiece Surface Malfunctions in Milling with Multiple Teeth Cutting Simultaneously.” *International Journal of Machine Tools and Manufacture* 49 (1): 53–65. <https://doi.org/10.1016/j.ijmachtools.2008.08.002>.
- Marinescu, Iulian, and Dragos A Axinte. 2008. “A Critical Analysis of Effectiveness of Acoustic Emission Signals to Detect Tool and Workpiece Malfunctions in Milling Operations.” *International Journal of Machine Tools and Manufacture* 48 (10): 1148–60. <https://doi.org/10.1016/j.ijmachtools.2008.01.011>.
- Marinov, V. 2004. “Tool Wear and Tool Life.” In *Manufacturing Technology*, 77–80.
- Mezentsev, Oleg A, Rixin Zhu, Richard E Devor, and William A Kline. 2002. “Use of Radial Forces for Fault Detection in Tapping.” *International Journal of Advanced Manufacturing Technology* 42 (4): 479–88.
- Mikell P. Groover. 2014. “Fundamentals of Modern Manufacturing: Materials, Processes, and Systems.” *Igarss 2014*. <https://doi.org/10.1017/CBO9781107415324.004>.
- Monostori, L., B. Kádár, T. Bauernhansl, S. Kondoh, S. Kumara, G. Reinhart, O. Sauer, G. Schuh, W. Sihn, and K. Ueda. 2016. “Cyber-Physical Systems in Manufacturing.” *CIRP Annals - Manufacturing Technology* 65 (2): 621–41. <https://doi.org/10.1016/j.cirp.2016.06.005>.
- Monostori, László. 2014. “Cyber-Physical Production Systems: Roots, Expectations and R&D Challenges.” *Procedia CIRP* 17: 9–13. <https://doi.org/10.1016/j.procir.2014.03.115>.
- Mourtzis, Dimitris, Ekaterini Vlachou, Nikolaos Milas, and Nikitas Xanthopoulos. 2016. “A Cloud-Based Approach for Maintenance of Machine Tools and Equipment Based on Shop-Floor Monitoring.” *Procedia CIRP* 41: 655–60. <https://doi.org/10.1016/j.procir.2015.12.069>.
- Mourtzis, Dimitris, Ekaterini Vlachou, Nikitas Xanthopoulos, Mohammad Givchchi, and Lihui Wang. 2016. “Cloud-Based Adaptive Process Planning Considering Availability and Capabilities of Machine Tools.” *Journal of Manufacturing Systems* 39: 1–8. <https://doi.org/10.1016/j.jmsy.2016.01.003>.
- Nath, Chandra, M Rahman, and S S K Andrew. 2007. “A Study on Ultrasonic Vibration Cutting of Low Alloy Steel.” *Journal of Materials Processing Technology* 193: 159–65. <https://doi.org/10.1016/j.jmatprotec.2007.04.047>.
- Nebot, José Vcte Abellán, Rubén Morales-Menéndez, Antonio J Vallejo Guevara, and Ciro A. Rodríguez. 2007. “Surface Roughness and Cutting Tool-Wear Diagnosis Based on Bayesian Networks.” In *Fault Detection, Supervision and Safety of Technical Processes 2006*. <https://doi.org/10.1016/B978-008044485-7/50069-5>.
- Oliveira, J, F Jr Ferraz, R Coelho, and E Silva. 2008. “Architecture for Machining Process and Production Monitoring Based in Open Computer Numerical Control.” *Journal of Engineering Manufacture* 222 (12): 1605–12. <https://doi.org/10.1243/09544054JEM1156>.

- Panda, S. S., D. Chakraborty, and S. K. Pal. 2008. "Flank Wear Prediction in Drilling Using Back Propagation Neural Network and Radial Basis Function Network." *Applied Soft Computing Journal* 8 (2): 858–71. <https://doi.org/10.1016/j.asoc.2007.07.003>.
- Park, Kyung Hee, Aaron Beal, Dave Dae Wook Kim, Patrick Kwon, and Jeff Lantrip. 2011. "Tool Wear in Drilling of Composite/Titanium Stacks Using Carbide and Polycrystalline Diamond Tools." *Wear* 271 (11–12): 2826–35. <https://doi.org/10.1016/j.wear.2011.05.038>.
- Patra, Karali, Surjya K. Pal, and Kingshook Bhattacharyya. 2007. "Artificial Neural Network Based Prediction of Drill Flank Wear from Motor Current Signals." *Applied Soft Computing Journal* 7 (3): 929–35. <https://doi.org/10.1016/j.asoc.2006.06.001>.
- Pittalà, G M, and M Monno. 2011. "A New Approach to the Prediction of Temperature of the Workpiece of Face Milling Operations of Ti-6Al-4V." *Applied Thermal Engineering* 31 (2–3): 173–80. <https://doi.org/10.1016/j.applthermaleng.2010.08.027>.
- Prakash, M, M Kanthababu, and K P Rajurkar. 2015. "Investigations on the Effects of Tool Wear on Chip Formation Mechanism and Chip Morphology Using Acoustic Emission Signal in the Microendmilling of Aluminum Alloy." *International Journal of Advanced Manufacturing Technology* 77 (5–8): 1499–1511. <https://doi.org/10.1007/s00170-014-6562-4>.
- Pritschow, G, and C Kramer. 2005. "Open System Architecture for Drives." *CIRP Annals - Manufacturing Technology* 54 (1): 375–78.
- Pujana, J, P J Arrazola, and J A Villar. 2008. "In-Process High-Speed Photography Applied to Orthogonal Turning." *Journal of Materials Processing Technology* 202 (1): 475–85. <https://doi.org/10.1016/j.jmatprotec.2007.10.007>.
- Qiao, X, and C Zhu. 2012. "Active Control of Milling Chatter Based on the Built-in Force Actuator." *Journal of Mechanical Engineering* 48 (1): 185–92.
- Quan, Y, M Zhou, and Z Luo. 1998. "On-Line Robust Identification of Tool-Wear via Multi-Sensor Neural- Network Fusion." *Engineering Applications of Artificial Intelligence* 11 (6): 717–22.
- Ramulu, M., and Mathew Spaulding. 2016. "Drilling of Hybrid Titanium Composite Laminate (HTCL) with Electrical Discharge Machining." *Materials* 9 (9). <https://doi.org/10.3390/ma9090746>.
- Rawat, Sanjay, and Helmi Attia. 2009. "Characterization of the Dry High Speed Drilling Process of Woven Composites Using Machinability Maps Approach." *CIRP Annals - Manufacturing Technology* 58 (1): 105–8. <https://doi.org/10.1016/j.cirp.2009.03.100>.
- Ren, Qun, Luc Baron, Marek Balazinski, Ruxandra Botez, and Pascal Bigras. 2015. "Tool Wear Assessment Based on Type-2 Fuzzy Uncertainty Estimation on Acoustic Emission." *Applied Soft Computing Journal* 31: 14–24. <https://doi.org/10.1016/j.asoc.2015.02.037>.
- René de Jesús, Romero-Troncoso, Herrera-Ruiz Gilberto, Terol-Villalobos Ivan, and Jáuregui-Correa Juan Carlos. 2004. "FPGA Based On-Line Tool Breakage Detection System for CNC Milling Machines." *Mechatronics* 14 (4): 439–54. [https://doi.org/10.1016/S0957-4158\(03\)00069-2](https://doi.org/10.1016/S0957-4158(03)00069-2).

- Rizal, Muhammad, Jaharah A. Ghani, Mohd Zaki Nuawi, and Che Hassan Che Haron. 2013. "Online Tool Wear Prediction System in the Turning Process Using an Adaptive Neuro-Fuzzy Inference System." *Applied Soft Computing Journal* 13 (4): 1960–68. <https://doi.org/10.1016/j.asoc.2012.11.043>.
- Rogers, L M. 1979. "The Application of Vibration Signature Analysis and Acoustic Emission Source Location to On-Line Condition Monitoring of Anti-Friction Bearings." *Tribology International* 12 (2): 51–58.
- Roy, Shibendu Shekhar. 2015. "An Application of ANFIS-Based Intelligence Technique for Predicting Tool Wear in Milling." *Advances in Intelligent Systems and Computing* 343: 299–306. https://doi.org/10.1007/978-81-322-2268-2_32.
- Rubio, E, and R Teti. 2009. "Cutting Parameters Analysis for the Development of a Milling Process Monitoring System Based on Audible Energy Sound." *Journal of Intelligent Manufacturing* 20 (1): 43–54. <https://doi.org/10.1007/s10845-008-0102-8>.
- Ryabov, O, K Mori, and N Kasashima. 1996. "An In-Process Direct Monitoring Method for Milling." *CIRP Annals - Manufacturing Technology* 45 (1): 97–100.
- Salgado, D R, and F J Alonso. 2006. "Tool Wear Detection in Turning Operations Using Singular Spectrum Analysis." *Journal of Materials Processing Technology* 171 (3): 451–58. <https://doi.org/10.1016/j.jmatprotec.2005.08.005>.
- Salgado, D R, F J Alonso, I Cambero, and A Marcelo. 2009. "In-Process Surface Roughness Prediction System Using Cutting Vibrations in Turning." *International Journal of Advanced Manufacturing Technology* 43 (1–2): 40–51. <https://doi.org/10.1007/s00170-008-1698-8>.
- Sanjay, C, M L Neema, and C W Chin. 2005. "Modeling of Tool Wear in Drilling by Statistical Analysis and Artificial Neural Network" 170: 494–500. <https://doi.org/10.1016/j.jmatprotec.2005.04.072>.
- Saoubi, Rachid M, Dragos Axinte, Leung Sein Soo, Christoph Nobel, Helmi Attia, Gregor Kappmeyer, Serafettin Engin, and Wei-ming Sim. 2015. "High Performance Cutting of Advanced Aerospace Alloys and Composite Materials." *CIRP Annals - Manufacturing Technology* 64 (2): 557–80. <https://doi.org/10.1016/j.cirp.2015.05.002>.
- Saravanan, S, G Yadava, and P Rao. 2006. "Condition Monitoring Studies on Spindle Bearing of a Lathe." *International Journal of Advanced Manufacturing Technology* 28 (9): 993–1005. <https://doi.org/10.1007/s00170-004-2449-0>.
- Scheffer, C, and P S Heyns. 2001. "WEAR MONITORING IN TURNING OPERATIONS USING VIBRATION AND STRAIN MEASUREMENTS." *Mechanical Systems and Signal Processing* 15 (6): 1185–1202. <https://doi.org/10.1006/mssp.2000.1364>.
- . 2004. "An Industrial Tool Wear Monitoring System for Interrupted Turning." *Mechanical Systems and Signal Processing* 18 (5): 1219–42. <https://doi.org/10.1016/j.ymsp.2003.09.001>.
- Schmidhuber, Jurgen, Daan Wierstra, Matteo Gagliolo, and Faustino Gomez. 2007. "Training Recurrent Networks by Evolino." *Neural Computation* 19 (3): 757–79.
- Segreto, T., A. Caggiano, and R. Teti. 2015. "Neuro-Fuzzy System Implementation in Multiple

- Sensor Monitoring for Ni-Ti Alloy Machinability Evaluation.” *Procedia CIRP* 37: 193–98. <https://doi.org/10.1016/j.procir.2015.08.020>.
- Segreto, T, A Simeone, and R Teti. 2014. “Principal Component Analysis for Feature Extraction and NN Pattern Recognition in Sensor Monitoring of Chip Form during Turning.” *CIRP Journal of Manufacturing Science and Technology* 7 (3): 202–9. <https://doi.org/10.1016/j.cirpj.2014.04.005>.
- Segreto, T, and R Teti. 2008. “Sensor Fusion of Acoustic Emission and Cutting Force for Tool Wear Monitoring during Composite Materials Machining.” In *6th CIRP International Conference on ICME*, 221–26. Naples.
- Sheikh-Ahmad, J., and J. P. Davim. 2011. “Tool Wear in Machining Processes for Composites.” In *Machining Technology for Composite Materials: Principles and Practice*. <https://doi.org/10.1016/B978-0-85709-030-0.50005-9>.
- Sheikh-Ahmad, Jamal Y., and João Paulo Davim. 2012. “Cutting and Machining of Polymer Composites.” In *Wiley Encyclopedia of Composites*. <https://doi.org/10.1002/9781118097298.weoc061>.
- Shinno, H, and H Hashizume. 1997. “Ln-Process Monitoring Method for Machining Environment Based on Simultaneous Multiphenomena Sensing.” *CIRP Annals - Manufacturing Technology* 46 (1): 53–56.
- Shunmugesh, K., and K. Panneerselvam. 2016. “Multi-Response Optimization in Drilling of Carbon Fiber Reinforced Polymer Using Artificial Neural Network Correlated to Meta-Heuristics Algorithm.” *Procedia Technology* 25 (Raerest): 955–62. <https://doi.org/10.1016/j.protec.2016.08.187>.
- Shy, D, DA Axinte, and NN Gindy. 2007. “Development of an Online Machining Process Monitoring System : A Case Study of the Broaching Process.” *International Journal of Advanced Manufacturing Technology* 34 (1–2): 34–46. <https://doi.org/10.1007/s00170-006-0588-1>.
- Shyha, I. S., S. L. Soo, D. K. Aspinwall, S. Bradley, R. Perry, P. Harden, and S. Dawson. 2011. “Hole Quality Assessment Following Drilling of Metallic-Composite Stacks.” *International Journal of Machine Tools and Manufacture* 51 (7–8): 569–78. <https://doi.org/10.1016/j.ijmachtools.2011.04.007>.
- Sick, Bernhard. 2002. “ON-LINE AND INDIRECT TOOL WEAR MONITORING IN TURNING WITH ARTIFICIAL NEURAL NETWORKS : A REVIEW OF MORE THAN A DECADE OF RESEARCH.” *Mechanical Systems and Signal Processing* 16 (4): 487–546. <https://doi.org/10.1006/mssp.2001.1460>.
- Silva, R. G., R. L. Reuben, K. J. Baker, and S. J. Wilcox. 1998. “Tool Wear Monitoring of Turning Operations by Neural Network and Expert System Classification of a Feature Set Generated from Multiple Sensors.” *Mechanical Systems and Signal Processing* 12 (2): 319–32. <https://doi.org/10.1006/mssp.1997.0123>.
- Simeone, A. 2008. “Ottimizzazione Di Lavorazione per Asportazione Di Truciolo Su Leghe a Bassa Lavorabilità.” University of Naples Federico II.
- Smit, J, K Stephan, C Moeller, and M Carlberg. 2016. *Industry 4.0*. Edited by EU: and Research and Energy European Parliament’s Committee on Industry.

- Smith, D A, S Smith, and J Tlusty. 1998. "High Performance Milling Torque Sensor." *Journal of Manufacturing Science and Engineering, Transactions of the ASME* 120 (3): 504–14.
- Song, Dong-yeul, Nobuo Otani, Takayuki Aoki, and Yuichiro Kamakoshi. 2005. "A New Approach to Cutting State Monitoring in End-Mill Machining." *International Journal of Machine Tools and Manufacture* 45: 909–21. <https://doi.org/10.1016/j.ijmachtools.2004.10.014>.
- Sousa, José A.G., Marcelo N. Sousa, Mark J. Jackson, and Álisson R. Machado. 2014. "Comparison of the Steel Machining Performance of New and Reground Cemented Carbide Drills." *Proceedings of the Institution of Mechanical Engineers, Part B: Journal of Engineering Manufacture* 228: 376–87. <https://doi.org/10.1177/0954405413502199>.
- Specht, Donald F. 1990. "Probabilistic Neural Networks." *Neural Networks* 3 (1): 109–18.
- Stephenson, D A, and J S Agapiou. 2006. *Metal Cutting Theory and Practice*. Edited by CRC Press - Taylor & Francis Group.
- Sun, J, G S Hong, M Rahman, and Y S Wong. 2004. "Identification of Feature Set for Effective Tool Condition Monitoring by Acoustic Emission Sensing." *International Journal of Production Research* 42 (5): 901–18. <https://doi.org/10.1080/00207540310001626652>.
- Tansel, Ibrahim Nur, Christine Mekdeci, and Charles McLaughlin. 1995. "Detection of Tool Failure in End Milling with Wavelet Transformations and Neural Networks (WT-NN)." *International Journal of Machine Tools and Manufacture* 35 (8): 1137–47.
- Tao, F, L Zhang, V C Venkatesh, Y Luo, and Y Cheng. 2011. "Cloud Manufacturing: A Computing and Service- Oriented Manufacturing Model." *Proceedings of the Institution of Mechanical Engineers, Part B: Journal of Engineering Manufacture* 225 (10): 1969–76. <https://doi.org/10.1177/0954405411405575>.
- Tarng, Y S, and B Y Lee. 1999. "Amplitude Demodulation of the Induction Motor Current for the Tool Breakage Detection in Drilling Operations." *Robotics and Computer-Integrated Manufacturing* 15 (4): 313–18.
- Teti, R. 2015. "Advanced IT Methods of Signal Processing and Decision Making for Zero Defect Manufacturing in Machining." *Procedia CIRP* 28: 3–15. <https://doi.org/10.1016/j.procir.2015.04.003>.
- Teti, R. 1995. "Fuzzy Logic Approach to Sensor Monitoring during Machining." In *WILF 95*, 189–99. Naples.
- . 2002. "Machining of Composite Materials." *CIRP Annals* 51: 611–34.
- Teti, R, I S Jawahir, K Jemielniak, T Segreto, S Chen, and J Kossakowska. 2006. "Chip Form Monitoring through Advanced Processing of Cutting Force Sensor Signals." *CIRP Annals* 55 (1): 75–80.
- Teti, R, K Jemielniak, G O Donnell, and D Dornfeld. 2010. "Advanced Monitoring of Machining Operations." *CIRP Annals - Manufacturing Technology* 59: 717–39. <https://doi.org/10.1016/j.cirp.2010.05.010>.
- Teti, R, and S R T Kumara. 1997. "Intelligent Computing Methods for Manufacturing Systems." *CIRP Annals - Manufacturing Technology* 46 (2): 629–52.

- Teti, R, and A Manzoni. 1998. "Tool Wear State Identification by Fuzzy Logic Processing of Fused Sensor Data." In *1st CIRP International Seminar on ICME*, 687–91. Capri.
- Teti, R, T Segreto, and C Harzbecker. 2008. "Sensor Monitoring Based Optimisation during Turning of Titanium Alloys." In *4th I*PROMS, Virtual International Conference on Innovative Production Machines and Systems*, 547–54. Berlin.
- Teti, R, T Segreto, R Neugebauer, and C Harzbecker. 2008. "Process Acceptability in Turning of Titanium Alloys Based on Cutting Force Sensor Monitoring." In *3rd International CIRP High Performance Cutting Conference*, 241–50. Dublin.
- Venuvinod, P. K., and A. Djordjevich. 1996. "Towards Active Chip Control." *CIRP Annals - Manufacturing Technology* 45 (1): 83–86. [https://doi.org/10.1016/S0007-8506\(07\)63021-2](https://doi.org/10.1016/S0007-8506(07)63021-2).
- Verl, A, U Heisel, M Walther, and D Maier. 2009. "Sensorless Automated Condition Monitoring for the Control of the Predictive Maintenance of Machine Tools." *CIRP Annals - Manufacturing Technology* 58 (1): 375–78. <https://doi.org/10.1016/j.cirp.2009.03.039>.
- Vijayaraghavan, A., and D. Dornfeld. 2010. "Automated Energy Monitoring of Machine Tools." *CIRP Annals - Manufacturing Technology* 59 (1): 21–24. <https://doi.org/10.1016/j.cirp.2010.03.042>.
- Wang, Guofeng, Chang Liu, Yinhu Cui, and Xiaoliang Feng. 2014. "Tool Wear Monitoring Based on Cointegration Modelling of Multisensory Information." *International Journal of Computer Integrated Manufacturing* 27 (5): 479–87. <https://doi.org/10.1080/0951192X.2013.814162>.
- Wang, Lihui, Martin Tornngren, and Mauro Onori. 2015. "Current Status and Advancement of Cyber-Physical Systems in Manufacturing." *Journal of Manufacturing Systems* 37: 517–27. <https://doi.org/10.1016/j.jmsy.2015.04.008>.
- Wang, W H, G S Hong, Y S Wong, and K P Zhu. 2007. "Sensor Fusion for Online Tool Condition Monitoring in Milling." *International Journal of Production Research* 45 (21): 5095–5116. <https://doi.org/10.1080/00207540500536913>.
- Wilhelm, Mark, Boeing Commercial, and Airplane Company. 2001. "Aircraft Applications." <https://doi.org/10.1361/asmhba0003477>.
- Wong, Y S, A Y C Nee, X Q Li, and C Reisdorf. 1997. "Tool Condition Monitoring Using Laser Scatter Pattern." *Journal of Materials Processing Technology* 63 (1–3): 205–10.
- Wu, Dazhong, Connor Jennings, Janis Terpenney, and Soundar Kumara. 2016. "Cloud-Based Machine Learning for Predictive Analytics: Tool Wear Prediction in Milling." *Proceedings - 2016 IEEE International Conference on Big Data, Big Data 2016*, 2062–69. <https://doi.org/10.1109/BigData.2016.7840831>.
- Wu, Dazhong, David W. Rosen, Lihui Wang, and Dirk Schaefer. 2015. "Cloud-Based Design and Manufacturing: A New Paradigm in Digital Manufacturing and Design Innovation." *CAD Computer Aided Design* 59: 1–14. <https://doi.org/10.1016/j.cad.2014.07.006>.
- Wu, S, P Li, Z Yan, L Zhang, X Qiu, and J Yang. 2014. "Wavelet Packet Analyses of Acoustic Emission Signal for Tool Wear in High Speed Milling." *Key Engineering Materials*, 600–

605.

- Wu, Ya, and R Du. 1996. "FEATURE EXTRACTION AND ASSESSMENT USING WAVELET PACKETS FOR MONITORING OF MACHINING PROCESSES." *Mechanical Systems and Signal Processing* 10 (1): 29–53.
- Xu, Xun. 2012. "From Cloud Computing to Cloud Manufacturing." *Robotics and Computer-Integrated Manufacturing* 28 (1): 75–86. <https://doi.org/10.1016/j.rcim.2011.07.002>.
- Yang, G, J Hou, W Zhou, L Zhu, and H Duan. 2014. "Non-Contact Temperature Measurement by Infrared Pyrometer in High Speed Milling." *Applied Mechanics and Materials*, 668–69.
- Zhang, Lin, Yongliang Luo, Fei Tao, Bo Hu Li, Lei Ren, Xuesong Zhang, Hua Guo, Ying Cheng, Anrui Hu, and Yongkui Liu. 2012. "Cloud Manufacturing: A New Manufacturing Paradigm." *Enterprise Information Systems* 8 (2): 167–87. <https://doi.org/10.1080/17517575.2012.683812>.
- Zhou, Z, Y Chen, J Fuh, and A Nee. 2000. "Integrated Condition Monitoring and Fault Diagnosis for Modern Manufacturing Systems 1." *CIRP Annals - Manufacturing Technology* 49 (1): 387–90.
- Zhu, Kunpeng, Yoke San Wong, and Geok Soon Hong. 2009. "Multi-Category Micro-Milling Tool Wear Monitoring with Continuous Hidden Markov Models." *Mechanical Systems and Signal Processing* 23 (2): 547–60. <https://doi.org/10.1016/j.ymsp.2008.04.010>.
- Zitoune, Redouane, Vijayan Krishnaraj, and Francis Collombet. 2010. "Study of Drilling of Composite Material and Aluminium Stack." *Composite Structures* 92 (5): 1246–55. <https://doi.org/10.1016/j.compstruct.2009.10.010>.
- Zitoune, Redouane, Mohamed El Mansori, and Vijayan Krishnaraj. 2013. "Tribo-Functional Design of Double Cone Drill Implications in Tool Wear during Drilling of Copper Mesh/CFRP/Woven Ply." *Wear* 302 (1–2): 1560–67. <https://doi.org/10.1016/j.wear.2013.01.046>.